An integrated communication and positioning system using geostationary satellites : a feasibility study

Peters, J.H.H.L.

Award date:
1994

EINDHOVEN UNIVERSITY OF TECHNOLOGY
DEPARTMENT OF ELECTRICAL ENGINEERING
TELECOMMUNICATIONS DIVISION (EC)

AN INTEGRATED COMMUNICATION AND POSITIONING SYSTEM USING GEOSTATIONARY SATELLITES

A feasibility study

Author: J.H.H.L. Peters

Master thesis
performed at the Satellite Communications Group of Virginia Tech (Blacksburg, VA)
from January until July 1994

Graduation professor: Prof.dr.ir. G. Brussaard
Supervisor: Dr. T. Pratt (Virginia Tech)

SUMMARY

The main objective of this study was to examine whether a communication system consisting of a number of geostationary satellites can be set up in such a way that system users can infer their own position from the transmitted data. The service area for such a system would be the Continental United States (CONUS).

Existing satellite positioning systems have been studied through an extensive literature search. The principles of operation and position accuracies of TRANSIT, GLONASS, NAVSAT and Starfix are given. The Global Positioning System (GPS) is described in detail.

Signals generated on earth and relayed by transponders on three geostationary satellites combined with an altitude input from an altimeter can yield sufficient information to a user receiver to determine its own position. Using QPSK direct sequence spread spectrum modulation, a carrier can be modulated with a short pseudo-noise code plus the general (e.g. weather) information on one channel and with a longer code plus the navigation message on the other channel. In this way acquisition times can be low. System specifications and receiver design are given.

The influence of the available number of satellites and their positions on the position accuracy of the system has been examined. Regarding system performance, cost and complexity, the optimal number of satellites is four. System operation can take place both at C- and Ku-band and horizontal accuracies of 51.9 - 131.3 m and 70.1 - 153.6 m are achievable across the CONUS when using C- and Ku-band satellites at optimal longitudes. These values compare well with the specified GPS accuracy of 100 m.

The proposed system is a communication system with integrated positioning capabilities. Maximum data rates on the information channel are 7.4 and 23.4 kbps at C- and Ku-band respectively.

TABLE OF CONTENTS

Preface

From January till July 1994, I have performed a Master thesis of the Eindhoven University of Technology, Department of Electrical Engineering, Telecommunications Division, at Virginia Tech in the United States of America.

At Virginia Tech, the work on this thesis has been done at the Bradley Department of Electrical Engineering, in the Satellite Communications Group. My graduation work has been supervised by Prof.dr.ir. G. Brussaard, professor at the Eindhoven University of Technology, Department of Electrical Engineering, Telecommunications Division. My coach at Virginia Tech has been Dr. T. Pratt.

I would especially like to thank Prof.dr.ir. G. Brussaard for giving me the opportunity to perform my Master thesis at Virginia Tech and to appreciate my "krankzinnig verzoek". I would also like to thank Dr. Pratt, who made my stay at Virginia Tech a pleasant one and who was always willing to make time for discussion, both on my project and other topics.

During my stay at Viriginia Tech I was very pleased to receive some considerable financial support from the Dutch Royal Engineering Institute (KIvI) and from the STIR-WO. Without this support my stay in the US would have been bothered by financial sorrows, not the things you need when writing a thesis.

I thank all members of the Satcom Group at Virginia Tech, for immediately accepting that tall Dutchman as one of them. A final word of appreciation to my fellow Dutch students at Virginia Tech for all those nights at PK's that turned me into a professional pool player.

John H.H.L. Peters

Eindhoven, August 1994

Chapter 1 Introduction

Radiopositioning systems that can determine a user's position based on the electromagnetic properties of radiowaves were used as early as World War II. Two terrestrial hyperbolic systems were introduced during the war: DECCA in the UK and Loran-A in the US. DECCA has mainly been used in Europe and the Loran-C system that was developed from Loran-A is still used in ships and aircraft around the world. In the 1960s work started to develop and build radiopositioning systems using satellite signals to overcome some of the problems and limitations of terrestrial systems. The first such system, TRANSIT, is described in more detail in Chapter 3.

The objective of this report was twofold

1. To study existing satellite positioning systems and to determine their main characteristics and accuracies
2. To examine whether a constellation of geostationary communication satellites can be used for positioning purposes.

The latter subject constitutes the main part of this report and is discussed in Chapter 5. It is important to keep in mind that the system proposed in that chapter is not a dedicated positioning system and it is not meant to replace any of the existing systems. It will be shown that a general communication system using geostationary satellites (e.g. a weather information distribution system) can be used for position measurements as well, provided that the satellite signals have a certain format. Using QPSK direct sequence spread spectrum modulation the general information, the data that a user needs to determine its position and a pseudo-noise code for range measurements can all be part of the same data stream.

Signals from three geostationary satellites combined with an altimeter input should yield sufficient information for a user anywhere in the Continental United States to produce its own position. Which satellites qualify to be used in such a system, system design, necessary timing and frequency control arrangements and achievable position accuracies are all topics to be covered in depth in Chapter 5.

A description of the main principles of (satellite) positioning systems can be found in Chapter 2. The error factors common to most systems are mentioned here. The effect of the atmosphere on range measurements and the influence of the geometry of the satellites, i.e. their position relative to the user and towards each other, are studied in more detail.

Chapter 3 gives an overview of currently existing satellite positioning systems. Its purpose is neither to list all existing systems nor to be exhaustive, but to give the reader a quick glance at the different concepts, the signal structures and the position accuracies of the following systems: TRANSIT, Navstar GPS, GLONASS, NAVSAT and Starfix.

The only time-continuous satellite positioning system with world-wide coverage functioning up to date is the US Global Positioning System. In spite of its limitations stemming from the system's military origin, it currently is the most used radio positioning system in the civil user community and will remain to be so in the nearby future. GPS is studied in detail in Chapter 4 and especially its signal structure, receiver operation and error budget where very much taken into account in the design of our system. Again it is stated here that our proposal for an integrated communication and positioning system by no means is intended as a replacement for GPS. Driven by the user needs from mainly the aviation community, attempts are currently being made to overcome some of the limitations of GPS by adding a civil component to the system. Latest developments in this area are also covered in Chapter 4.

The final chapter of this report contains the most important conclusions and some recommendations for future work. A list of references and seven appendices are included to provide specific details to the interested reader.

Chapter 2 Principles of satellite positioning systems

2.1 Introduction

Radiopositioning systems can be divided into two categories: terrestrial and extraterrestrial systems. Examples of the former category are Omega, Loran-C and VOR/DME. This study concentrates on satellite positioning systems, part of the latter category. In this report satellite positioning refers to the positioning of objects by means of satellites, not to the positioning of satellites. Usually positions are determined in Cartesian coordinates in the Conventional Terrestrial System. Most users however want to know their position in latitude (φ), longitude (λ) and height above the geoid (h). Therefore a transformation of coordinates is needed.

The determination of the position of stationary or moving objects is called static and kinematic positioning respectively. In point or absolute positioning, a position is determined with respect to a well-defined (geocentric) coordinate system. Determining a position with respect to another point is known as relative positioning.

Although the term radiopositioning system has no legal international definition or standing, this term is widely used and will be used throughout this report. The official ITU definitions are [Blanchard, 1989]

Radiodetermination - The determination of the position, velocity and/or other characteristics of an object, or the obtaining of information relating to these parameters, by means of the propagation properties of radiowaves. Radiodetermination Satellite Service (RDSS) is a subset of this general classification.

Radionavigation - Radiodetermination used for the purposes of navigation, including obstruction warning.

Radiolocation - Radiodetermination used for purposes other than navigation.

The last distinction has been made because only radionavigation systems are regarded as 'safety-of-life' systems. Exclusive frequency bands (1215-1260 MHz and 1559-1610 MHz) have been allocated to radionavigation systems, whereas radiolocation systems have to share their frequencies with other systems.

From the design point of view the main difference is that in a radiolocation system it can be assumed that the user is stationary during the measurement period. This allows for a long integration period and post-processing of the data. In a radionavigation system the user will generally be moving during the measurement period. The dynamical behavior of this motion determines the design parameters of various filters in the receiver and the integration period normally has to be short.

2.2 Range measurements

Positions can be determined by using the ranging method. If we know the distance r_1 between the receiver and a transmitter at a known location, the receiver has to be on a circle with radius r_1 centered at the transmitter's location. This circle is called a Line Of Position, LOP. When we use two transmitters, the position of the receiver corresponds to the intersection of the two LOPs. In 3-D space the circles become spheres and the intersection of three spheres represents the location of the receiver.

The distance between a transmitter and a receiver is determined by multiplying the propagation time of a radiated pulse with the propagation speed, which is the speed of light. In reality one extra transmitter is needed to account for the time bias introduced by the fact that the time of emission and the time of reception are measured in different time frames (at the transmitter and receiver respectively). The measured ranges are therefore called pseudo-ranges.

Timing problems are also eliminated in the case of hyperbolic positioning, which is based on the measurement of the difference in range to two transmitters. By measuring the difference in arrival time of the pulses (assuming synchronization of the transmitters so that the pulses were sent at the same time) a hyperbolic LOP can be defined, which corresponds to a constant difference in range between two transmitters. The use of two pairs of transmitters results in two LOPs. The receiver's position corresponds to the intersection of the two hyperbolas. In 3-D space the receiver's position will be determined by the intersection of three hyperbolic surfaces of revolution.

Based on the satellite signal a receiver can measure the following entities

- The time shift required to line up a received code, modulated on the signal, with a replica generated in the receiver. This method to determine pseudo-ranges was first used in GPS and is described in Chapter 4.
- The Doppler shift of the carrier frequency. How the receiver's location can be inferred from this is described in Section 3.1.

- The phase of the carrier frequency. The problems of cycle ambiguity can normally not be solved in real-time. As phase measurements can yield very accurate positions they are widely used in geodetic applications. This report however will not deal with this type of measurements, the interested reader is referred to [Seeber, 1993].

Carrier phase measurements have been used for a long time in multi-tone ranging. Multiple coherent tones at different frequencies modulate a single carrier. The frequency of the lowest tone is chosen such that the period is longer than the propagation delay between the transmitter and a receiver. By comparison of the phases the receiver can measure the range based on the unique phase relationship of the tones that depends on the position of the receiver. The range resolution is limited by the receiver's ability to measure the tone's phases.

2.3 Applications

Satellite positioning systems can be used for a wide range of applications. Some examples are

- surveying and mapping
- in-car navigation (e.g. the Philips CARIN system)
- vehicle monitoring/fleet management
- marine navigation
- en route navigation and (non-)precision approach landing of airplanes
- positioning/navigation of other space vehicles (e.g. LEO satellites)
- military (e.g. missile guidance)

2.4 Performance parameters

The accuracy of a satellite positioning system is determined by a large number of factors

- accuracy of received satellite ephemerides (if needed)
- remaining timing errors
- errors introduced by the receiver
- multipath problems
- influence of atmosphere
- geometry of the satellites

The first five factors together result in a user range error. Combined knowledge of this error and the geometry leads to a certain error in position. As the last two factors are common to most systems they will be dealt with in the remaining two sections of this chapter.

During the last few years there has been a shift in focus from accuracy to reliability and integrity of radio positioning systems. The 1992 Federal Radionavigation Plan uses the following definitions

Accuracy - The degree of conformance between the estimated or measured position and/or velocity of a platform at a given time and its true position or velocity. Radionavigation system accuracy is usually presented as a statistical measure of system error and is specified as

- **Predictable** - The accuracy of a radionavigation system's position solution with respect to the charted solution. Both the position solution and the chart must be based upon the same geodetic datum.
- **Repeatable** - The accuracy with which a user can return to a position whose coordinates have been measured at a previous time with the same navigation system.
- **Relative** - The accuracy with which a user can measure position relative to that of another user of the same navigation system at the same time.

Availability - The percentage of time that the services of a navigation system are usable.

Reliability - The probability of performing a specified function without failure under given conditions for a specified period of time.

Integrity - The ability of a system to provide timely warnings to users when the system should not be used for navigation.

External integrity means that the failure of a navigation system can be communicated to a user of that system. When there is some redundancy in the navigational data available to the receiver then the receiver is able to determine the quality of the position fix itself. This is known as Receiver Autonomous Integrity Monitoring (RAIM).

2.5 Atmospheric effects

In the ideal situation a radio wave would propagate in a straight line from a satellite to a receiver at a known constant velocity c_0. Because of the presence of molecules in the troposphere and free electrons in the ionosphere the velocity differs slightly from c_0. This atmospheric influence can be described by the

refractive index n, defined as c_0/v. Because of its small deviation from 1, very often the refractivity N, defined as
$(n\text{-}1)\cdot 10^6$, is used instead. For example an atmospheric delay of only 1 ns will already lead to a 0.3 meter error in the range measurement.

When measurements are carried out at the carrier wave frequency of a signal, the phase velocity of the radio wave has to be considered, given by

$$v_p = c_0/n \tag{2.1}$$

where c_0 equals $2.99792458\cdot 10^8$ m/s. If the measurements are based on the modulation of the radio wave, the group velocity of the radio wave has to be used, given by

$$v_g = \frac{c_0 \cdot n}{n^2 + \frac{1}{2}\cdot\omega\cdot\frac{dn^2}{d\omega}} \tag{2.2}$$

where ω is the angular frequency of the radio wave.

If signal path bending is small the range error in an electromagnetically measured distance is given by

$$\Delta r = \int_{\substack{geometric\\ path}} \{n(s)-1\}ds = 10^{-6}\cdot \int_{\substack{geometric\\ path}} N(s)ds \tag{2.3}$$

2.5.1 Troposphere

When speaking of the troposphere, we mean mostly the lower and neutral (non-ionized) 50 km of the earth's atmosphere. For frequencies up to 20 GHz the refractivity N of moist air is given by [Smith & Weintraub, 1953]

$$N = k_1\cdot\frac{p}{T} + \left[k_3 + 273\cdot(k_2 - k_1)\right]\cdot\frac{e}{T^2} \tag{2.4}$$

where

$k_1 = 77.604\ \mathrm{K/mbar}$
$k_2 = 64.8\ \mathrm{K/mbar}$
$k_3 = 3.776 \cdot 10^5\ \mathrm{K^2/mbar}$
} empirically determined constants [Thayer, 1974]

p = total pressure of moist air (mbar)

e = partial pressure of water vapor (mbar)

T = temperature (K)

The refractive index of the troposphere is practically independent of the frequency of the radio wave. Therefore the group velocity and the phase velocity are both equal to c_0/n. The first term in equation 2.4 is often referred to as the dry, or more accurately, the hydrostatic term. The last term is called the wet term. It is convenient to also write the tropospheric delay as the sum of a dry and a wet component

$$\Delta r = \Delta r_d + \Delta r_w \tag{2.5}$$

The tropospheric delay for a satellite at elevation angle E can be written as the product of the delay at zenith and a mapping function which relates this zenith delay to the delay at elevation angle E [De Jong, 1991]

$$\Delta r(E) = F(E,\underline{P}) \cdot \Delta r(90°) \tag{2.6}$$

where the mapping function $F(E,\underline{P})$ is always a function of the elevation and sometimes a function of other parameters, contained in the vector $\underline{P}$. Based on real data, Hopfield has found a height-dependent function of the dry and wet component given by [Hopfield, 1971]

$$N_d(h) = N_{d_0} \cdot \left(\frac{h_d - h}{h_d - h_s} \right)^4 \tag{2.7}$$

$$N_w(h) = N_{w_0} \cdot \left(\frac{h_w - h}{h_w - h_s} \right)^4 \tag{2.8}$$

with

$$N_{d_0} = k_1 \cdot \frac{p_s}{T_s} \tag{2.9}$$

$$N_{w_0} = [k_3 + 273 \cdot (k_2 - k_1)] \cdot \frac{e_s}{T_s} \tag{2.10}$$

$$h_d = 40136 + 148.72 \cdot (T_s - 273.16) \tag{2.11}$$

where

h_d = height (m) of the dry neutral atmosphere above the geoid

h_w = height of the wet neutral atmosphere above the geoid, mean value is 11,000 m

h = height above the geoid

h_s = surface height above the geoid (height of the receiver)

p_s = surface air pressure

T_s = surface temperature

e_s = surface partial water vapor pressure

This model is based on the assumptions that the temperature decreases with height as 6.71°C/km, the dry atmosphere behaves like an ideal gas, the atmosphere is built up in spherical layers and the refractivity does not change with time. The expression for the wet component has the same form as the expression for the dry component. Although there is no supportive theoretical foundation to support the correspondence, this expression has been widely used [Seeber, 1993].

The tropospheric zenith delay is then given by

$$\begin{aligned}\Delta r(90°) = \Delta r_d(90°) + \Delta r_w(90°) &= 10^{-6}\cdot\left[\int_{h_s}^{h_d} N_d(h)dh + \int_{h_s}^{h_w} N_w(h)dh\right] \\ &= 0.2\cdot 10^{-6}\cdot\left[N_{d_0}\cdot(h_d - h_s) + N_{w_0}\cdot(h_w - h_s)\right]\end{aligned} \tag{2.12}$$

When using typical values then $\Delta r_d(90°)$ is about 2.3 m and changes relatively slowly with time. $\Delta r_w(90°)$ is less than 0.4 m. As it can change quickly with time it is the main source of remaining tropospheric errors.

To calculate the dry and wet tropospheric delay at elevation E from the zenith values a number of models have been developed. Blacks' model has been widely used and is given by [Black, 1978]

$$\Delta r(E) = \Delta r_d(90°)\cdot\left[1-\left(\frac{\cos E}{1+0.15\cdot h_d/r_s}\right)^2\right]^{-1/2} + \Delta r_w(90°)\cdot\left[1-\left(\frac{\cos E}{1+0.15\cdot h_w/r_s}\right)^2\right]^{-1/2} \tag{2.13}$$

where r_s is the distance between the receiver and the center of the earth. This can be written as (compare with equations 2.20 and 2.21)

$$\Delta r(E) = \frac{\Delta r_d(90°)}{\sin E'} + \frac{\Delta r_w(90°)}{\sin E''} \tag{2.14}$$

with

$$\cos E' = \frac{r_s}{r_s + 0.15 \cdot h_d} \cdot \cos E \tag{2.15}$$

$$\cos E'' = \frac{r_s}{r_s + 0.15 \cdot h_w} \cdot \cos E \tag{2.16}$$

Another mapping function is given by [Seeber, 1993]

$$\Delta r(E) = \frac{\Delta r_d(90°)}{\sin(E^2 + 6.25)^{\frac{1}{2}}} + \frac{\Delta r_w(90°)}{\sin(E^2 + 2.25)^{\frac{1}{2}}} \tag{2.17}$$

The results of both mapping functions compare well.

In most satellite positioning systems the measured ranges are corrected using models like this. It is fair to conclude that for very high accuracy applications tropospheric delays cannot be determined accurately enough from empirical models. In Figure 2.1 the resulting tropospheric range error is shown as a function of the elevation angle. In this example T_s, p_s and e_s were assumed to be equal to 290 K, 1000 mbar and 10 mbar respectively.

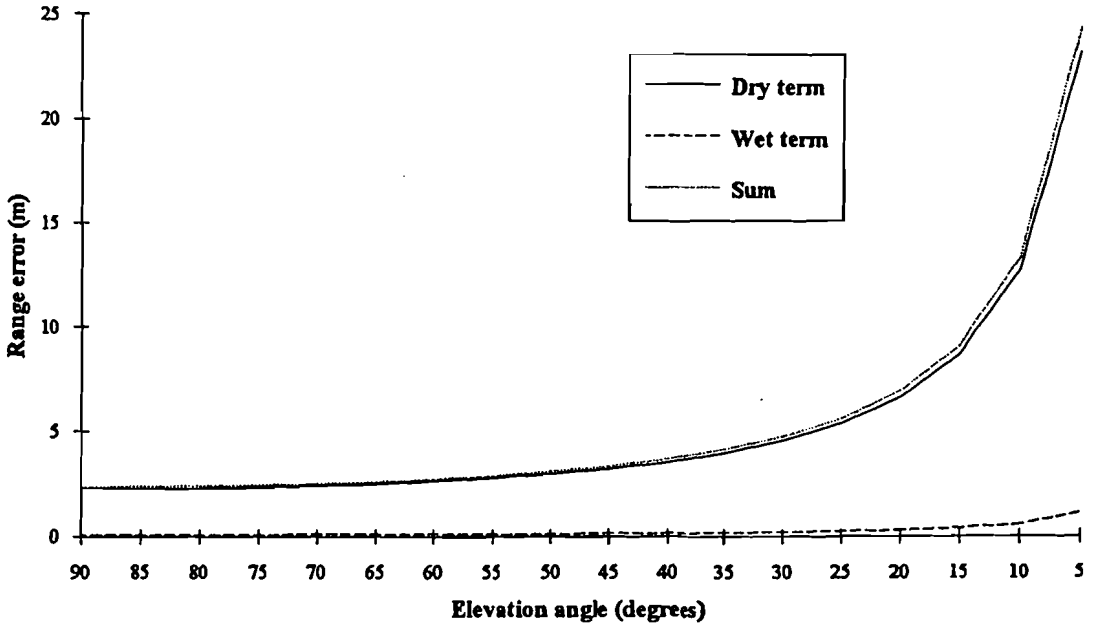

Figure 2.1 Tropospheric range error under standard conditions

2.5.2 Ionosphere

The ionosphere can be considered as a spherical shell around the earth, roughly ranging from 100 to 1000 km above its surface. Due to solar radiation it contains free electrons and positive ions. The electron density increases up to a height of 300-400 km, after which it decreases again. For frequencies above 100 MHz the refractive index of the ionosphere can be approximated by

$$n_i = 1 - 40.3 \cdot \frac{N_e}{f^2} \tag{2.18}$$

where N_e is the free electron density in m^{-3} and f is the frequency in Hz. As a result the ionospheric range error is given by

$$\Delta r_i = -\frac{40.3}{f^2} \cdot \int_{\substack{geometric \\ path}} N_e(s)ds = -\frac{40.3}{f^2} \cdot TEC \tag{2.19}$$

where TEC is the Total Electron Content of the ionosphere corresponding to the total number of electrons per m^2 along the signal propagation path. The ionosphere increases the phase velocity of a signal and decreases its group velocity. Both effects are equal in magnitude, but opposite in sign. The TEC is usually smaller at high than at low and middle latitudes, although at high latitudes it tends to fluctuate more rapidly. Due to the difference in solar activity the ionospheric range error during the day is about 4 times as high as during the night. A typical daytime value is $50 \cdot 10^{16}$. Unfortunately the TEC also strongly depends on the geographical position and time of year.

The ionospheric range error at elevation E is related to $\Delta r_i(90°)$ by (compare with equations 2.14 and 2.15)

$$\Delta r_i(E) = \frac{\Delta r_i(90)}{\sin E'} \tag{2.20}$$

$$\cos E' = \frac{R_e}{R_e + H} \cdot \cos E \tag{2.21}$$

where R_e is the earth radius and H the height of the ionospheric layer above the earth's surface ($\approx$ 400 km).

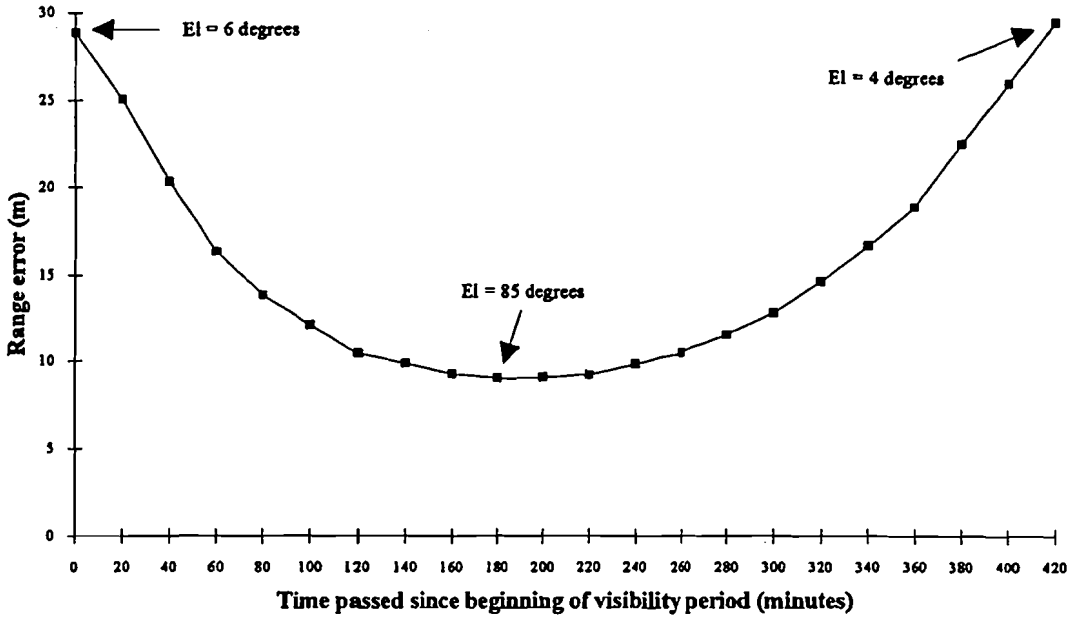

Figure 2.2 Ionospheric range error during a satellite pass

The ionospheric range error can be calculated for example for a pass of a GPS satellite. The result of such a calculation is shown in Figure 2.2. Based on the ground trace of the satellite (available from Global Satellite Software) the elevation angle of the satellite can be determined during the satellite pass. The TEC is assumed to have a constant value of $50 \cdot 10^{16}$. The obtained values apply to a receiver located at Blacksburg, VA, but the figure gives a general impression for the variation in range error which can occur during measurements.

If simultaneous range measurements at frequencies f_1 and f_2 are available, the ionospheric effect can be practically eliminated. The corrected range is given by

$$R = \frac{f_1^2}{f_1^2 - f_2^2} \cdot R_1 - \frac{f_2^2}{f_1^2 - f_2^2} \cdot R_2 \tag{2.22}$$

where R_1 and R_2 are the uncorrected ranges measured at frequencies f_1 and f_2 respectively.

When performing phase measurements at two frequencies the corrected phase at f_2 is given by

$$\phi_2' = \frac{f_1 f_2}{f_1^2 - f_2^2} \cdot \phi_1 - \frac{f_2^2}{f_1^2 - f_2^2} \cdot \phi_2 \tag{2.23}$$

As the ionospheric range error can easily be 10 meters, the use of a dual-frequency receiver is preferable to the use of its single-frequency counterpart, despite the possibility of accounting for ionospheric effects by using models. A drawback of dual frequency measurements is that the accuracy of the corrected range is worse than that of the measured ranges. For this reason f_1 and f_2 should not be chosen too close together.

Third order ionospheric effects are usually neglected, but for extreme TEC values they may be of the order of a few cm. In order to reduce the ionospheric effects to a sub-centimeter level it would be useful to have a third frequency available.

2.6 Geometrical influence on accuracy

The position error is determined by a combination of the user range error and the geometry of the selected satellites. According to Figure 2.3 the following vectors can be defined

$\mathbf{R}_u$ = unknown position vector of the user, originating from the earth's center
$\mathbf{R}_i$ = known position vector of the ith satellite, originating from the earth's center
$\mathbf{D}_i$ = vector from the user to the ith satellite
$1 \le i \le n$, $n \ge 4$

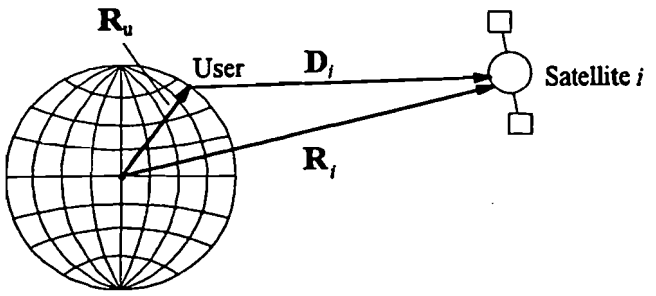

Figure 2.3 Definition of the vectors

By defining $\mathbf{e}_i$ as the unity vector from the user to the satellite i, the length of $\mathbf{D}_i$ is given by both

$$D_i = \mathbf{e}_i \cdot \mathbf{D}_i = \mathbf{e}_i \cdot \mathbf{R}_i - \mathbf{e}_i \cdot \mathbf{R}_u \qquad (2.24)$$

and

$$D_i = \rho_i - B_u - B_i \tag{2.25}$$

where ρ_i is the measured pseudo-range and B_u and B_i are the range equivalents of user and satellite clock offset respectively. Combining equations 2.24 and 2.25 gives

$$\mathbf{e}_i \cdot \mathbf{R}_u - B_u = \mathbf{e}_i \cdot \mathbf{R}_i - \rho_i + B_i \ , \ i = 1,2,...,n \tag{2.26}$$

Writing this equation in matrix form gives

$$\mathbf{G}_u \mathbf{X}_u = \mathbf{A}_u \mathbf{S} - \mathbf{r} \tag{2.27}$$

where

$$\mathbf{G}_u = \begin{bmatrix} e_{1x} & e_{1y} & e_{1z} & -1 \\ \vdots & \vdots & \vdots & \vdots \\ e_{nx} & e_{ny} & e_{nz} & -1 \end{bmatrix} \tag{2.28}$$

$$\mathbf{X}_u = \begin{bmatrix} x_u & y_u & z_u & B_u \end{bmatrix}^T \tag{2.29}$$

$$\mathbf{A}_u = \begin{bmatrix} (e_{1x}, e_{1y}, e_{1z}, 1) & \mathbf{0} & \cdots & \mathbf{0} \\ \mathbf{0} & (e_{2x}, e_{2y}, e_{2z}, 1) & & \\ \vdots & & & \\ \mathbf{0} & & & (e_{nx}, e_{ny}, e_{nz}, 1) \end{bmatrix} \tag{2.30}$$

$$\mathbf{S} = \begin{bmatrix} (x_1, y_1, z_1, B_1) & \cdots & (x_n, y_n, z_n, B_n) \end{bmatrix}^T \tag{2.31}$$

$$\mathbf{r} = \begin{bmatrix} \rho_1 & \cdots & \rho_n \end{bmatrix}^T \tag{2.32}$$

A least squares solution leading to an estimate of $\mathbf{X}_u$ is given by

$$\hat{\mathbf{X}}_u = [\mathbf{G}_u^T \mathbf{G}_u]^{-1} \cdot \mathbf{G}_u^T \cdot [\mathbf{A}_u \mathbf{S} - \mathbf{r}] \tag{2.33}$$

An initial estimate of the user position has to be made. Provided that $[\mathbf{G}_u^T \mathbf{G}_u]^{-1}$ exists, equation 2.33 then gives estimates of e_{ij}, which lead to a new position. After a few steps this iterative procedure leads to the user position. The covariance matrix of the error $\delta \mathbf{X}_u$ in $\hat{\mathbf{X}}_u$ is given by

$$\mathrm{cov}(\delta \mathbf{X}_u) = (\mathbf{G}_u^T \mathbf{G}_u)^{-1} \cdot \mathbf{G}_u^T \cdot \mathrm{cov}[\delta (\mathbf{A}_u \mathbf{S} - \mathbf{r})] \cdot [(\mathbf{G}_u^T \mathbf{G}_u)^{-1} \cdot \mathbf{G}_u^T]^T \tag{2.34}$$

Assuming that the range errors for each satellite are mutually independent with standard deviation σ_0 then equation 2.34 is reduced to

$$\mathrm{cov}(\delta \mathbf{X}_u) = \sigma_0^2 \cdot (\mathbf{G}_u^T \mathbf{G}_u)^{-1} = \sigma_0^2 \cdot \begin{bmatrix} \sigma_{xx}^2 & \sigma_{xy}^2 & \sigma_{xz}^2 & \sigma_{xt}^2 \\ \sigma_{yx}^2 & \sigma_{yy}^2 & \sigma_{yz}^2 & \sigma_{yt}^2 \\ \sigma_{zx}^2 & \sigma_{zy}^2 & \sigma_{zz}^2 & \sigma_{zt}^2 \\ \sigma_{tx}^2 & \sigma_{ty}^2 & \sigma_{tz}^2 & \sigma_{tt}^2 \end{bmatrix} \tag{2.35}$$

Independent of the coordinate system, the following figures of merit which reflect the geometry of the system can be defined

$$\mathrm{GDOP} = \text{Geometric Dilution Of Precision} = \sqrt{\mathrm{Trace}(\mathbf{G}_u^T \mathbf{G}_u)^{-1}} = \sqrt{\sigma_{xx}^2 + \sigma_{yy}^2 + \sigma_{zz}^2 + \sigma_{tt}^2} \tag{2.36}$$

$$\mathrm{PDOP} = \text{Position Dilution Of Precision} = \sqrt{\sigma_{xx}^2 + \sigma_{yy}^2 + \sigma_{zz}^2} \tag{2.37}$$

$$\mathrm{HDOP} = \text{Horizontal Dilution Of Precision} = \sqrt{\sigma_{xx}^2 + \sigma_{yy}^2} \tag{2.38}$$

$$\mathrm{VDOP} = \text{Vertical Dilution Of Precision} = \sigma_{zz} \tag{2.39}$$

$$\mathrm{TDOP} = \text{Time Dilution Of Precision} = \sigma_{tt} \tag{2.40}$$

So for example the horizontal position error is given by the product of HDOP and σ_0.

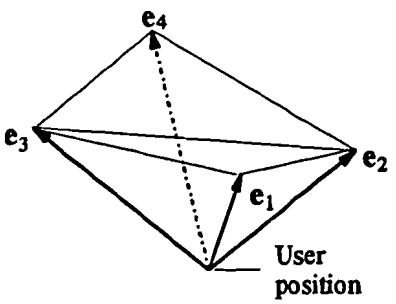

Figure 2.4 Definition of the tetrahedron

The four unity vectors together define a tetrahedron shown in Figure 2.4. Its volume is given by

$$V = \frac{1}{6} \cdot \begin{vmatrix} e_{2x} - e_{1x} & e_{2y} - e_{1y} & e_{2z} - e_{1z} \\ e_{3x} - e_{2x} & e_{3y} - e_{2y} & e_{3z} - e_{2z} \\ e_{4x} - e_{3x} & e_{4y} - e_{3y} & e_{4z} - e_{3z} \end{vmatrix} \tag{2.41}$$

Combining equation 2.28 for n=4 and equation 2.41 leads to

$$V = \frac{1}{6}\cdot|\mathbf{G}_u| \tag{2.42}$$

Without loss of generality a rectangular coordinate system with origin at the user's position can be defined, in which the x-coordinate coincides with the $\mathbf{e}_1$ direction and the xy plane contains $\mathbf{e}_2$. This gives

$$|\mathbf{G}_u| = \begin{vmatrix} 1 & 0 & 0 & -1 \\ e_{2x} & e_{2y} & 0 & -1 \\ e_{3x} & e_{3y} & e_{3z} & -1 \\ e_{4x} & e_{4y} & e_{4z} & -1 \end{vmatrix} \tag{2.43}$$

The GDOP can be written as a function of $|\mathbf{G}_u|$, so there is a high correlation between the volume of the tetrahedron and the GDOP. Maximizing the volume leads to (close to) minimum GDOP. It can be shown [Kihara, 1984] that an optimal GDOP of 1.5811 is achieved by

$$\mathbf{G}_u = \begin{bmatrix} 1 & 0 & 0 & -1 \\ -\frac{1}{3} & \frac{2\sqrt{2}}{3} & 0 & -1 \\ -\frac{1}{3} & -\frac{\sqrt{2}}{3} & \frac{\sqrt{6}}{3} & -1 \\ -\frac{1}{3} & -\frac{\sqrt{2}}{3} & -\frac{\sqrt{6}}{3} & -1 \end{bmatrix} \tag{2.44}$$

which means that all unity vectors have the same angle δ of 109.47° ($\cos\delta = -1/3$) to each other.

In practice there is an additional requirement that the elevation angle to a satellite needs to exceed a certain minimum. When more than four satellites fulfill this requirement the following selection method can be used [Kihara, 1984]

1. Select the first satellite at the largest elevation angle
2. Select the second satellite with an angle to the first satellite closest to 109.47°
3. Select the third satellite which maximizes the volume given by

$$V_{max} = \frac{1}{6}\cdot\left[\sqrt{2\cdot(1-e_{2x})\cdot(1+e_{3x})\cdot(1-e_{2x}e_{3x}-e_{2y}e_{3y})}+\left|e_{2y}e_{3z}\right|\right]\cdot(1-e_{3x}) \tag{2.45}$$

4. Select the fourth satellite which maximizes the volume of the tetrahedron given by equation 2.42. When more than one satellite leads to near maximum volumes choose the one which gives minimum GDOP.

Optimum geometry can only be established by calculating the GDOP for all possible combinations of satellites. The described method however gives near optimum results and it requires much less computing power.

Chapter 3 Existing satellite positioning systems

3.1 TRANSIT

3.1.1 Satellites and signal format

The position of a receiver can be calculated from the Doppler shift of the signals from satellites in known orbits. This was the basis of the development of the first satellite navigation system called TRANSIT, also known as NNSS (Navy Navigation Satellite System). It was developed for and by the US Navy, but was released for civil use in 1967. The system contains 5 satellites in (nearly) circular and polar orbits with an altitude over the earth's surface of 1075 km. The orbit period is about 107 minutes. The coverage of the system is not time-continuous and the average waiting time increases with decreasing latitudes.

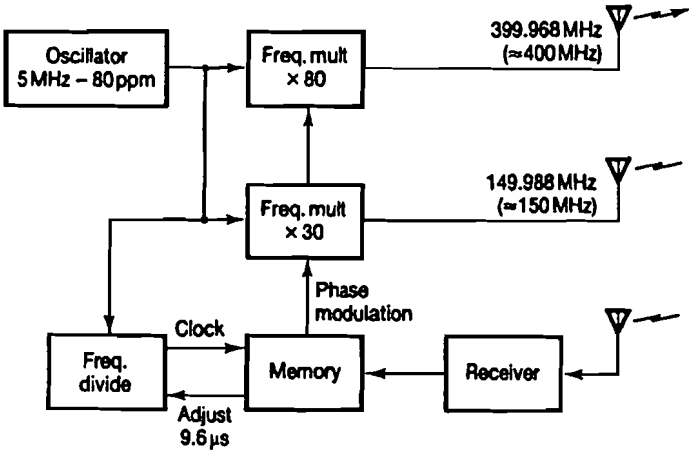

Figure 3.1 Block diagram of a TRANSIT satellite [Stansell, 1978]

A simple block diagram of a TRANSIT satellite is shown in Figure 3.1. The satellite transmits at two frequencies, 149.988 MHz and 399.968 MHz. Orbital parameters are computed at the control station and received by the satellite. This data is phase modulated on to the carrier wave. A complete message takes precisely 2 minutes and consists of 26 rows with 39-bit words in 6 columns plus a 19-bit final word, giving a total data rate of 6103 bits per 2 minutes. Only every sixth word is available to a civil user. The messages both give an update on the satellite's position and synchronize the receiver. The phase modulation, shown in Figure 3.2, is organized in such a way that the data transmission does not influence the position determination [Van Willigen, 1993].

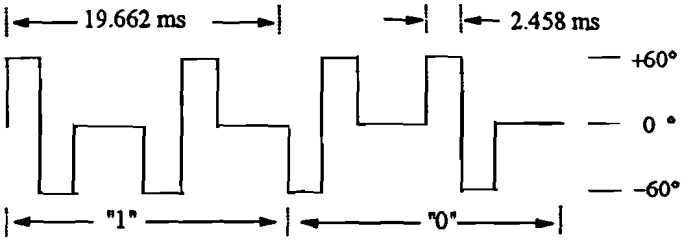

Figure 3.2 Phase modulation of the signal

3.1.2 Position measurement

The receiver usually has stable frequency references, f_g, at 150 and 400 MHz. Because the satellite transmits at 149.988 and 399.968 MHz and the Doppler shift is in the interval ± 8 kHz, the frequency of the received signal, f_r, is always lower than f_g. The frequency difference between the received signal and the local reference varies during a satellite pass as shown in Figure 3.3. The Doppler shift is zero at the time of the Closest Point of Approach. The slope of the Doppler curve increases with increasing elevation.

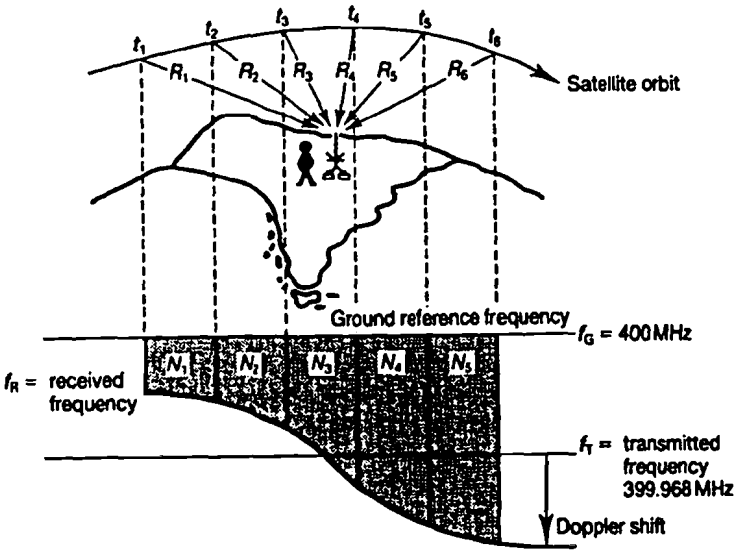

Figure 3.3 Principle of Doppler count [Stansell, 1978]

The receiver counts the number of periods of the difference frequency between 2 time marks, signaled by the satellite. As the time marks are received at $t_1 + \Delta t_1$ and $t_2 + \Delta t_2$, the content of the counter, called the Doppler count, is given by

$$N_1 = \int_{t_1+\Delta t_1}^{t_2+\Delta t_2} (f_g - f_r)dt \tag{3.1}$$

The received frequency is given by

$$f_r = f_t \cdot (1+v_r/c) \tag{3.2}$$

where v_r is the velocity component of the satellite towards the receiver. The distance change is given by

$$\Delta R = R_1 - R_2 = c \cdot (\Delta t_1 - \Delta t_2) = \int_{t_1+\Delta t_1}^{t_2+\Delta t_2} v_r dt \tag{3.3}$$

This gives

$$N_1 = (f_g - f_t) \cdot (t_2 - t_1) + \frac{f_g}{c} \cdot (R_2 - R_1) \tag{3.4}$$

or more generally

$$N_i = (f_g - f_t) \cdot (t_{i+1} - t_i) + \frac{f_g}{c} \cdot (R_{i+1} - R_i) \tag{3.5}$$

This leads to the basic observation equation of Doppler positioning

$$\begin{aligned} N_i = \frac{f_g}{c} \cdot [\{(X_{i+1} - X_u)^2 + (Y_{i+1} - Y_u)^2 + (Z_{i+1} - Z_u)^2\}^{\frac{1}{2}} - \\ \{(X_i - X_u)^2 + (Y_i - Y_u)^2 + (Z_i - Z_u)^2\}^{\frac{1}{2}}] + (f_g - f_t) \cdot (t_{i+1} - t_i) \end{aligned} \tag{3.6}$$

So the distance difference can be determined from the Doppler count and it is measured in the same way as in a terrestrial hyperbolic system. However instead of using several transmitting stations at fixed points, we have one transmitter moving from one point to the other. By measuring a number of Doppler counts during a satellite pass, the receiver's position is found at the intersection point of the hyperbolas. The usable satellite pass lasts for about 10-18 minutes. Because of slight frequency drift, f_g - f_t is usually treated as an additional unknown.

In practice, the position calculation is based on the assumption that the receiver is at a certain position. The Doppler count at this assumed position is computed and compared to the real count. Iteration is used to make the assumed and the measured results coincide.

3.1.3 Accuracy and performance

During a Doppler count the receiver either has to be stationary or has to know its speed and course, usually available from another system like Loran-C. Using an incorrect velocity in the E-W direction shifts the whole Doppler curve upwards or downwards and mainly results in an error in latitude. A velocity error in the N-S direction will mainly result in an error in longitude.

Up till now it has been assumed that the height of the receiver is known. An error in the estimated (antenna)height results mainly in a longitude error, which increases as the longitude separation between the receiver and the orbit projection decreases. Using more than one satellite pass makes it possible to determine the height above the reference geoid as well. In general the position accuracy can be improved by utilizing a larger number of satellite passes and averaging the results.

Simultaneous reception of two frequencies allows for correction of the ionospheric effect, not of the tropospheric effect however. Obviously orbital errors will lead to errors in position. Only passes with elevation angles between 15° and 70° should be used.

The predictable accuracy (2σ) for dual and single frequency operation is specified to be 25 and 500 m respectively. The specified values for the repeatable accuracy are lower, 15 and 50 m respectively [FRP 1992]. The accuracy can be highly improved by making use of a second TRANSIT receiver at an exactly known location, because of a strong correlation in the position errors. This method is called translocation or differential positioning.

Major disadvantages of TRANSIT include

1. Long time to fix, therefore not suitable for aircraft or other highly dynamic users.
2. Insufficient knowledge of course and speed of receiver will result in severe position errors.
3. Discontinuous system.
4. System operation by the DOD will be discontinued in 1996 [FRP 1992].
5. As the receiver can only operate on one signal at the time, problems occur when more than one satellite is visible.

3.2 Navstar GPS - System overview

The Navstar Global Positioning System (GPS) is the result of a combined effort of the US armed forces to develop a highly accurate space-based navigation system [Milliken, 1978]. GPS comprises a space, control and user segment, which are described in more detail in Chapter 4.

The GPS satellites transmit L-band signals modulated by one or two PN codes and a navigation message, which contains the time of transmission and the position of the satellite at that time. A GPS receiver generally consists of an L-band antenna, tracking loops, a data processor and a control display unit, as shown in Figure 3.4. By generating replicas of the PN codes and shifting them in time, the receiver can determine the pseudo-ranges from each satellite. The basic navigation equations can be written as

$$[(X-X_i)^2+(Y-Y_i)^2+(Z-Z_i)^2]^{1/2} + CB = PR_i \ , \ i=1,2,3,4 \qquad (3.7)$$

where X, Y, Z and X_i, Y_i, Z_i are the user and satellite position coordinates respectively, PR_i is the measured pseudo-range and CB is the range equivalent of the clock bias introduced by the GPS receiver. Delta range values (i.e. the changes in time of the measured pseudo-ranges), which yield the user's velocity, are determined by measuring the Doppler shift on the carrier wave.

In practice the user's position and velocity are determined by means of a Kalman filter implemented in the data processor. When switched on, a receiver either utilizes the last determined user position available in its memory or a position estimate manually put in by the user. The computed pseudo-range and delta-range values based on this initial estimate are then compared with the measured values and adjusted to give the current position and velocity.

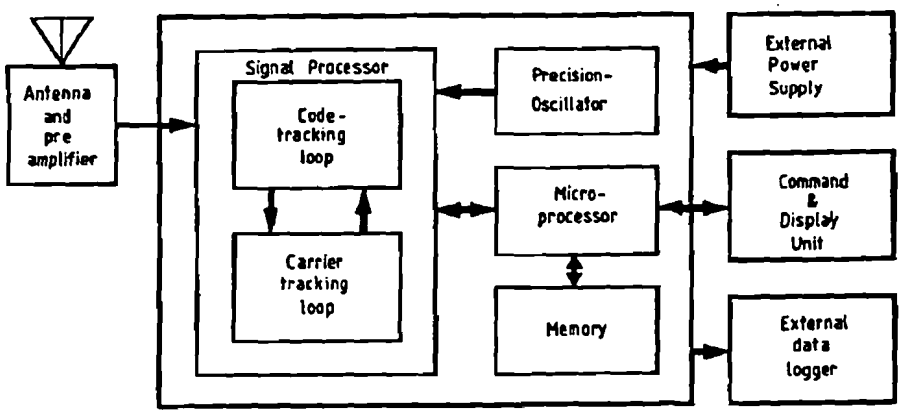

Figure 3.4 Block diagram of a GPS receiver

3.3 GLONASS

3.3.1 System configuration

GLONASS (Global Navigation Satellite System) can be considered as the CIS version of GPS. Like GPS the system consists of three components: the satellite subsystem, the monitoring and control subsystem and the user terminals.

GLONASS satellites are launched three at a time by Proton launchers into circular orbits with a height of 19,100 m and an inclination of 64.8°. The orbital period is 11 h 15 min 44 sec. The final constellation, which will not be achieved before 1996, will consist of 24 satellites in three orbital planes, separated in RAAN (Right Ascension of the Ascending Node) by 120°. Within the planes the satellites are separated by 45° The satellites in the second and third plane have a displacement of +30° and -30° respectively with reference to the first plane. As a result all satellites will pass through a position with a given subsatellite point within an 8-day period. Planes 1 and 3 will be filled first before launching any satellites into plane 2. According to the most recent information [Daly, 1993] the current status is 8 satellites in plane 1 and 6 satellites in plane 3. The estimated satellite life is 3.14 years [Kazantsev, 1992].

The monitoring and control subsystem consists of one ground control center, central synchronizer and navigation signal phase control center (all in Moscow), 4 TT&C stations, 5 "quantum optical" stations and navigation field control equipment at 3 locations [Kazantsev, 1992]. The subsystem runs three independent processes: calculation of ephemerides and almanacs, calculation of frequency-time corrections and navigation field monitoring.

Up till now the development of civil user equipment has lead to integrated GPS/GLONASS receivers rather than stand alone GLONASS receivers. 3S Navigation has produced a 12 channel integrated receiver capable of simultaneously tracking up to 12 GLONASS satellites, up to 7 GPS satellites or a combination of both. Position errors have shown to be considerably lower than the errors which result from the use of GPS alone. [Beser, 1993].

3.3.2 Signal structure

GLONASS uses two carrier frequencies in L-band, modulated by spread-spectrum codes and a data sequence. FDMA is applied instead of CDMA, so each satellite sends the same code but at a different

carrier frequency. Satellites are distinguished by channel number i and the L_1 and L_2 frequencies are given by

$$L_1 = 1602 + i \cdot 05625\,, \quad i = 1,2,\ldots,24$$
$$L_2 = 7/9 \cdot L_1 \tag{3.8}$$

The signals transmitted by the satellites are right-hand circularly polarized. A low-precision (C/A) code is transmitted at L_1 and a high-precision (P) code is transmitted at both frequencies. The code rates are 0.511 and 5.11 Mbps respectively. The C/A-code, generated by a 9-stage shift register, has a length of 511 bits, resulting in a period of 1 ms. Although the P-code is probably generated by a 25-stage shift-register this code has a period of only one second. [Forssell, 1991] Compared to CDMA the FDMA scheme reduces the crosstalk between signals from different satellites [Ivanov, 1992]. As the P-code requires a bandwidth of about 10 MHz the total frequency spectrum will range from 1597-1620.5 MHz.

Potential interference problems have arisen since WARC '92 where frequency bands of 1610-1626.5 MHz and 1610.6-1613.8 MHz were allocated to LEO communication satellites and radio-astronomy respectively. As radio-astronomy has a protected status it was decided to shift the GLONASS channels with center frequencies in the radio-astronomy band to lower channels by allowing antipodal satellites to employ the same transmit frequencies [Daly, 1993].

The GLONASS data message consists of two blocks, one containing both clock corrections and ephemeris, the other containing the almanacs. Ephemerides are transmitted as a set of ECEF position and velocity coordinates (x,y,z) at a given reference time, whereas almanacs are transmitted as Kepler elements. The navigation message is modulo-2 added to both codes at 50 bps. The information is structured into superframes of 2.5 minutes, consisting of 5 frames with fifteen lines of 2 s each. Ephemerides and almanacs are normally updated every day.

3.3.3 Comparison with GPS

The main differences between GPS and GLONASS are listed in Table 3.1. The main problems for dual mode operation are the use of two different time frames and geodetic coordinate systems. The respective solutions are to include a fifth satellite in the navigation solution and to clearly define the relationship between the two coordinate systems. Because of the applied FDMA a receiver needs a frequency synthesizer to generate the LO frequencies for each carrier frequency. Frequency and code synthesis are realizable at IF by means of DSP.

Table 3.1 Comparison of GLONASS and GPS system parameters

Parameter	GLONASS	GPS
Multiple access	FDMA	CDMA
Number of orbit planes	3	6
Orbit inclination	64.8°	55°
Orbit altitude	19,100 km	20,200 km
Orbital period	11 h 15 min 44 sec	11 h 58 min
Ephemeris presentation	ECEF position, velocity and acceleration	Kepler elements of orbits
Geodetic coordinate system	SGS-90	WGS-84
Time synchronization	UTC (SU)	UTC (USNO)
Almanac content	120 bit	152 bit
Time to transmit complete almanac	2.5 min	12.5 min
Frequency spectrum	1241 - 1261.5 MHz	1217.37 - 1237.83 MHz
	1597 - 1620.5 MHz	1565.19 - 1585.65 MHz
Type of C/A code	Maximum length	Gold code
C/A-code frequency	0.511 MHz	1.023 MHz
Crosstalk in two adjacent levels	- 48 dB	- 21.6 dB
Synchronization period	2 s	6 s
Selective Availability	No	Yes

3.4 NAVSAT

3.4.1 System configuration

The NAVSAT system was developed by the European Space Agency as an attempt to come up with a civil alternative to GPS and GLONASS. Although the system never left the design stage it was the first step towards a civil global navigation satellite system.

The space segment, shown in Figure 3.5 consists of 12 HEO (highly elliptical orbit) and 6 GEO satellites. The HEO satellites are spread over six orbital planes (three planes for each hemisphere) with an inclination of 63.45°. The GEO satellites are equally spaced around the equator. All the satellites were supposed to be communication satellites with a C/L-band transponder for relaying the navigation signals.

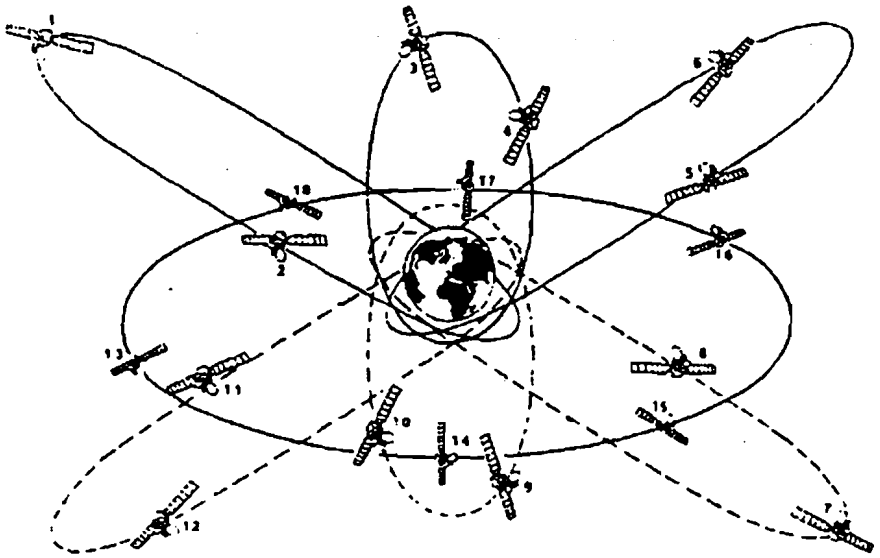

Figure 3.5 NAVSAT satellite constellation

The control segment consists of one master control station and six ground stations. All communications between the different stations can take place through one or more of the GEO's. The control segment is responsible for the navigation signal uploading, time synchronization, ionospheric delay correction, satellite health status control and ephemeris determination and prediction. The ground stations compute the range and range rate to the satellites. By applying timing and Doppler-offset arrangements all L-band navigation signals leave the satellites at NAVSAT system time and frequency.

3.4.2 Signal structure

NAVSAT uses a TDMA format. Antipodal satellites can share time slots so one frame only has to contain nine bursts. The bursts last for 230 ms and are separated by guard bands of 120 ms. This leads to a frame duration of 3.15 s. The navigation signal contains a high power carrier wave component for Doppler measurements, a PN code for range measurements and a data stream containing the navigation message. After a proposal by INMARSAT the PN code (same for each satellite) was chosen to have a 1.023 MHz chiprate and 1 ms duration to allow for interoperability with GPS [Diederich, 1989].

3.4.3 Performance

The user range error (1σ) has been specified as 5 m [Rosetti, 1986], but this seems rather optimistic. The Global Satellite Software package can be used to calculate the Position Dilution Of Precision values. We have created a grid of points on the earth surface to cover the Continental United States and Europe and a 7 degrees elevation mask has been chosen. The resulting values are comparable to the GPS case. Main difference is the occurrence of large peaks (PDOP > 6) for certain geographic locations. For a large number of locations however the variation of the PDOP with time is smaller than in the GPS case.

Major advantages of NAVSAT are that there is no need for dedicated satellites and that it is possible to start with a reduced constellation to cover a selected geographic area. Except for some CIS satellites the required HEO satellites are not available yet.

3.5 The Starfix system

3.5.1 System configuration

Starfix is a privately owned location system, not a navigation system, used primarily in the Gulf of Mexico by oil companies since 1986. In a personal communication to the author, Starfix Vice-President Prewitt announced that the system is still operational but only for a short time to come. Major components of the system are: a constellation of at least three satellites, uplink facilities, a tracking network (remote sites), a master site and passive users. Starfix makes use of transponders on geostationary communication satellites, specifically Galaxy II (286° E), Westar IV (261° E, not in orbit anymore), Spacenet I (240° E) and Satcom FIR (221° E, not in orbit anymore). All the timing is accomplished on the ground and a precisely timed signal is transmitted simultaneously to all satellites. The only timing requirement on the satellite is that the delay introduced by the transponder has to be reasonably constant.

Starfix receivers use four horn antennas pointed at the satellites. A receiver is calibrated at dockside by comparing the surveyed coordinates with the measured coordinates. The basic equation to be solved is

$$(R_u + dt) - R_d = \left[(X_u - X_s)^2 + (Y_u - Y_s)^2 + (Z_u - Z_s)^2\right]^{1/2} - \left[(X_d - X_s)^2 + (Y_d - Y_s)^2 + (Z_d - Z_s)^2\right]^{1/2} \quad (3.9)$$

R_u and R_d are the range measurements at the user and remote site respectively, X_s, Y_s, Z_s and X_d, Y_d, Z_d the known space coordinates of the satellite and remote site respectively. Unknown are X_u, Y_u, Z_u, the space coordinates of the user, and dt, the clock offset error. Because of the limited geometry of three or more geostationary satellites the geodetic height of the user has to be known, which gives an extra equation. Together with the basic equations resulting from measurements to three satellites the user position can be determined.

The positions of the satellites are determined at the master site. The remote sites send their range measurements twice per second and satellite positions are determined by solving

$$(R_r + dt) - R_m = \left[(X_r - X_s)^2 + (Y_r - Y_s)^2 + (Z_r - Z_s)^2\right]^{1/2} - \left[(X_m - X_s)^2 + (Y_m - Y_s)^2 + (Z_m - Z_s)^2\right]^{1/2} \quad (3.10)$$

The unknown variables are the space coordinates of the satellites and the clock offset of each remote site. At least five remote sites are needed, a larger number (13) is used to increase the confidence in the solution. The positions and velocities of the satellites are determined by using a Kalman filter and this information is uplinked every 180 s.

3.5.2 Signal structure

Starfix uses direct sequence spread spectrum modulation The PN code has a length of 16384 bits and the data rate is 150 bits/sec. This gives a chip rate of 2.4576 MHz and an occupied bandwidth of about 5 MHz. The processing gain in the receiver is 41 dB. The ambiguity is 2000 km (based on 150 bps). Up and down link frequencies are about 6 and 4 GHz respectively.

The navigation message consists of

1. Time-tagged range measurement from each remote site
2. Health status of each remote site
3. Time tagged satellite positions
4. Health status of each satellite
5. Base of time measurements
6. User messages

3.5.3 Accuracy and performance

The horizontal accuracy (2 drms) of Starfix is stated to be 5 m [Ott 1988]. Starfix has a number of limitations. Most important one is that a very accurate height input is needed, which is only available at sea level. The system does not work in polar regions and near the equator. Main advantage is the use of available transponder bandwidth instead of dedicated satellites. Adding a number of inclined orbit satellites could change the system into a true navigation system.

Chapter 4 The Global Positioning System

4.1 The space segment

The GPS satellites are in near circular orbits at an altitude of about 20200 km resulting in an orbital period of 12 sidereal hours. There are 6 orbital planes equally spaced around the equator. The final constellation consists of 4 satellites in each plane, resulting in a total of 24 satellites. The satellite orbit has to be corrected once a year, causing a three days' period of unavailability of a satellite during the corrections. Any user on earth is supposed to have at least five satellites in view above 5° elevation with a Position Dilution Of Precision (PDOP) of six or less [FRP 1992].

Between 1978 and 1985 11 Block I satellites were built of which 10 were successfully launched into orbit Three satellites are currently mission capable. The orbits of these prototype satellites, mainly developed for testing, have an inclination angle of 63°. Since 1989 23 Block II/IIA satellites have been launched into orbit, all of them are currently mission capable. The original intent was to use the Space Shuttle for launching and therefore an inclination angle of 55° was selected, even though this is not the optimum angle for coverage. The Challenger disaster however caused a change of plan and a delay in launch schedule. It was decided to use Delta II launch vehicles instead.

The Block II satellites have an on orbit weight of 845 kg and a design lifetime of 7.5 years [Wells, 1986]. They deploy 12 helix array antennas, with a maximum gain of 15 dB, which radiate right-hand circularly polarized waves. The orientation of the satellites is such that the antennas will always point to the earth. This is established by means of a gravity gradient boom. A few days per year the satellites are periodically eclipsed by the earth during a fraction of one orbital period. The satellites are controlled by particularly jam resistant S-band signals at 1783.74 MHz uplink and 2227.5 MHz downlink [Ananda, 1988]. The satellites are designed to function without any ground contact for a period of 180 days with gradually decreasing accuracy.

After 1996 twenty replenishment (Block IIR) satellites will be launched. These will all have crosslink ranging capabilities, which will result in a 180 day autonomous performance without degraded accuracy. Production of the follow-on (Block IIF) satellites will not start until 1999 [Wiedemer, 1993].

4.2 The control segment

The Control Segment (CS) is operated by the US Air Force Space Command and performs the following functions

- tracking the GPS satellites
- providing the GPS satellites with ephemeris and clock parameter corrections
- monitoring and maintaining the status, health and configuration of the satellites.

The CS consists of three parts: one Master Control Station (MCS), 5 monitor stations and 4 uplink ground antennas, all shown in Figure 4.1. All the downlink data-processing and the computation of the periodical updates to be sent to the satellites takes place at the MCS. It is responsible for the control and management of both the operational satellites and the other CS elements.

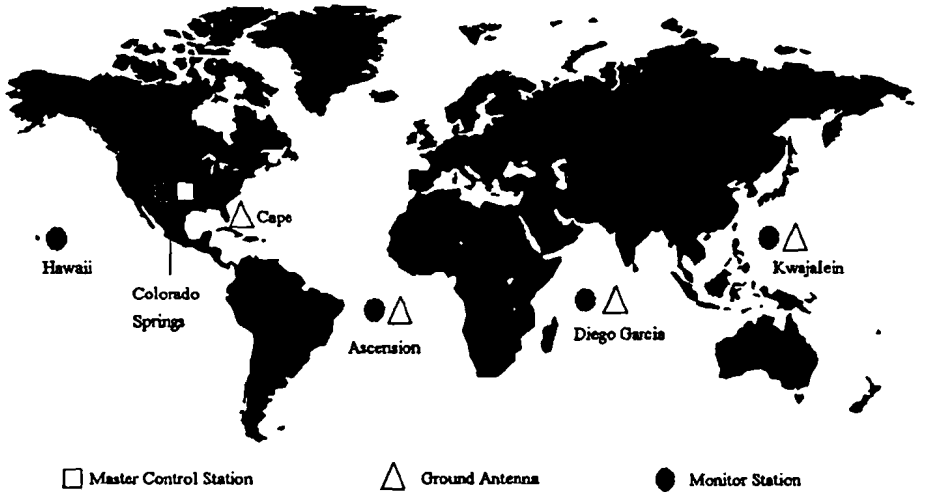

Figure 4.1 The GPS control segment

The monitor stations are globally dispersed in longitude to provide maximum constellation coverage. Their task is to track the satellites, to measure the apparent pseudo-ranges and to collect navigation messages in order to estimate trajectory and clock calibration for each satellite and to monitor the navigation service provided to the user. The positions of the monitor stations are very well known and they are equipped with extremely accurate receivers, controlled by Cesium clocks, and antennas with a 14 dB multipath rejection ratio for elevation angles greater than 15 degrees. Satellite positions can be determined within 1 meter and clock drift in the satellites can be surveyed. Corrections for tropospheric delay can be approximated based on data from meteorological sensors.

Like the monitor stations the ground antennas are unmanned. Control signals and updates of the navigation messages are transmitted to the satellites at S-band. The satellites receive these updates and a prediction of their orbits three times a day. The predictions enable the satellites to continue the navigational service to the user community even in case of CS malfunctioning.

4.3 Signal structure

4.3.1 Design considerations

In the design phase of GPS there were several key performance objectives which distinguished GPS from then existing satellite and land based radionavigation systems. Some of them were [Spilker, 1978]

- high accuracy 10-30 meter rms position error
- real-time navigation for users with high dynamics
- world-wide operation
- tolerant to nonintentional or intentional interference
- no need for extremely accurate receiver clock
- short time to fix

The GPS signal had to be a RF representation of the satellite clock and in addition the signal had to carry data indicating satellite position and clock error parameters. The following requirements formed the basis of design [Spilker, 1978]

- allow accurate real-time pseudo-range measurements ($\sigma_\tau < 10$ ns) without ambiguity
- allow accurate Doppler shift measurements (< 0.1 Hz)
- provide dual frequency signals to enable ionospheric group delay measurements (>20% frequency separation)
- provide an efficient data channel
- provide a rapid acquisition navigation capability with good accuracy along with a high accuracy capability for more demanding users
- good multiple access properties
- good interference rejection properties
- ability to reject or greatly reduce multipath interference problems where the differential multipath delay is 200 ns or greater

GPS frequencies were chosen in L-band in favor of VHF-band because of the large bandwidth demand and the smaller effect of (uncorrected) ionospheric delay. C-band was not chosen because of the larger space losses. GPS uses two carrier frequencies which are coherently generated from the 10.23 MHz clock (purposely set slightly lower to correct relativistic effects)

$$L_1 = 154 \cdot 10.23 = 1575.42 \text{ MHz}$$
$$L_2 = 120 \cdot 10.23 = 1227.6 \text{ MHz} \tag{4.1}$$

The frequency separation is 28.3 % relative to L_2, sufficient to permit measurement of ionospheric group delay. Clock stability is obtained by using two Cesium and two Rubidium frequency standards. The control segment can adjust the satellite clocks in order to keep the time frames of the different satellites within 1 ms of GPS time. Remaining clock errors are transmitted as part of the navigation message.

4.3.2 The use of codes

GPS makes use of two pseudo-random noise (PN) codes which are modulated on the carrier frequencies.

C/A-code

The C/A-code (Coarse Acquisition Code) is a relatively short code of 1023 bits at a 1.023 Mbps chiprate, resulting in a 1 ms period. The C/A-codes are Gold codes, formed as the product of two 1023 bit PN codes $G_1(t)$ and $G_2(t)$, represented as

$$C_i(t) = G_1(t) \cdot G_2(t + 10iT_c) \tag{4.2}$$

where i is the satellite number which determines the phase offset between G_1 and G_2. This results in a different C/A-code for each satellite. As the cross-correlation between the Gold codes is very low, they are well suited for the intended multiple access purposes. G_1 and G_2 are generated by 10-stage maximum length linear shift registers which are both reset at X_1 epoch (i.e. every 1.5 s). The generator polynomials are given by [Spilker, 1978]

$$G_1(X) = 1 + X^3 + X^{10}$$
$$G_2(X) = 1 + X^2 + X^3 + X^6 + X^8 + X^9 + X^{10} \tag{4.3}$$

The various delay offsets are generated by making use of the cycle-and-add property of PN codes. This means that by tapping of on different points of the G_2 register and modulo-2 adding the two sequences, a delayed version of the G_2 sequence is created. The block diagram of the C/A-code generator is shown in Figure 4.2.

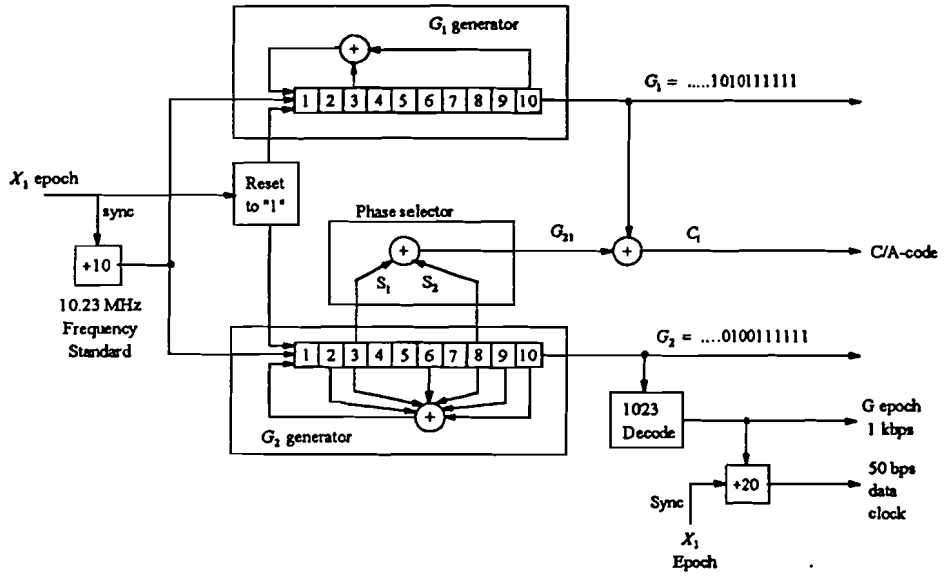

Figure 4.2 C/A-code generator

As the period of the C/A-code is only 1 msec, there will be a range ambiguity of 300 km. This ambiguity is normally resolved by the initial estimate of the user position.

P-code

The P-code (Precision Code) for each satellite i is the product of two PN codes, $X_1(t)$ and $X_2(t+iT_c)$. Both X_1 and X_2 are clocked in phase at chip rate $1/T_c$ = 10.23 MHz. X_1 has a period of 1.5 s or 15,345,000 chips, whereas the period of X_2 is 37 chips longer. Each satellite has a unique code offset iT_c, where $0 \le i \le 36$. Because of the different code lengths of X_1 and X_2 the P-code would have a period of 266.4 days. Each satellite however has been assigned a certain part of the code of one week's length in such a way that there is no overlap between the different parts. To assure this 7 days' period both X_1 and X_2 are reset each Sunday at 00:00h. Due to the long period of the P-code the measured pseudo-ranges are unambiguous.

The Z-count is defined as the number of X_1 periods since the beginning of the week and is reset at the same time as X_1 and X_2. By means of the Hand-Over-Word (HOW) at the beginning of each subframe

the Z-count is transmitted to the user. This enables the receiver to acquire the P-code at the beginning of the next subframe. It is important to notice that tracking the P-code without using the C/A-code would take a very long time. When the C/A-code has been tracked however, the combined knowledge of C/A-code epoch, data subframe epoch and HOW gives exact phasing of the P-code.

In the Block-II satellites the P-code can be encrypted. This mode of operation is called anti-spoofing, which means that the system is protected against the deliberate transmission of incorrect information. Only users authorized by the US Department of Defense have access to the code keys needed by the receiver to decrypt the information. The encrypted P-code is called the Y-code [Nieuwejaar, 1988].

Assuming that a receiver can measure arrival times with an accuracy of 0.01 T_c, the obtainable resolutions of the C/A- and P-code will be 3 and 0.3 meter respectively.

4.3.3 The navigation message

The navigation message is the information supplied from a GPS satellite to users. It is superimposed on both the P-code and the C/A-code by modulo-2 addition at a rate of 50 bps. Combined with the measured pseudo-ranges this information enables the receiver to do the navigational calculations. The message is formatted into a frame of 1500 bits, which takes 30 s to transmit. Each frame has five 300-bit subframes, which in turn are subdivided into ten 30-bit words.

Each subframe starts with a Telemetry Word (TLM) which contains information about the state of the satellite and of the message itself and a Handover Word (HOW). The HOW contains the subframe identification and a number which, when multiplied by 4, gives the Z-count at the beginning of the next subframe. Subframe 1 contains clock correction parameters, the age of the transmitted data and various flags (Datablock I). Subframes 2 and 3 contain the ephemeris information of the transmitting satellite (Datablock II). Subframes 1 to 3 are repeated every 30 s.

Subframe 5 contains one page of a series of 25 pages, which together contain the almanac data for 24 satellites (pages 1 through 24) and the health status for these satellites (page 25). It thus takes 12.5 minutes before this information (Datablock III) is completely received. The almanac data is a reduced-precision subset of the clock and ephemeris parameters, which helps the receiver in the acquisition of the other satellite signals once the first satellite has been tracked. Subframe 4 amongst other things contains ionospheric parameters and is organized into 25 pages as well. A more detailed description of the subframes can be found in Appendix 1 [Van Dierendonck, 1978].

4.3.4 The transmitted signal

A 90° phase shifted version (quadrature component) of the L_1 carrier is modulated by the C/A-code. Both the in phase component of the L_1 carrier and the L_2 carrier are modulated by the P-code. As a result the following signals are transmitted by the satellite

$$S_{L_1}(t) = A_P P_i(t) D_i(t) \cos(\omega_1 t + \phi_i) + A_C C_i(t) D_i(t) \sin(\omega_1 t + \phi_i)$$
$$S_{L_2}(t) = B_P P_i(t) D_i(t) \cos(\omega_2 t + \phi_i) \tag{4.4}$$

where

ω_1, ω_2 = angular frequency of L_1, L_2 carrier waves
ϕ = phase noise and oscillator drift
A_c, A_p and B_p = signal amplitudes ($A_c = A_p\sqrt{2}$)

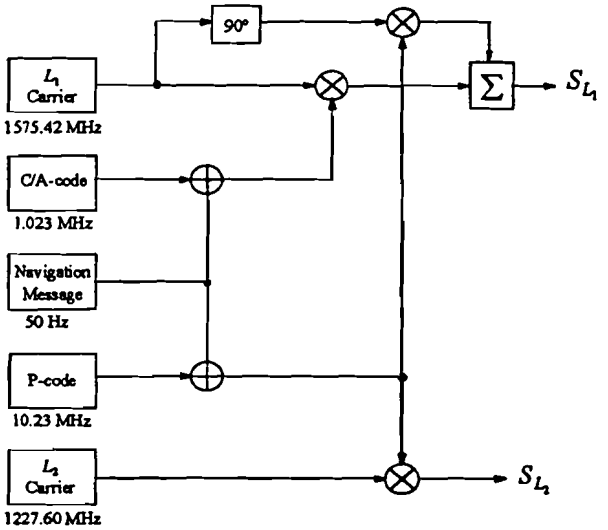

Figure 4.3 GPS signal modulation

GPS makes use of direct sequence spread spectrum techniques because of the following reasons

- shared use of allocated frequency spectrum by a number of transmitters
- PN codes can be used for real-time positioning
- insensitive to interference
- possibility of limited access to authorized users only

As a result the bandwidths are 2.046 and 20.46 MHz for the C/A-code and P-code respectively.

4.4 Link budget

The link budget for GPS is given in Table 4.1. The process gain is given by [Dixon, 1984]

$$\text{Process gain} = \frac{\text{RF bandwidth}}{\text{information bit rate}} \tag{4.5}$$

Usually the compression process is not 100 % efficient, so gain is typically 1 dB less than this value. The receiver antenna is omnidirectional with a minimum gain of 0 dB.

Table 4.1 GPS link budget

Carrier	L_1		L_2
Code	**C/A-code**	**P-code**	**P-code**
$EIRP_s$ (dBW)	26.8	23.8	19.7
Space and atmospheric loss (dB)	- 186.8	- 186.8	- 185.7
P_r (dBW)	- 160	- 163	- 166
N (dBW)	- 141.2	- 131.2	- 131.2
C/N (dB)	- 18.8	- 31.8	- 31.8
Process gain (dB)	46.1	56.1	56.1
S/N (dB)	27.3	24.3	21.3

4.5 GPS receivers

4.5.1 Introduction

Bandwidth reduction can be achieved in two different ways. When the transmitted PN codes are known, duplicates are generated in the receiver and bandwidth is reduced by using the correlation properties of the codes. This sort of receiver is called a code-correlation receiver.

The satellite signals can also be used without any knowledge of the codes. Code-free receivers were developed in the light of Selective Availability. Bandwidth reduction is achieved either by deploying a squaring channel or a code phase channel. In both channels the incoming signal is first translated to an IF signal. In a squaring channel this signal is squared to obtain the carrier wave, which then can be used for phase measurements. In a code phase channel the IF signal is multiplied by a delayed version of itself, with a delay equal to half the chip period (487 and 49 ns for C/A- and P-code respectively). The resulting signal has a code frequency component. By passing the signal through a BPF at center frequency $1/T_c$ a clock signal at the code frequency is obtained. This clock signal can then be used for phase measurements.

In both cases the navigation message is not retrieved, so the receiver needs an external almanac. Real-time positioning is not possible and therefore the use of code-free receivers is limited to geodetic applications. A more detailed description of this class of receivers can be found in [Wells, 1986]; the rest of this section will focus on code-correlation receivers.

4.5.2 The code-correlation receiver

Suppose a user has N satellites in view, all transmitting at frequency L_1. The received signal will then be given by

$$s(t) = \sum_{i=1}^{N} \begin{bmatrix} A'_{P_i} \cdot P_i(t-\tau_i) \cdot D_i(t) \cdot \cos\{(\omega_1 + \omega_{d_i})t - \varphi_i(l_i) + \phi_i\} + \\ A'_{C_i} \cdot C_i(t-\tau_i) \cdot D_i(t) \cdot \sin\{(\omega_1 + \omega_{d_i})t - \varphi_i(l_i) + \phi_i\} \end{bmatrix} \quad (4.6)$$

where

ω_d = angular frequency of Doppler shift on L_1
τ_i = propagation delay
$\varphi(l)$ = phase shift due to path length l

To enable measurements to a certain satellite m, a duplicate of the specific C/A-code is generated and multiplied with the received signal. After correlation the signal from satellite m is given by

$$s(t) = A'_{C_m} \cdot R(\tau_m - \tau) \cdot D_m(t) \cdot \sin\{(\omega_1 + \omega_{d_m})t - \varphi_m(l_m) + \phi_m\} + n(t) \quad (4.7)$$

where R is the autocorrelation function and $n(t)$ is the total noise caused by finite cross-correlation values.

To account for the propagation delay between satellite and receiver the duplicate code is shifted in time until maximum autocorrelation is achieved. The time-shift needed is a direct measure for the pseudo-range to the satellite. This shift has to be adapted continuously as the range is changing with time. This process is known as code tracking.

To enable the electronic implementation of the tracking process, the frequency of the signal given by equation 4.6 has to be converted to the IF range first. This is done by multiplying it with a signal from a local oscillator and passing it through a BPF. The LO-frequency has to conform to

$$\omega_{LO} = \omega_1 + \omega_{d_m} + \omega_{IF} \tag{4.8}$$

As the Doppler-shift ω_{d_m} is changing with time, the LO-frequency has to be adapted continuously to keep the signal within the BPF bandwidth. This is realized by the carrier tracking loop. The adjustment needed to match the receiver-generated frequency with the incoming carrier frequency yields the relative velocity between the receiver and the satellite. Based on the relative velocities to four satellites the receiver can calculate its own velocity.

Normally, code tracking is achieved by means of a delay-lock loop (DLL), shown in Figure 4.4. A DLL tracks the delay of a (code) modulation signal in a way similar like a PLL tracks the phase of a sinusoidal signal. The outputs of the correlator channels are subtracted from each other to form a correction signal v, which drives the VCO. The VCO with gain g_c is described by [Ziemer, 1985]

$$\frac{\hat{\tau}(t)}{T_c} = g_c \int_0^t v(\lambda) d\lambda \tag{4.9}$$

The output of the BPF is envelope detected to remove the data modulation. In addition the punctual channel (which utilizes an "on time" replicate of the code) is used for despreading the signal, which results in the data-modulated carrier wave at the output.

Sometimes a τ-dither loop is used instead. It utilizes only one correlator channel in which the early and late signals are processed in time sequence instead of in parallel. The implementation of this loop is more simple, but the performance is poorer. Both loops only work when the difference between the codes is less than one chip period T_c. Therefore the tracking process has to be preceded by an acquisition process.

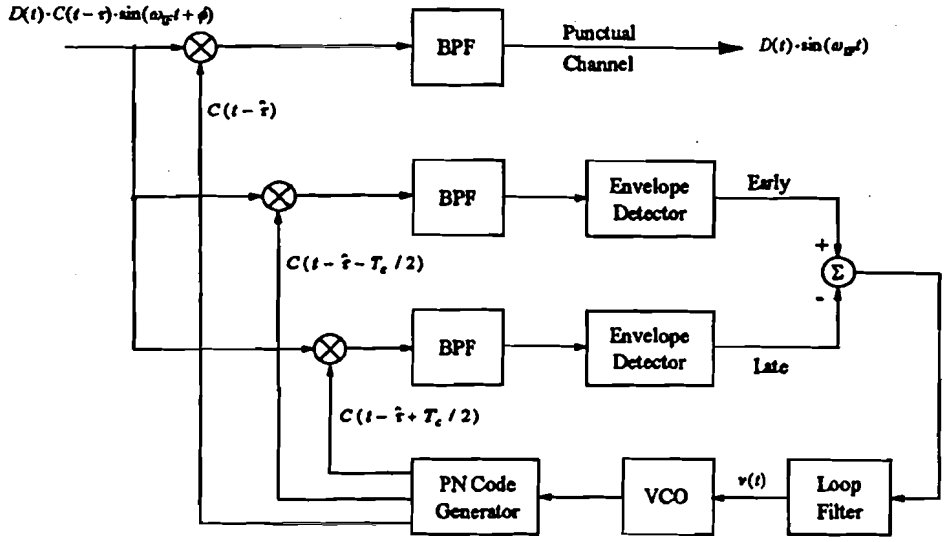

Figure 4.4 Non-coherent delay-lock loop

Carrier tracking is established by a phase-lock loop or more specifically a Costas loop, shown in Figure 4.5. The input signal is the output of the DLL punctual channel. This signal is tracked in frequency by the reference signal at the output of the VCO. A phase-locked version of the carrier wave is regenerated when $\phi = \hat{\theta} - \theta = 0$. The loop filter is the filter with the smallest bandwidth and determines the loop characteristics.

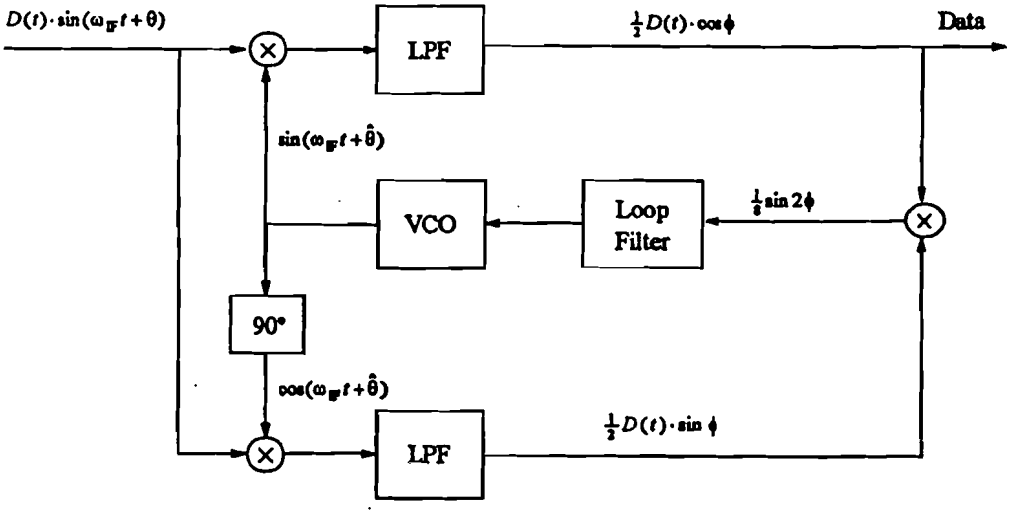

Figure 4.5 The Costas loop

Before the tracking process can start, the difference between the received and the duplicate code has to be less than 1 code chip. As the user receiver may initially have little knowledge of either the time of arrival of the C/A-code or the Doppler shift on the carrier frequency, an acquisition process takes place first. The time/frequency uncertainty region is shown in Figure 4.6. Each cell has a width of half a chip (≈ 0.5 μs) in time and one IF bandwidth ($\approx$ 1 kHz) in frequency. The maximum Doppler shift of about 4 kHz is based on the motion of the satellites relative to the user. The "cold start" acquisition time is in the order of one minute.

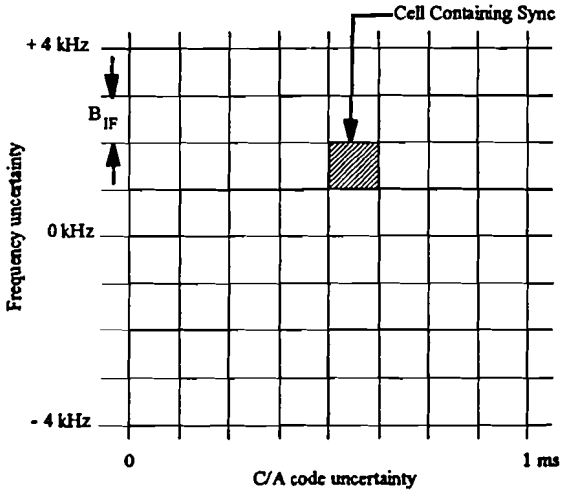

Figure 4.6 Time/frequency uncertainty region

All cells are scanned by measuring the output power in the IF bandwidth, integrating this power and comparing it with a threshold. If one cell exceeds the threshold with a certain likelihood (e.g. three out of four times), then the receiver is declared in-lock and the search is stopped. As the Doppler shift is changing with time, this process has to be repeated depending on the rate of change.

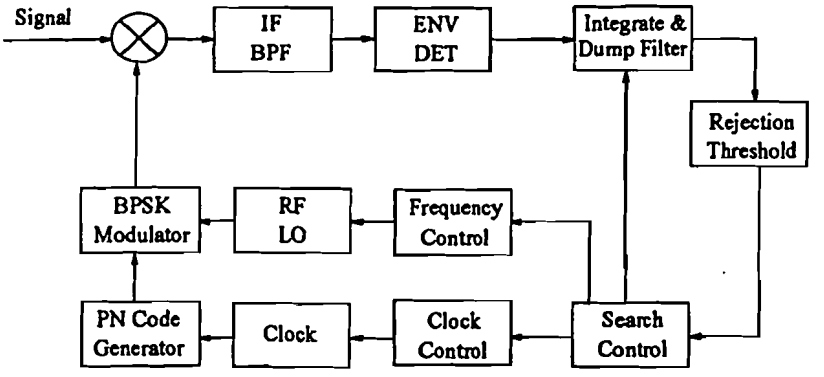

Figure 4.7 Acquisition of the signal

In order to receive the P-code a second DLL, controlled by a P-code generator, has to be added.

4.5.3 Receiver types

A dual-frequency receiver is needed to correct the ionospheric delay as much as possible. The front-end for such a receiver is shown in Figure 4.8. If the Y-code is transmitted instead of the P-code, then this type of receiver does not offer any advantages to civil users anymore. Compared to the single-frequency version it is more expensive.

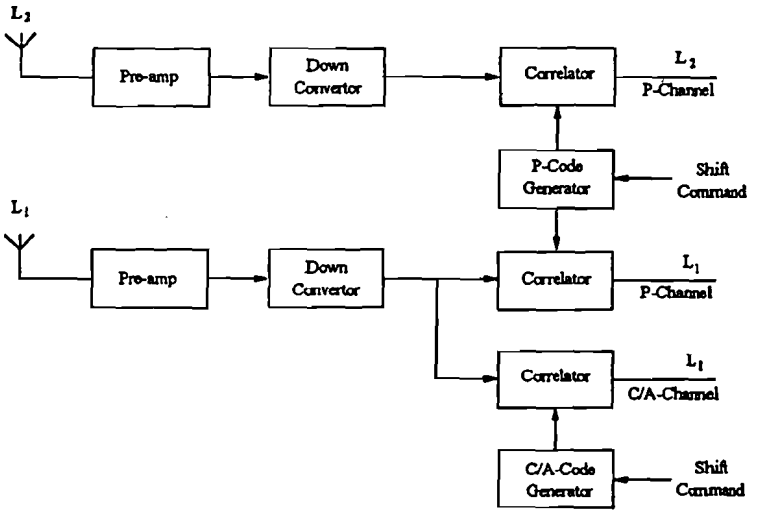

Figure 4.8 Simplified front end of dual-frequency receiver

For most applications it is necessary to track at least four satellites at the same time. The common hardware of a receiver is that part used for tracking all the satellites. It consists of the antenna, pre-amplifier and down-converter. The hardware dedicated to a specific satellite for code-correlation and Doppler tracking is called the channel hardware, e.g. code generators and correlation channels.

A multichannel receiver has four or more dedicated channels so it can simultaneously perform measurements of at least four satellites without interruption. A fifth channel is often added in order to track a new satellite without disturbing the measurements from the other four. The calibration of inter-channel biases is a problem which has to be resolved. This receiver used to be the more expensive type, mainly used for highly dynamic applications. A sharp decline in price has made it the most widely used type of receiver however.

Instead of a multichannel receiver a time sharing receiver can be used in which one channel samples signals from more than one satellite. It is less expensive, but the software will be more complex and the signal to noise ratio is lower after integration because it tracks each satellite for only a part of the time. There a two types, a sequential and a multiplex receiver.

A sequential receiver switches between satellites and it usually tracks one satellite for a period (dwell) of 1 s. Therefore it takes at least 4 s to get the position/velocity information, which makes this type of receiver not very suitable for highly-dynamic applications. Because of the long time between dwells a short acquisition process has to take place at the beginning of each dwell and the receiver cannot be used for Doppler measurements.

A multiplex receiver completes a cycle of measurements from 4 or 5 satellites within the length of one data bit (20 ms), resulting in a dwell time of 5 or 4 ms respectively. The sample frequency is about 200 times higher than in the sequential receiver which eliminates the need for an acquisition process at the beginning of each dwell. The tracking loops track the signals of each satellite continuously through the software. In order to maintain the lock in the carrier loop, receiver time control has to make sure that a bit transition in the data signal never occurs within a track interval of a satellite.

4.5.4 Receiver antennas

The radio waves that leave the GPS satellites are right-hand circularly polarized. A single dipole can be used as a receiver antenna, but then only half the signal power can be received. To receive full signal power two crossed dipoles can be used, combined with a phase network. All dipoles are narrow band antennas and require a ground plane to reduce multipath interference. The main advantage is their simplicity.

A commonly used receiver antenna is the quadrifilar helix or volute. These are narrow band devices as well but they have better gain patterns than dipoles and do not require a ground plane. Disadvantage is the more complicated design and construction. For dual frequency operation a spiral helix can be used. It has a good gain pattern as well, but its high profile can be a disadvantage. Microstrip antennas can be used for both single and dual frequency operation. Their low profile makes them a first choice for airborne or other highly mobile applications. Disadvantage is their relatively low gain.

In general the GPS receiver antenna must have a full upper hemispherical coverage with no zenith nulls. For most applications (near to) zero gain is required at low elevation angles to avoid multipath problems. Due to satellite movement the antenna phase center will be changing with time, which has to

be accounted for. Due to the correlation properties of the PN codes multipath is only a cause of concern in pseudo-range measurements if the difference in path length is less than 1.5 chip lengths (< 450 meters for the C/A-code).

4.6 Differential GPS

Many applications require a higher accuracy than GPS can provide in the stand-alone mode. The acceptable solution for most of them is differential GPS in which one or more reference receivers are located at very accurately known positions. As the major errors are introduced by the satellites and the atmosphere, range errors are highly correlated in a local (300-600 km) geographical area. A large portion of the range error can be eliminated when an estimate of this error is obtained at a reference station in the same area and transmitted to the user. This concept is illustrated in Figure 4.9. A distinction can be made between Local Differential GPS (LDGPS), in which a local reference receiver is used, and Wide Area Differential GPS (WADGPS) which utilizes a network of remote reference stations.

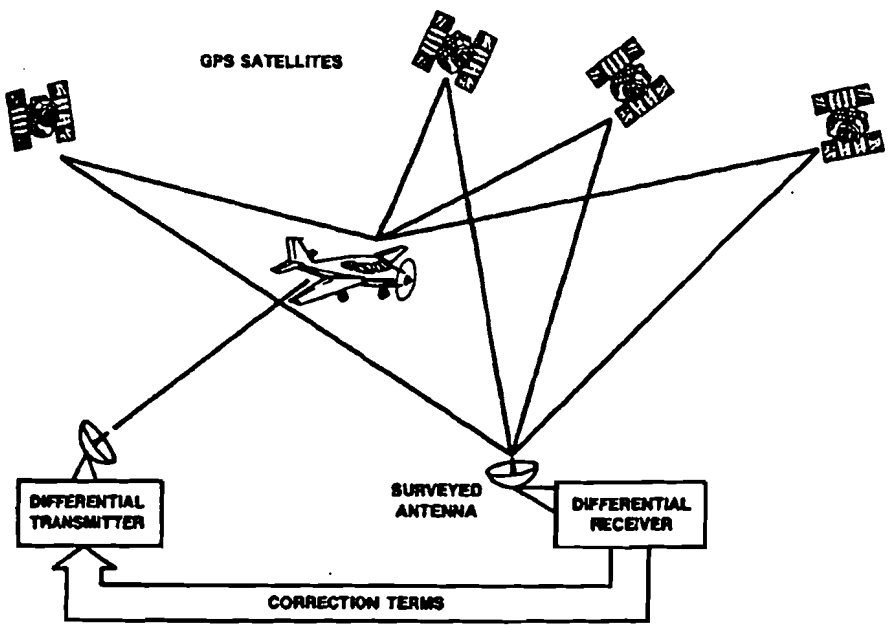

Figure 4.9 Concept of differential GPS [Denaro, 1988]

The reference station can either transmit the corrections of the pseudo-ranges to all visible satellites or it can send a correction of the measured position. The first option is preferable, because the reference station does not know which satellites the user has in view and would therefore have to transmit the position corrections for a large number of combinations of satellites. Two other responsibilities of the reference station are integrity monitoring and integrity management. This respectively means alerting the user when satellite signals are outside some specified threshold in accuracy and assuring that the differential corrections are an actual improvement of the accuracy. Depending on the application the reference receiver may utilize an atomic clock instead of a quartz clock.

Generally ionospheric and tropospheric delay can be well compensated by differential GPS. Due to the small angular difference between the user and the reference receiver satellite ephemeris and clock errors become negligibly small. The range error due to multipath however is largely determined by antenna design and placement at the user's site. This part cannot be eliminated by differential operation and the reference receiver's antenna has to be designed very carefully so as not to enlarge the multipath error. As receiver noise at the reference station and the user are not correlated this still leads to errors. The largest potential source of error in differential GPS is Selective Availability, described in the next section. Its actual influence depends on the time interval between differential corrections and the rate of change of the range error due to SA. Tests have shown that horizontal accuracies of 2-3 m are achievable.

Another way of increasing the accuracy and also the integrity of GPS is by integrating it with another system like GLONASS or Loran-C. As this has turned out to be a field of study of its own, this report will not deal with integrated systems.

4.7 Error budget and accuracy

The accuracy of GPS is divided into two classes, SPS and PPS which stands for Standard and Precise Positioning Service respectively. SPS is based on C/A-code pseudo-range measurements. As the obtainable accuracy turned out to be much higher than the 100 m intended by the DOD, it was decided to add errors to the ephemeris and clock information in the navigation message. This is known as Selective Availability (SA) and it was implemented to prevent enemies of the US from having high accuracy missile guidance systems based on GPS. The horizontal accuracy of SPS with SA is specified to give an error of less than 100 m for 95% of the time. PPS is only available to a selected group of users, authorized by the DOD, because it is based on encrypted P-code pseudo-range measurements.

The User Range Error (URE) is the error vector along the line of sight between a GPS receiver and a GPS satellite. It is the projection of all system errors stemming from the space, control and user segment. An indication of expected range errors for both P-code and C/A code measurements in both stand alone and differential mode is given in Table 4.2, which only applies to static applications. The 2 drms values of 100.2 and 20.1 m relate well to the 100 and 21 m accuracies specified by the DOD [FRP 1992]

Table 4.2 Error budget

	P-code		C/A-code	
Error source	**Absolute**	**Differential**	**Absolute**	**Differential**
Satellite clock error	3.5	0	3.5	0
Ephemeris error	4.3	0	4.3	0
SA error	N/A	N/A	32.0	0
Ionospheric delay	2.3	0	6.4	0
Tropospheric delay	2.0	0	2.0	0
Receiver noise	1.5	1.5	2.4	2.4
Interchannel bias	0.6	0.6	0.6	0.6
Multipath	1.3	1.3	3.0	3.0
URE (1σ)	6.7	2.0	33.4 [9.5]	3.9
Assumed HDOP	1.5	1.5	1.5	1.5
Horizontal accuracy (drms)	10.1	3.0	50.1 [14.3]	5.9
Horizontal accuracy (2 drms)	20.1	6.0	100.2 [28.6]	11.8

[ ] : without SA

URE = User Range Error HDOP = Horizontal Dilution of Precision drms = distance root mean square

Usually an elevation mask of 5° and 7° is used in PPS and SPS respectively. The higher elevation mask for SPS is caused by the limited ability of a SPS (= single frequency) receiver to compensate for high ionospheric delays at low elevation angles. Based on interferometric measurements, not dealt with in this report, accuracies in the cm-range or even mm-range are achievable.

4.8 GPS and beyond

4.8.1 The INMARSAT geostationary overlay

Driven by the aviation community's need for a GPS integrity channel (GIC) to result in real-time warnings of degraded system performance, Inmarsat has proposed to implement a set of geostationary repeaters to serve as an overlay to GPS (and GLONASS). The Inmarsat Geostationary Overlay (IGO) consists of navigation packages on four Inmarsat-3 spacecraft to be launched in 1995, resulting in a coverage pattern shown in Figure 4.10. As the navigation payload only constitutes a small portion of the overall costs of an Inmarsat-3 satellite, the total expenses are much lower than the costs of launching additional GPS satellites to result in the same improvement in coverage and availability. In a study carried out for INMARSAT, COMSAT has estimated a service price of $ 2,200,000 per year per satellite, based on an expected 13 year-lifetime of the satellite [Zachmann, 1992].

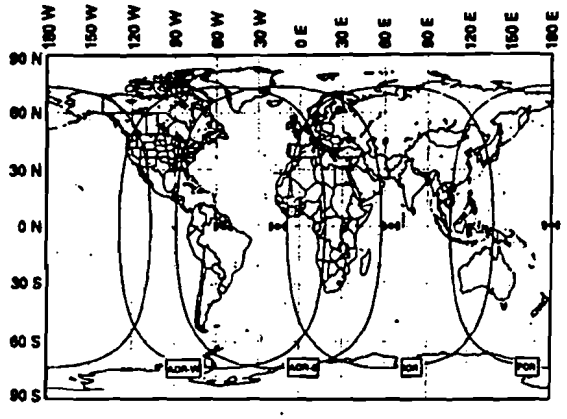

Figure 4.10 INMARSAT-3 four ocean region coverage [Kinal, 1992]

The Inmarsat-3 navigation payload is shown in Figure 4.11. A GPS-like signal is received from a special ground station at C-band (6455.6 MHz) and translated to a downlink frequency of 1575.42 MHz. To enable a conventional GPS receiver to use the signal, the bandwidth will be 2.2 MHz centered at 1575.5 MHz and the (saturated) output EIRP provided by a global coverage antenna beam is 27.5 dBW. By careful selection of PN codes the transponders are no more a cause of interference to a GPS signal than any other GPS satellite [Van Dierendonck, 1992]. It has been shown that the payload design is resistant to plausible levels of interference and that a spoofing signal can only be a possible cause of harm in a small geographic area for a limited period of time [Kinal, 1993].

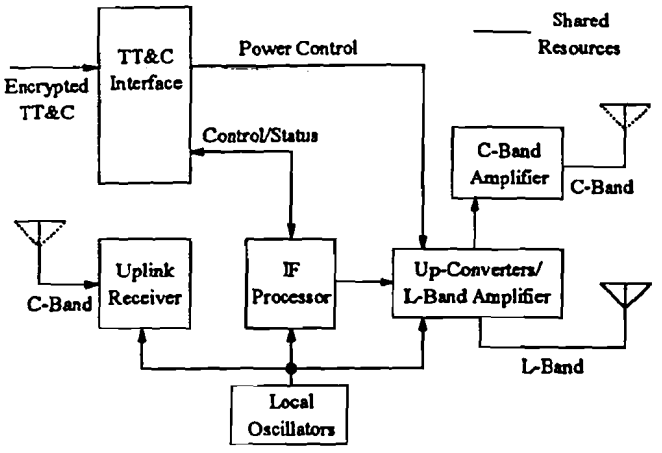

Figure 4.11 INMARSAT-3 navigation payload

A low-power C-band downlink (0 dBW at center frequency 3630.6 MHz) is specified to create a parallel C-C band path which will be employed by the ground station for timing adjustments. The PN signal has to appear as if it had been clocked at the satellite. To achieve this, the uplink station performs a closed-loop timing adjustment of the PN code clock and the carrier frequency, based on a comparison of the received downlink signal with what is desired. Inmarsat's extensive worldwide network of earth stations can be used for the necessary accurate tracking of the satellites.

Although the overlay results in increased coverage and availability, its main purpose is to enhance the integrity of GPS, which is achieved in two ways. Integrity status/warnings are generated by an independent civil integrity monitoring network and transmitted to the users through the GIC. It gives pseudo-range error estimates for each satellite, which resemble true differential corrections, and a "don't use" signal can be employed. The data is transmitted at a rate of 50 bps or possibly higher and is generated within the 10-second warning time required by the FAA [Kinal, 1990]. As the overlay increases the number of navigation satellites visible to a user, the RAIM is also enhanced, because a receiver can now more easily detect a malfunctioning satellite, provided that the number of channels in the receiver is sufficient. The combination of the ranging signal from the satellite and the integrity channel is called RGIC.

The advantages of employing geostationary transponders compared to increasing the number of GPS/GLONASS satellites are

- the repeaters are much cheaper, simpler and potentially more reliable than autonomous satellites driven by military requirements
- both external and internal integrity is enhanced

- the quality of the navigation solution will improve because the selection of one or more geostationary satellites will generally lead to a lower PDOP
- signals from geostationary satellites do nut suffer from SA
- signals can be changed in real time at the ground station
- control of supervision by an international (civil) organization rather than one country's military arm
- as the navigation message originates from the ground its format can be changed at any time during the system's development or operation
- geostationary satellites are constantly visible in a certain geographic area

Combined use of GPS and GLONASS, together often referred to as GNSS (Global Navigation Satellite System) certainly offers some benefits like increased coverage and availability. This will be however at the expense of more complicated and therefore more expensive user equipment. Uncertainties about the viability of GLONASS and its higher susceptibility to interference from mobile L-band communications are some other disadvantages.

4.8.2 The next step

Driven by the following concerns related to the civil use of GPS there is a growing international interest in a future more capable (civil) GNSS

- degradation of system accuracy due to SA
- unavailability of a usable signal at a second frequency for ionospheric correction and precision applications
- final GPS constellation will still result in areas of degraded performance with further degradation in case of (temporary) satellite failures
- limited integrity monitoring possibilities
- continuity of service

Apart from the described geostationary overlay there are other options for the augmentation of GPS/GLONASS, possibly leading to a fully capable civil GNSS. Before taking a look at these options in more detail it is important to notice that for a number of reasons any system should have a high degree of backward compatibility. Among those reasons are the large number of GPS receivers already in use and the availability of the required high-tech components.

One option would be to make use of the future LEO communications satellites. The low orbits however result in very large Doppler shifts and very short visibility periods. Use of signals from LEO satellites in a way compatible with GPS would be extremely difficult.

Another option is to launch satellites into Intermediate Circular Orbits (ICO). These could either be multimission satellites (communications plus navigation payload) or low-cost dedicated navigation satellites, sometimes referred to as Econosats [McDonald, 1993]. The latter will be much cheaper than GPS satellites because of the following factors

- no need for 180 days navigation message storage $\Rightarrow$ lower memory requirement
- no need for P-code or P-code encryption
- no need for SA or A-S processing
- no nuclear events detection capability and nuclear effects hardening
- no cross-link communications or ranging facilities
- relaxation of frequency standard stability requirements
- use of commercial instead of military standards for spacecraft components
- reduced launch costs (more than one satellite per launch vehicle)

Independent of the choice of the ICO satellite, transmission would take place at L_1 and L_2, frequencies possibly slightly offset from the GPS frequencies to avoid interference. Carrier-to-code clock ratios can be maintained to allow use of GPS processors with minor modifications. The PN codes can be chosen from the same family of Gold codes. The C/A-code can be modulated on L_2 as well to enable receivers to determine the ionospheric delay. Signal bandwidth of 20 MHz can be maintained to allow the use of narrow correlator techniques. Navigation message format and contents can be kept the same as in GPS except for leaving out the military parts. Integrity information can be sent on the L_1 link and differential data possibly on both links. A functional diagram of an ICO satellite navigation payload is shown in Figure 4.12.

A comparison of (estimates of) payload requirements for different satellites is given in Table 4.3. It is clear that in any case the mass (and therefore the costs) of the navigation payload is small compared to the GPS case.

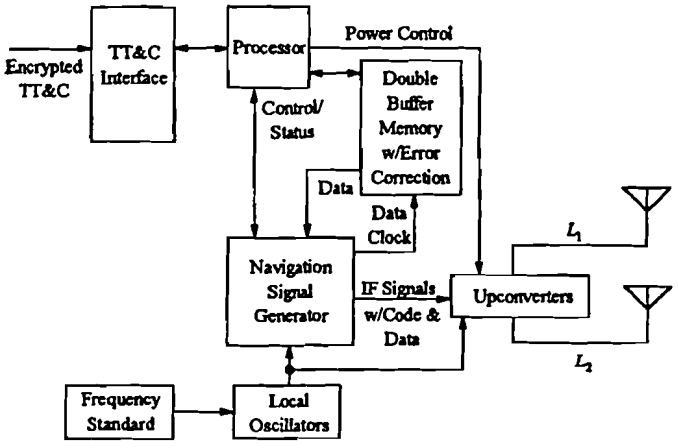

Figure 4.12 ICO satellite navigation payload

Table 4.3 Preliminary estimates of size, power and mass requirements [Van Dierendonck, 1993]

	Inmarsat-3 (Actual)	Future Generation GEO Satellite	ICO Communications Satellite Host	Low-Cost Navigation Satellites	GPS Block IIR Satellites
Navigation payload size (m^3)$^{incl. antennas}$	0.5	0.5	0.75	0.75	1.0
Navigation payload power (Watt)	90	150	175	205	385
Navigation payload mass (kg)	7.1	20	50	70	200
Total payload mass (kg)$^{exc. TT\&C}$	207	500	470	70	280
Total dry satellite mass (kg)	853	1600	1400	275	980

For global coverage with 4 or more satellites visible a constellation of 32 ICO satellites would be sufficient [McDonald, 1993]. Solely for communications purposes a number of 12 satellites would be enough. Solution might be a mix of multimission and navigation-only satellites. The latter are less complex and much lower in cost, both in terms of the costs of the satellite itself and the costs of launching it into orbit.

As an example the PDOP plot for a possible future constellation of 30 ICO plus 6 geostationary satellites is given in figure 4.13. The performance is better than in the final GPS constellation.

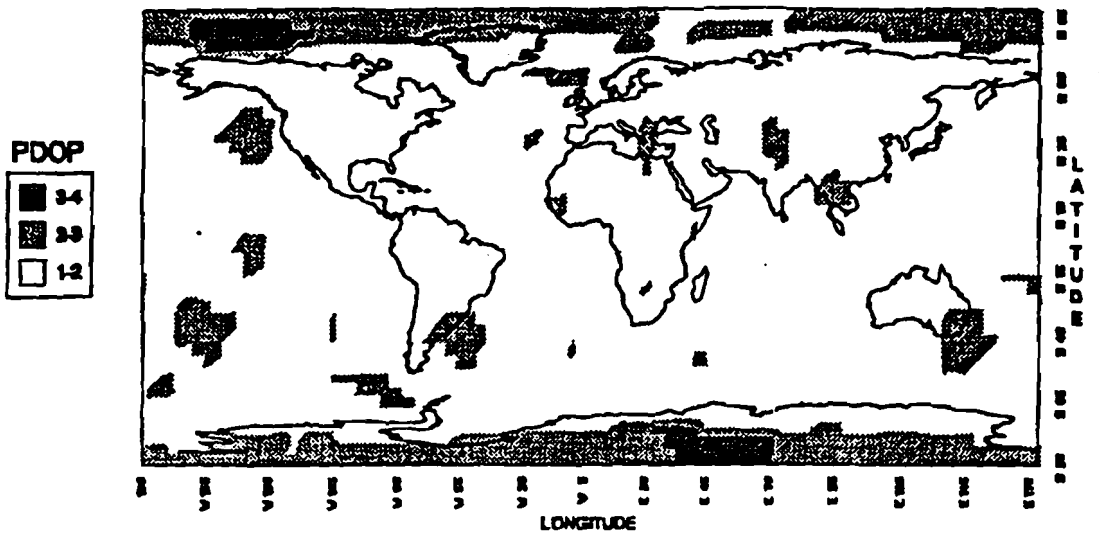

Figure 4.13 PDOP plot for 30 ICO and 6 geostationary satellites [Van Dierendonck, 1993]

Chapter 5 An integrated communication and positioning system using geostationary satellites

5.1 Introduction

In this chapter the possibility of using geostationary satellites, which are part of a communication system for mobile users, for position measurements will be examined. The assumption is that transponder bandwidth on a number of geostationary satellites will be leased to provide the information demand of mobile users, e.g. airplanes and cars. This information might be local weather information, road and traffic information or anything else wanted by the group of users.

If the transmitted signals are modulated with a PN code and have some sort of navigation message as part of the data stream, then the transponders on geostationary satellites can be used to replace dedicated navigation satellites.

Theoretically four such transponders could form a positioning system for a limited geographic area. Unfortunately this will result in a very high (on the order of 10^4) dilution of precision (DOP), because all the satellites are coplanar. This can be seen easily just by looking at the very small volume of the tetrahedron defined by the four satellite positions and the user position. This leads to the conclusion that any positioning system based on geostationary satellites needs at least one input from another source. This might be an altimeter or a satellite in a (highly) inclined orbit.

In this chapter the obtainable accuracy will be investigated of a system which receives signals from at least three geostationary satellites and has altitude information available from an altimeter. The datarates which such a system could support are determined.

5.2 Geometry considerations

The obtainable accuracy of any positioning system is for a large part defined by the geometry of the satellites, i.e. the DOP values. Based on the theoretical background given in Section 2.6 a program has been written in Matlab to calculate these values. Specific care has to be taken in the transformation of user and satellite position coordinates to a common coordinate system. Two systems are generally used

- a space-fixed, inertial reference system for the description of satellite motion
- an earth-fixed, terrestrial system for the positions of the users

The first system is known as the Conventional Inertial System (CIS). The origin of the system coincides with the geocenter. The positive z-axis is oriented towards the north-pole and the positive x-axis to the First Point of Aries. In the Conventional Terrestrial System (CTS), also known as the Earth Centered Earth Fixed (ECEF) system, the positive z-axis coincides with the mean position of the earth's rotational axis and the positive x-axis is defined by the intersection of the Greenwich Meridian with the equator. Transition from CIS coordinates to CTS coordinates can be realized through a sequence of rotations that account for precession, nutation, earth rotation and polar motion. It is beyond the scope of this text to describe the rotation matrices which account for all these effects. The interested reader is referred to [Seeber, 1993] for a more detailed description.

As a first approximation the following rotation matrix to transform CIS to CTS coordinates can be used

$$\mathbf{x}_{CTS} = \begin{bmatrix} \cos(GMST) & \sin(GMST) & 0 \\ -\sin(GMST) & \cos(GMST) & 0 \\ 0 & 0 & 1 \end{bmatrix} \cdot \mathbf{x}_{CIS} \tag{5.1}$$

where $GMST$ is the Greenwich Mean Sidereal Time, which is the angle between the Greenwich Meridian and the mean vernal equinox at a given time. If this angle is known at 0.00 h UTC and equal to α, then the $GMST$ at t minutes after 0.00 h UTC is given by [Pratt, 1986]

$$GMST = \alpha + 0.25068447 \cdot t \quad \text{(degrees)} \tag{5.2}$$

The position of a user is generally known or required to be known in ellipsoidal coordinates φ (latitude), λ (longitude) and h (height). These coordinates are related to the ECEF coordinates by

$$\mathbf{x}_{CTS} = \begin{bmatrix} x \\ y \\ z \end{bmatrix} = \begin{bmatrix} (N+h)\cdot\cos\varphi\cdot\cos\lambda \\ (N+h)\cdot\cos\varphi\cdot\sin\lambda \\ [(b^2/a^2)\cdot N+h]\cdot\sin\varphi \end{bmatrix} \tag{5.3}$$

where N is the radius of curvature in the prime vertical, which is related to the semi-axes a, b of the reference ellipsoid by

$$N = \frac{a^2}{\sqrt{a^2\cos^2\varphi + b^2\sin^2\varphi}} \tag{5.4}$$

To calculate DOP values, unity vectors from the user position to the satellite positions have to be determined. As a last step a Cartesian coordinate system is defined with the origin at the user location ($\mathbf{x}_u$), the z-axis coinciding with the local vertical, the x-axis in the E-W direction and the y-axis in the N-S direction. The new coordinates of the satellite positions are given by [Kaula, 1966]

$$\mathbf{x}'_s = \begin{bmatrix} -\sin\lambda_u & \cos\lambda_u & 0 \\ -\sin\varphi_u \cdot \cos\lambda_u & -\sin\varphi_u \cdot \sin\lambda_u & \cos\varphi_u \\ \cos\varphi_u \cdot \cos\lambda_u & \cos\varphi_u \cdot \sin\lambda_u & \sin\varphi_u \end{bmatrix} \cdot (\mathbf{x}_s - \mathbf{x}_u)_{CTS} \tag{5.5}$$

To check the correctness of the code, DOP values have been calculated for GPS satellites. The source code can be found in Appendix 2A. The satellite positions in CIS coordinates are obtained from the GSS software package. DOP values have been calculated for several combinations of GPS satellites. The calculated results hardly differ from the values given by GSS.

One way to solve for the coplanar nature of geostationary satellites is to use an altimeter reading as one input, which is the same as placing one satellite in the center of the earth. In this case the Geometric Dilution Of Precision is given by [Stein, 1986]

$$\mathrm{GDOP}_a = \sqrt{\mathrm{trace}(\mathbf{G}_a^T \cdot \mathbf{R} \cdot \mathbf{G}_a)^{-1}} \tag{5.6}$$

where

$$\mathbf{G}_a = \begin{bmatrix} 0 & 0 & -1 & 0 \\ x'_{s1} & y'_{s1} & z'_{s1} & -1 \\ x'_{s2} & y'_{s2} & z'_{s2} & -1 \\ x'_{s3} & y'_{s3} & z'_{s3} & -1 \end{bmatrix} \tag{5.7}$$

with

$$\sqrt{x'^2_{si} + y'^2_{si} + z'^2_{si}} = 1 \quad , \quad i = 1, 2, 3 \tag{5.8}$$

and

$$\mathbf{R} = \begin{bmatrix} 1/r^2 & 0 & 0 & 0 \\ 0 & 1 & 0 & 0 \\ 0 & 0 & 1 & 0 \\ 0 & 0 & 0 & 1 \end{bmatrix} \tag{5.9}$$

with r the ratio of the altimeter error (σ_a) to the pseudo-range error (σ_0).

As a common basis for further studies the assumption is made here that the service area for an integrated communication and positioning system will be the Continental United States (CONUS) with longitudes ranging from 125 W to 70 W and latitudes ranging from 25 N to 50 N. Possible locations of geostationary satellites depend on the required minimum elevation angle. To determine which subsatellite points result in satellite visibility in a certain area the following relations can be used [Pratt, 1986]

$$\cos(El) = \frac{\sin(\gamma)}{\sqrt{1.02274 - 0.301596 \cdot \cos(\gamma)}} \tag{5.10}$$

$$\cos(\gamma) = \cos(\varphi_e) \cdot \cos(\lambda_s - \lambda_e) \tag{5.11}$$

where φ_e and λ_e are the latitude and the longitude of an earth based user, λ_s is the longitude of the subsatellite point and γ is the great circle distance between the user station and the subsatellite point.

Using the most northern latitude (≈50°) of the CONUS, the maximum separation in longitude between an earth user and the subsatellite point can be calculated for the case of a required minimum elevation angle. Longitudes of the subsatellite points in case of n ($n \geq 3$) available geostationary satellites are calculated based on the following initial assumptions

1. In case of four available satellites, the most eastern and western satellites each have to be visible in at least half the CONUS. More in general: most eastern and western satellites have to be visible at $1/(n - 2)$ part of the longitudes at latitude 50 N.
2. Satellites are equally displaced in longitude.

The resulting base positions of the satellites, shown in Table 5.1, can be used for further analysis of the selection of available satellites.

Table 5.1 Base positions of geostationary satellites

El	$\Delta\lambda$	$\lambda_s, n=3$	$\lambda_s, n=4$	$\lambda_s, n=5$	$\lambda_s, n=6$
10°	61°	131 98 64	158 118 77 37	167 132 98 63 28	172 142 112 83 53 23
15°	52°	122 98 73	149 115 80 46	158 128 98 67 37	163 137 110 84 57 31
20°	43°	113 98 82	140 112 83 55	149 123 98 72 46	154 131 109 86 64 41

To obtain an initial set of DOP values at different locations in the CONUS, a grid of 72 points, separated in latitude and longitude by five degrees, has been chosen. The Matlab source code for the case of five available geostationary satellites can be found in Appendix 2B. The criteria for satellite selection in case there are more than three satellites visible from a certain location are straightforward: the first and second satellite are respectively the most eastern and western satellites which are still visible and the third satellite is the one closest to overhead. For all grid positions HDOP values have been calculated for the three, four, five and six satellite scenario, for different values of the altimeter error to range error ratio r, in the case of an elevation mask of 15°. The results are shown in Table 5.2.

Table 5.2 Average HDOP values in CONUS for satellites at base positions and an elevation mask of 15°

HDOP	Number of available satellites			
r	3	4	5	6
0.5	18.0	8.3	7.2	6.6
1	18.0	8.4	7.3	6.7
2	18.2	8.7	7.7	7.1
3	18.4	9.3	8.3	7.8
4	18.8	10.0	9.1	8.7
5	19.2	10.8	10.0	9.6

5.3 System operation

The receiver antenna system has to track three visible system satellites that yield best geometry. The tracking software in the receiver has to implement the flow chart shown in Figure 5.1. For simplicity reasons the use of four available satellites and four independently steerable antennas or antenna beams has been assumed.

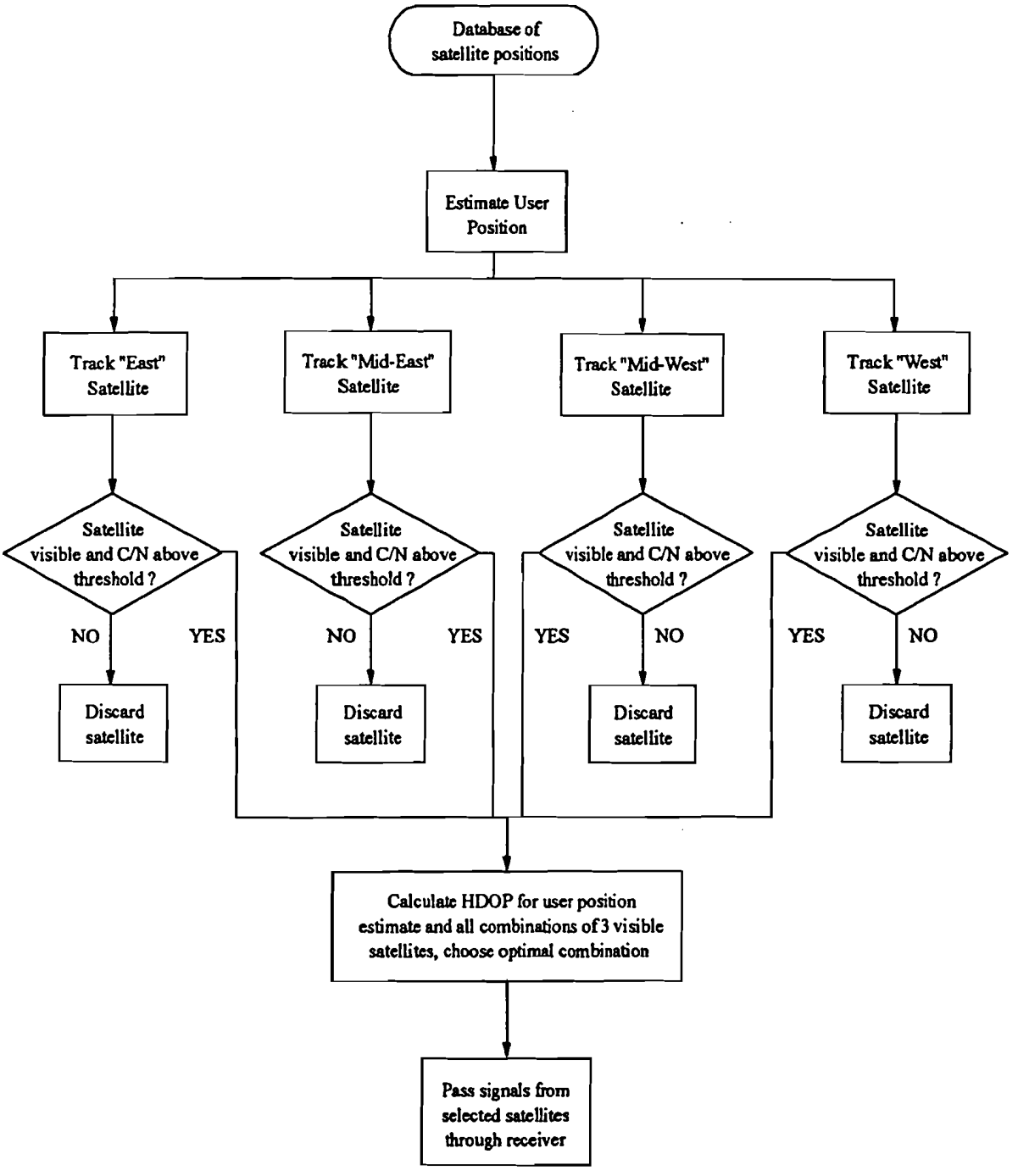

Figure 5.1 Flow chart of satellite tracking process

After the navigation message has been decoded the time of transmission and the position of the satellite at the time of transmission are known. When maximum correlation between the received and locally generated PN code is achieved the pseudo-range to the satellite can be determined. The measured pseudo-ranges to three satellites are adjusted for tropospheric and ionospheric delay and can then be used to solve for the following set of navigation equations

$$PR_i + CB = [(X_u - X_s^i)^2 + (Y_u - Y_s^i)^2 + (Z_u - Z_s^i)^2]^{\frac{1}{2}} \quad i = 1,2,3$$
$$[(X_u - h_a \cdot u_x)^2 + (Y_u - h_a \cdot u_y)^2 + (Z_u - h_a \cdot u_z)^2]^{\frac{1}{2}} = R \qquad (5.12)$$

where

PR_i	=	pseudo-range measurement to satellite i
CB	=	clock offset error between user clock and system time
X_u, Y_u, Z_u	=	space coordinates of the user
X_s^i, Y_s^i, Z_s^i	=	space coordinates of satellite i
h_a	=	altimeter reading (= altitude above the reference ellipsoid)
(u_x, u_y, u_z)	=	unit vector from the user position to the earth center
R	=	earth radius

Further research is required to determine the possible advantages of using delta-range measurements and an external velocity measurement as extra inputs to the navigation processor. The user's position can be determined using a 4 or 7 state (depending on the use of delta-range measurements) Kalman filter implemented in the navigation processor of the receiver.

5.4 The altimeter

As the accuracy of the positioning part of the system depends very much on the accuracy of the altimeter input, a brief description will be given of this device. In an airplane an altimeter indicates the vertical distance above ground level. The altimeter is a pressure measuring device and it is actuated by the static pressure of the atmosphere. The static pressure is sensed by static holes in a static-pressure probe or by a set of holes in the side of an aircraft fuselage, called fuselage vents or static ports. The holes have to be located at points where the local velocity and pressure are equal to the free stream velocity and static pressure. The pressure that is sensed is conveyed to a pressure-sensing element, generally in the form of a capsule. A pressure capsule is formed by joining together two corrugated diaphragms which are about

2 inches in diameter. The absolute-pressure (or aneroid) capsule is evacuated and sealed. The principle of the altimeter is shown in Figure 5.2

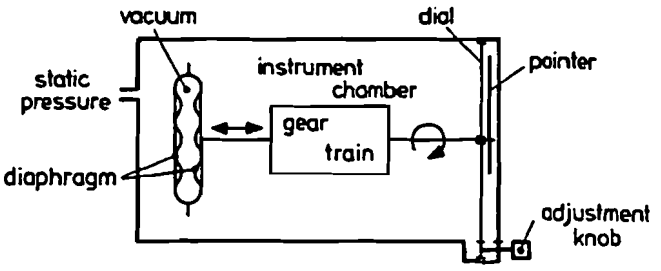

Figure 5.2 Principle of altimeter [Ruijgrok, 1990]

The capsule or diaphragm unit reacts to a change in the static pressure inside the instrument chamber. When the pressure decreases the capsule will expand. This deflection, which is very small, is amplified through a system of gears and levers (gear train), to rotate the indicator point in front of the scale on the dial of the instrument.

To provide an indication of height, the scale is calibrated according to the pressure-height relationship in the International Standard Atmosphere (ISA). For use in the troposphere the so called geopotential pressure altitude H_p for $H_p \leq 11{,}000$ m is given by [Ruijgrok, 1990]

$$H_p = \left[\left(\frac{p}{p_0}\right)^{-\frac{R\cdot\lambda}{g_0}} - 1\right]\cdot\frac{T_0}{\lambda} \tag{5.13}$$

with

p_0 = 101325 N/m², the pressure at sea level
T_0 = 288.15 K, the temperature at sea level
R = 287.05 m²/s²K, the gas constant
λ = -0.0065 K/m, the temperature gradient
g_0 = 9.80665 m/s², the acceleration of gravity at sea level

When the atmospheric conditions depart from the values assumed in the ISA an altimeter is in error. The geopotential pressure altitude then provides the actual air pressure but only gives an approximation of the geometric or true height above the ground. The greatest error is caused by the influence of the sea-

level pressure p_0. To correct the altimeter for the occurring pressure at ground level the adjustment knob can be turned until the altimeter reads the correct height of the airport above mean sea level (MSL).

The reading of the altimeter is also subject to inaccuracies in the instrument itself. The indications of the instrument may be affected by static-pressure errors of the static probe or static ports, errors due to system lag during alterations of height or speed and to imperfections in the instrument mechanism. The last category of errors depends on the elastic properties of the pressure capsule (scale error, hysteresis and drift) and the effects of temperature, acceleration and friction of the linkage mechanism. The static-pressure error and scale-error are systematic and can be determined by calibration, so corrections can be applied. The time lag errors vary with the rate of change of altitude and the other instrument errors are generally random [Gracey, 1980].

Altimeters can be expected to have an accuracy better than 75 feet ($\approx$ 22.5 m). It would be advisable to put meteorological data on the information stream to users of the integrated system to allow for regular resetting of the altimeter. In this way the disturbing influence of local high or low pressures on the accuracy of the altimeter can be minimized.

5.5 Selection of the satellites

5.5.1 Requirements

The selection of the geostationary satellites to be used in our system is governed by a number of factors

- The number and position of the satellites determine the average HDOP across the CONUS, which must be kept as low as possible.
- Different satellites and satellite positions result in different EIRP footprints. A selection criterion would be to select those satellites that give maximum EIRP for a certain geographic area.
- The total number of satellites has to be kept low, because each extra transponder increases the system cost and makes the satellite tracking system in the receiver more complicated.
- It may be advantageous to lease transponder bandwidths on satellites run by the same operator.
- Transponder bandwidth has to match the required system bandwidth.
- Satellites should ideally remain in their orbit for at least five years or be replaced within that period with equivalent satellites.
- The satellite antennas all have to use either circular or linear polarization.

- All satellites have to be visible from the master control/uplink station. Assuming a ground control station latitude of about 40° this yields a maximum orbital separation of the most eastern and western satellites of 131° and 144° for elevation masks of 10° and 15° respectively.
- Possibility and financial terms of leasing transponder bandwidth on a certain satellite.

Some of the requirements are conflicting so the selected combination of satellites will generally be a compromise.

5.5.2 Horizontal position accuracy

For the evaluation of the obtainable horizontal position accuracy of our system the Matlab source code described in Section 5.2 has been adapted. Longitudinal and latitudinal separation of the grid points has been reduced to 1°, leading to a total number of 1456 points. Possible satellite combinations are defined in arrays and the average horizontal, E-W and N-S error factors are calculated for each combination. Elevation masks can be chosen freely, but the analysis has been limited to masks of 10° and 15°. The final source code for the case of 5 available satellites can be found in Appendix 2C.

The E-W error factor is determined only by the position of the satellites relative to the user and is independent of the altimeter error. In the analysis the ratio of altimeter error to range error was chosen to be one. This is rather optimistic and a more realistic ratio would be three or four. HDOP values have also been calculated using a ratio of four for the satellite combinations which were found to give most favorable results for a ratio of one.

In order to get an acceptable satellite geometry at least four satellites are needed. To fulfill the communication purposes the system would not need more than four satellites. The choice of having additional satellites has to be justified by a (considerable) improvement in position accuracy. A small advantage of a system built up of more than four satellites is the decreased susceptibility to positioning system malfunctioning due to one satellite failure.

5.5.3 Analysis of C-band satellite systems

A short description of geostationary satellites which possibly have transponder bandwidth available at C-band can be found in Appendix 3A [Long, 1992]. All satellites have transponders with a bandwidth of 36 MHz. In ITU Region 2 there are 17 satellites available which leads to a large degree of freedom in the choice of satellites at longitudes between 69 W and 137 W. These satellites all have a minimum

EIRP in the CONUS of 35 dBW and variation between satellites is less than 3 dBW. In ITU Region 1 there are four possible candidates: NASA's TDRSS-41 and Intelsat satellites at 27.5 W, 34.5 W and 53 W. The only candidate in ITU Region 3 is NASA's TDRSS-174. The EIRP of satellites in Region 1 and 3 is about 3 dB lower which results in either a lower data rate or a reduced interference margin. At the moment of writing this report (July 1994) uncertainty still existed about the possibility of leasing transponder bandwidth on any of the NASA satellites.

Obtainable horizontal, E-W and N-S error factors for a large number of four and five satellite systems can be found in Appendix 4A and B respectively. The results for the most favorable combinations are summarized in Table 5.3.

Table 5.3 Summary of C-band 4 satellite system results

Average HDOP	15° Elevation mask[1]		10° Elevation mask	
Satellite positions (°W)	$r = 1$	$r = 4$	$r = 1$	$r = 4$
34.5 69 103 137	8.42	9.98	7.47	9.19
34.5 69 101 137	8.50	10.05	7.47	9.20
41 69 103 137	8.51	10.05	7.48	9.18
41 69 101 137	8.57	10.12	7.45	9.16
34.5 69 99 137	8.64	10.18	7.51	9.25
41 69 99 137	8.69	10.23	7.45	9.17

[1] a few locations have elevation angles smaller than 15°

r is the altimeter error to range error ratio

The "East" satellite can either be Intelsat VI-F3 (34.5 W) or NASA TDRSS-41 (41 W). The "West" satellite can be (in order of preference) Aurora II (137 W), Satcom C3 (135 W) or Galaxy I-R (133 W). Spacenet IIR (69 W) is preferable to Galaxy VI (79 W) as the "Mid-East" satellite. The "Mid-West" satellite can either be Spacenet IR (103 W), Spacenet IV (101 W) or Galaxy IV-H (99 W).

As can be seen in Appendix 4B, adding a fifth satellite in case of an elevation mask of 15° does not give increased system performance. In case of an elevation mask of 10°, adding a fifth satellite only makes sense when NASA's TDRSS-174 can be used. In that case HDOP of about 6.2 is feasible.

5.5.4 Analysis of Ku-band satellite systems

Usable geostationary satellites with Ku-band transponders are briefly described in Appendix 3B. When compared to C-band transponders two differences appear: a wider variety in transponder bandwidths (27, 36, 43, 54 and 72 MHz) and a wider range of satellite EIRP (42 to 50 dBW).

In ITU Region 1 there are six satellites available: three Intelsat satellites, two Orion satellites and one PAS satellite. Twelve satellites are available in Region 2 between longitudes 69 W and 125 W. ITU Region 3 again is the bottleneck. The Columbiasat 1 may be available at 165 W and there is one Intelsat satellite at 177 W, but even for an elevation mask of 10° this satellite is only visible in a small part of the US. Horizontal, E-W and N-S error factors have been calculated for four and five satellite systems. The results can be found in Appendix 4C and D.

4 satellites - Elevation mask 15°

Best obtainable HDOP is about 10.5. The difference with the much lower value of 8.5 for the C-band case can be explained by the lack of a Ku-band satellite around 135 W. A summary of the results is given in Table 5.4.

Table 5.4 Summary of Ku-band 4 satellite system results, 15° elevation mask[1]

	Average HDOP	
Satellite positions (°W)	$r = 1$	$r = 4$
37.5 69 97 125	10.49	11.83
47 69 97 125	10.49	11.76
47 69 97 123	11.09	12.30
37.5 69 97 123	11.13	12.41
47 79 101 125	12.40	13.62

[1] a few locations have elevation angles smaller than 15°

r is the altimeter error to range error ratio

The East satellite can either be Orion 1 (37.5 W) or Orion 2 (47 W). The West satellite can be GSTAR IV (125 W) or SBS 5 (123 W). Spacenet II (69 W) is preferable to Satcom Hybrid-1 (79 W) as Mid-East satellite. The Mid-West satellite is best chosen to be AT&T's Telstar 401 (97 W) or Galaxy IV-H (99 W).

10° elevation mask

Obtainable HDOP values with or without using Columbiasat 1 are summarized in Table 5.5 and 5.6. With Columbiasat 1, HDOP can be about 0.7 better than in the C-band case. Without Columbiasat 1, HDOP is more than 2.2 worse than in the C-band case however.

Table 5.5 Summary of Ku-band 4 satellite system results
10° elevation mask, without Columbiasat

	Average HDOP	
Satellite positions (°W)	$r = 1$	$r = 4$
37.5 69 97 125	9.66	11.08
47 69 97 125	9.75	11.10
37.5 69 97 123	10.26	11.62
47 69 101 123	10.34	12.15
47 79 99 125	10.93	12.26

r is the altimeter error to range error ratio

Table 5.6 Summary of Ku-band 4 satellite system results
10° elevation mask, with Columbiasat

	Average HDOP	
Satellite positions (°W)	$r = 1$	$r = 4$
47 79 125 165	6.74	8.57
47 87 125 165	6.79	8.61
53 87 125 165	7.21	8.97
47 69 125 165	7.48	9.23

r is the altimeter error to range error ratio

5 satellites

Without the availability of Columbiasat 1 adding a fifth satellite cannot be justified. When using Columbiasat 1, HDOP values of about 6.0 are obtainable for an elevation mask of 10° (see Appendix 4D). This yields an improvement of about 0.8 compared to the 4 satellite case. Adding a fifth satellite only really makes sense when using a 15° elevation mask. In this case (using Columbiasat 1) HDOP goes down from about 10.5 to 7.8.

5.5.5 Summary of results

The results of the analysis are summarized in Table 5.7.

Table 5.7 Summary of obtainable HDOP values averaged across the CONUS for optimal constellations

Obtainable HDOP	Elevation mask is 15°		Elevation mask is 10°	
System	$r = 1$	$r = 4$	$r = 1$	$r = 4$
4 C-band satellites	8.5	10.0	7.5	9.2
5 C-band satellites	8.3	9.9	6.2 (7.3)[1]	8.1
4 Ku-band satellites	10.5	11.8	6.8 (9.7)[2]	8.6 (11.1)[2]
5 Ku-band satellites	7.8 (10.7)[2]	9.4	6.0 (9.3)[2]	7.9

[1] TDRSS-174 not available

[2] Columbiasat 1 not available

r is the altimeter error to range error ratio

Assuming that Columbiasat 1 is not available then the average accuracy of a C-band system using either four or five satellites is higher than the accuracy of a Ku-band system. Another important difference is that the distribution of HDOP values across the CONUS is much more homogeneous in the C-band case. The Ku-band system is characterized by much higher (> 12) HDOP values in the western part of the US than in the eastern part.

To get an indication of the range of HDOP values across the CONUS the 72 point grid has been used to obtain the 90% ranges for different constellations assuming a (worst case) altimeter error to range error ratio of four. The results are summarized in Table 5.8. The 90% ranges for the ratios of the E-W error to range error, which are independent of the altimeter error to range error ratio and show little variation for elevation masks of 10° and 15°, are shown in Table 5.9.

Main conclusion is that our system should consist of four satellites. Even if the possibility exists to use TDRSS-174 at C-band or Columbiasat 1 at Ku-band, the improvement in positioning accuracy would not outweigh the increase in system cost and complexity.

Table 5.8 90% ranges of HDOP values across the CONUS

90% range of HDOP	Elevation mask	
System	15°	10°
4 C-band satellites	5.4 - 13.4	5.3 - 13.0
5 C-band satellites	5.2 - 12.9	5.2 - 11.1
4 Ku-band satellites[1]	7.5 - 16.0	7.3 - 15.0
5 Ku-band satellites	5.4 - 12.6	4.9 - 11.3

[1] Columbiasat 1 not available

Table 5.9 90% ranges of E-W error to range error ratios

System	Error ratios
4 C-band satellites	0.9 - 2.2
5 C-band satellites	0.8 - 1.5
4 Ku-band satellites[1]	1.0 - 4.0
5 Ku-band satellites	0.9 - 1.5

[1] Columbiasat 1 not available

Table 5.9 shows that the horizontal position error is for the biggest part an error in the N-S direction.

It might be cheaper to use one the older Intelsat satellites in ITU Region 1 (not listed in Appendix 3) whose lifetime is being prolonged by means of the Satcom maneuver. This usually results in an increasing inclination of the orbit and the effect of a (worst case) inclination of 5° on the HDOP has been examined for the case of three "real" geostationary satellites at 69 W, 103 W and 137 W and one inclined orbit satellite at 41 W. HDOP decreases a little bit when the inclined orbit satellite moves from zero latitude to the south, but increases when the satellite crosses the equator heading north. The use of an inclined-orbit satellite will therefore not result in a substantial change in accuracy when compared to using a geostationary satellite at the same longitude. It may be slightly more difficult to determine the position of an inclined-orbit satellite as accurate as the position of a geostationary satellite.

5.6 Link budgets

5.6.1 C-band link budget

The link budget for a system based on C-band (6/4 GHz) geostationary transponders is given below. Ω_{sat} and $(G/T)_{sat}$ vary from satellite to satellite, given values are typical. As can be seen in Appendix 3A, 36 dBW is the typical EIRP of a ITU-2 Region satellite. A derivation of the receiver system noise temperature can be found in Appendix 7. A receiver antenna gain of 8 dB is assumed to be feasible; more attention to the antenna system is paid in Section 5.7.6.

Uplink

Ω_{sat}	=	- 83 dBW/m^2 (saturated power flux density at satellite)
$(G/T)_{sat}$	=	- 1 dB/K
$c^2/4\pi f^2$	=	- 37 dB
k	=	- 228.6 dBW/K-Hz
$(C/N_0)_u$	=	107.6 dB-Hz $(= \Omega_{sat} \cdot (c^2/4\pi f^2) \cdot (G/T)_{sat} \cdot (1/k))$
$4\pi d^2$	=	163 dB-m^2
Loss margin L	=	2 dB
EIRP	=	82 dBW $(= \Omega_{sat} \cdot 4\pi d^2 \cdot L)$

Downlink

$EIRP_{sat}$	=	36 dBW (at edge of coverage zone)
Output backoff	=	1 dB
Path loss	=	196.5 dB
Pointing loss	=	2 dB (of receiver antenna)
Margin	=	2 dB
k	=	- 228.6 dBW/K-Hz
T_r	=	23.6 dB-K
G_r	=	8 dB
$(C/N_0)_d$	=	47.5 dB-Hz (carrier to noise ratio at receiver LNA input)

As expected, the influence of the uplink on the overall carrier to noise ratio can be neglected. At the demodulator input, the energy per information bit to noise ratio is given by

$$\frac{E_b}{N_0} = \left(\frac{C}{N_0}\right)_d - 10 \cdot \log(R_b) - L_i \qquad (5.14)$$

where R_b is the information channel bit rate and L_i is the implementation loss in the receiver, estimated to be 1 dB. For a probability of bit error of 10^{-6}, the required (E_b/N_0) without any coding is 10.5 dB. When a rate R = ½ convolutional code of constraint length $K = 7$ is used with Viterbi soft-decision then only 4.8 dB is required. In this case the bitrate is twice the data rate. Using equation 5.14 the maximum possible data rates can be determined. This gives data rates of 4.0 kbps and 7.4 kbps without and with FEC respectively. For satellites in ITU Region 1 or 3 nominal EIRP will be about 3 dB lower. As a result the maximum data rates are halved.

5.6.2 Interference analysis

The receiver antenna in our system will have four independent steerable beams with beamwidths sufficiently narrow to achieve the required antenna gain. There are a number of possible sources of interference

1. Cochannel interference. As the carrier components are modulated by different codes, the interference between the information channel and the range channel (see Section 5.7) can be neglected.

2. Adjacent channel interference. Interference from adjacent satellites will be rejected by a combination of the lower antenna gain in the direction of these satellites and the despreading process in the receiver.

3. Interference from system satellites. The antenna gain pattern should be sufficient to reject this interference because of the large orbital separation between the satellites. By choosing a different Gold code and m-length code for each satellite any remaining interference will be eliminated in the correlation process.

4. Interference from terrestrial radio systems. This is only a cause of concern at C-band. Received power from a terrestrial transmitter can be orders of magnitude higher than the received signal power. A high processing gain is required to reject this interference.

5. Intentional jamming. As our system will not be a military system this should not be a real factor. The processing gain in both channels is sufficient to have some tolerance for jamming.

The maximum tolerable interference from a terrestrial system can be derived using the following equation [Ha, 1990]

$$\frac{E_b}{\mathcal{N}_0} = \left[\left(\frac{E_b}{N_0}\right)^{-1} + \frac{R_b}{R_c}\cdot\frac{J}{C}\right]^{-1} \tag{5.15}$$

where

$\frac{E_b}{\mathcal{N}_0}$ = determined by the required P_b

$\frac{E_b}{N_0}$ = given by Equation 5.14

R_b = information channel bit rate (equal to the data rate R_d for a non-coded system and twice the data rate in case of FEC)

R_c = code chip rate

J/C = ratio of received interference power and signal power

Here is an example to see how much interference power can be tolerated when using FEC.

$P_b = 10^{-6} \Rightarrow E_b/\mathcal{N}_0 = 4.8$ dB

R_d = 2 kbps

R_c = 15 Mcps

C/N_0 = 47.5 dB-Hz

E_b/N_0 = 13.5 dB

J/C = 29.6 dB

Without FEC the margin would be 25.2 dB. Because of the higher interference margin and the possibility to use higher data rates the choice is made to use FEC at the cost of increased system complexity. Table 5.10 shows the interference margins for a number of combinations of data rates and chip rates. Because of the low data rate of the navigation message, the use of FEC on the range channel (see Section 5.7) is not mandatory.

Further study is required to determine which interference levels from terrestrial microwave systems can be expected throughout the US.

Table 5.10 C-band interference margins for different data rates and chip rates

Interference margin (dB)	Chiprate (Mcps)		
Data rate (kbps)	10	15	18
1	31.6	33.3	34.1
2	27.8	29.6	30.4
4	22.8	24.5	25.3
7	11.0	12.8	13.6

5.6.3 Ku-band link budget

The link budget for Ku-band geostationary transponders is complicated by the wider range of nominal EIRP and the need to include a rain margin. The EIRP values are obtained from Appendix 4B. A down link rain margin of 5 dB was chosen. This should be sufficient to account for both the effect of attenuation and an increase in receiver noise temperature due to rain for 99.9 % of the year. Values for Ω_{sat} and $(G/T)_{sat}$ again are typical. An antenna gain of 12 dB should be feasible at Ku-band.

Uplink

Ω_{sat}	=	- 82 dBW/m^2 (saturated power flux density at satellite)
$(G/T)_{sat}$	=	2 dB/K
$c^2/4\pi f^2$	=	- 44.5 dB
k	=	- 228.6 dBW/K-Hz
$(C/N_0)_u$	=	104.1 dB-Hz $(= \Omega_{sat} \cdot (c^2/4\pi f^2) \cdot (G/T)_{sat} \cdot (1/k))$
$4\pi d^2$	=	163 dB-m^2
Rain margin	=	8 dB
EIRP	=	89 dBW $(= \Omega_{sat} \cdot 4\pi d^2 \cdot L)$

Downlink

$EIRP_{sat}$	=	42 to 50 dBW (at edge of coverage zone)
Output backoff	=	1 dB
Path loss	=	206 dB
Atmospheric attenuation	=	0.3 dB [Maral, 1993]
Pointing loss	=	2 dB (of receiver antenna)
Rain margin	=	5 dB
k	=	- 228.6 dBW/K-Hz
T_r	=	23.8 dB-K
G_r	=	12 dB
$(C/N_0)_d$	=	44.5 to 52.5 dB-Hz (carrier to noise ratio at receiver LNA input)

For the given range of available satellite EIRP and assuming the use of FEC, the range of maximum data rates is given by

$$3.7 \text{ kbps} \leq R_{d,\max} \leq 23.4 \text{ kbps} \tag{5.16}$$

So even for the lowest values of satellite EIRP a data stream at a reasonable bitrate is still possible. Some extra margin is useful however to allow for the use of antennas with lower gain.

5.6.4 The effect of Doppler

Relative motion between a receiver and a satellite results in a Doppler shift on both the carrier frequency and the code clock rate. The maximum velocity of a geostationary satellite relative to an earth based stationary receiver is about 30 m/s. This results in Doppler shifts of 400 Hz and 1200 Hz for C-band and Ku-band carriers respectively and 1.5 cps for a 15 Mcps code rate.

For receivers located in moving cars the worst case relative velocity will be about 60 m/s leading to doubled Doppler shift values. The effect of Doppler shift only really becomes noticeable in the case of receivers installed in airplanes. In this case the maximum relative velocity will be about 1000 km/h leading to Doppler shifts of about 3.7 and 11.1 kHz for C-band and Ku-band carriers respectively and 14 cps for a 15 Mcps code rate.

5.7 System design

5.7.1 Signal analysis

Instead of using BPSK for both data modulation and spread spectrum modulation, QPSK can be used for modulating the PN code(s) on the carrier. QPSK direct sequence spread spectrum offers a number of interesting features

1. Opportunity to modulate the in-phase and quadrature carrier components with different data and at different data rates.
2. Opportunity to modulate the carrier components with PN codes of different length.
3. Decreased sensitivity to some types of jamming or interference [Ziemer, 1985].

The PN code to modulate the general information can be short because it will not be used for range measurements. Because of the short period of this information code, acquisition times will be short. A different Gold code is chosen for each satellite signal because of the low cross-correlation of Gold codes. A code period of 1023 bits is chosen. It can be arranged that the code epochs of both the short Gold code and the longer range code occur simultaneously. As a result the range code period can be selected long enough to allow for high unambiguous ranges in the pseudo-range measurements. For an elevation mask of 10° the slant range from a user anywhere in or above the CONUS lies somewhere between 36500 km and 40800 km. An unambiguous range of 4500 km will therefore be sufficient to exclude the need for any user input or other information to resolve for the ambiguity of the range measurements. As a result the range code lenght has to be at least 0.015 s. A truncated 18 stage maximum length code with a code period of 256*1023 = 261,888 bits can be chosen, in case of a chip rate of about 15 Mcps. This results in a code length of about 0.017 s.

Apart from the advantage of having the opportunity to transmit both a short Gold code for quick acquisition and a long range code for unambiguous range measurements another advantage of QPSK spreading modulation is the possibility to transmit the general information and the navigation message simultaneously but separated. In case of BPSK spreading modulation the navigation message can either be transmitted for only part of the time or has to be embedded in the general information.

For dual-channel QPSK the transmitted signal is given by

$$s(t) = \sqrt{P}\cdot d_g(t)\cdot c_G(t)\cdot\cos(\omega_0 t) + \sqrt{P}\cdot d_n(t)\cdot c_r(t)\cdot\sin(\omega_0 t) \qquad (5.17)$$

where

P = the total transmitted power

$d_g(t)$ = the general information

$c_G(t)$ = the Gold code to spread the general information

$d_n(t)$ = the navigation message

$c_r(t)$ = the range code to spread the navigation message

ω_0 = the carrier frequency

Ignoring the frequency and timing control arrangements, which will be discussed in Section 5.9.2, the transmitter block diagram looks like in Figure 5.3. Any non-linearity in the power amplifier will regenerate the $[(\sin x)/x]^2$ spectrum suppressed by the BPF. In practice a second filter after the power amplifier will have to be included.

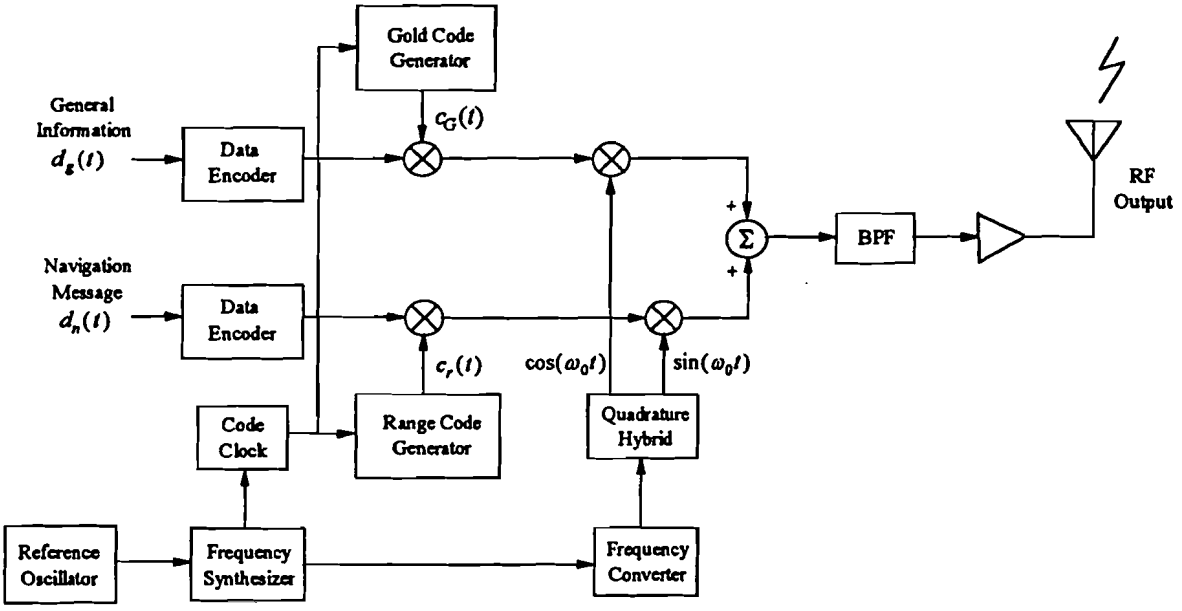

Figure 5.3 Transmitter block diagram

A summary of the signal parameters is given below.

Carrier frequency	:	6/4 GHz or 14/12 GHz
Spread spectrum modulation	:	Dual-channel QPSK direct sequence
Spreading code rate	:	15,345 Mcps (15,000*1023)
Spreading codes	:	1023 bit Gold code on information channel
		truncated 18-stage m-sequence, period 261,888 bits on range channel
RF bandwidth	:	30.69 MHz ($2*R_c$, using square root raised cosine filters with α=1)
Data modulation	:	BPSK
Data rates	:	> 1 kbps on information channel
		50 bps on range channel
Forward error correction	:	R=½, K=7 convolutional code with Viterbi soft decision

5.7.2 The navigation message

There should be sufficient information in the navigation message about the positions of the satellites to enable the receiver to perform all the necessary (position) calculations. It would be most efficient to include the ECEF position, velocity and acceleration of the transmitting satellite at a given time, as computed by the Master Control Station. To aid satellite tracking, the position of the other three satellites can also be included. Table 5.11 lists the parameters that should be part of the navigation message. Scale factors are included to indicate the attainable range of the parameters for the given bit allocations.

A more complicated alternative is to transmit a set of Kepler elements plus orbit correction parameters like it is done in GPS. This results in a longer navigation message and requires more computational power in the receiver. The different parameters that would be transmitted in this case and the procedure to compute the ECEF satellite coordinates from those parameters are given in Appendix 5. Assuming that comparable accuracies of satellite positions can be achieved, the first method is preferable.

To keep a reference time frame, all code generators should be reset on each Sunday at 00.00 UTC. The week number indicates the number of weeks that have passed since the beginning of system operation.

Table 5.11 Navigation message parameters

Group	Parameter	No. of bits	Scale factor	Information
Status	Satellite accuracy	4		Predicted user range accuracy
	Satellite health	6		Health status of the transmitting satellite
	Use/don't use flag	2		Warning in case of satellite malfunctioning
	Week No.	10		Number of the week in UTC time
Ephemeris	IODE	8		Issue of Data Ephemeris
	x (m)	32*	2^{-12}	Satellite position in ECEF coordinates
	y (m)	32*	2^{-12}	
	z (m)	32*	2^{-12}	
	$\dot{x}$ (m/s)	32*	2^{-23}	Satellite velocity in ECEF coordinates
	$\dot{y}$ (m/s)	32*	2^{-23}	
	$\dot{z}$ (m/s)	32*	2^{-23}	
	$\ddot{x}$ (m/s^2)	32*	2^{-23}	Satellite acceleration in ECEF coordinates
	$\ddot{y}$ (m/s^2)	32*	2^{-23}	
	$\ddot{z}$ (m/s^2)	32*	2^{-23}	
Ionospheric	α_0 (s)	8*	2^{-30}	For description see Appendix 6
correction	α_1 (s/semi-circle)	8*	2^{-27}	
parameters	α_2 (s/semi-circle^2)	8*	2^{-24}	
	α_3 (s/semi-circle^3)	8*	2^{-24}	
	β_0 (s)	8*	2^{11}	
	β_1 (s/semi-circle)	8*	2^{14}	
	β_2 (s/semi-circle^2)	8*	2^{16}	
	β_3 (s/semi-circle^3)	8*	2^{16}	
Positions of	t_{oa} (s)	8	2^{12}	Reference time of satellite positions
other system	x (m)	24*	2^{-4}	Satellite position in ECEF coordinates
satellites	y (m)	24*	2^{-4}	
	z (m)	24*	2^{-4}	
Status of other	Satellite accuracy	4		
system satellites	Satellite health	6		
	Use/don't use flag	2		

*Sign bit (+ or -) occupies the MSB

Parameters which enable a receiver to (partially) compensate for the ionospheric delay can be included in the navigation message. Appendix 6 describes how the receiver can compute the ionospheric time delay, based on data in the navigation message. As this requires quite some computational power from the receiver, it seems appropriate to include ionospheric correction parameters only in the navigation message of a C-band system, because the uncompensated ionospheric range error at Ku-band is smaller than 1 m anyway.

The data can be structured into words and subframes like in GPS. A telemetry word (TLM) and time-of-week word (TOW) can be included at the beginning of each subframe. An indication of the total length of the navigation message is given below, assuming the use of 30 bit words and 3 subframes of 12 words each.

Table 5.12 Possible structure of navigation message

Group	No. of bits	No. of words (including parity bits)
Status	22	1
Ephemeris	296	13
Ionosphere	64	3
System satellites	276	13
TLM and TOW	48	2

In case of a total length of 1080 bits and a bitrate of 50 bps it will take only 22 s to receive a complete navigation message, compared to 12.5 min in GPS.

5.7.3 Code acquisition

As discussed in Chapter 4, the process of synchronizing the local and received PN codes is accomplished in two stages. Initially a coarse alignment of the two PN codes is produced to within a small (typically half a chip) residual relative timing offset. This is known as the acquisition process. The tracking process then has to bring the two codes into a much finer synchronism (typically 1% of a chip).

As the acquisition process normally precedes the carrier tracking process, the carrier phase must be assumed to be unknown and therefore a non-coherent detector is needed. The most common acquisition system for a Direct Sequence Spread Spectrum system is the single dwell serial PN acquisition system shown in Figure 5.4. The phase of the local PN code is, at uniform increments in time, advanced by

typically half a chip. This sweep of the uncertainty region is a unidirectional search from one end of the region to the other in case of no a priori information about the received PN code phase. If some information about the code phase is available an expanding window serial search, starting in the region of highest code phase certainty, is more appropriate. A single dwell time detector can utilize either partial or full period code correlation, depending on the ratio of code length and dwell time.

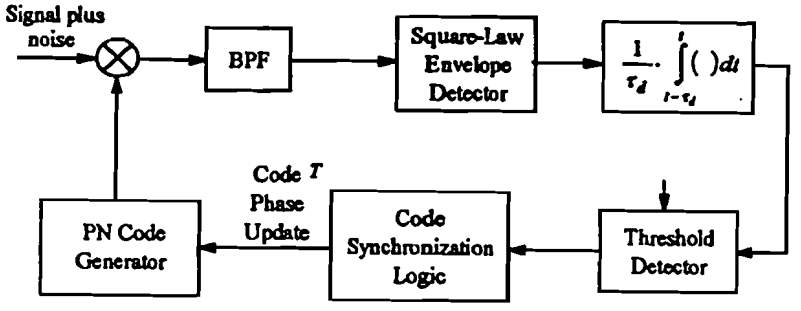

Figure 5.4 Block diagram of single dwell serial PN acquisition system

The received signal plus noise is actively correlated with the local PN code and then passed through a bandpass (pre-detection) filter with bandwidth B large enough to pass the data modulation and account for any remaining Doppler offset.

$$B = 2\cdot\left(|\Delta f_c| + R_b\right) \tag{5.18}$$

The filter output is then square-law envelope detected to remove the unknown information modulation and unknown carrier phase. The detector output is integrated for a fixed time τ_d (the dwell time) in an integrate-and-dump (I&D) circuit and then compared to a preset threshold. If the I&D output is above the preset threshold then a "hit" is declared. If the correct code phase has been determined then the search comes to an end and the detector is in lock. If the hit is a false alarm the search must continue after an extended dwell time $K\tau_d$, the "penalty" of obtaining a false alarm. Typically K is about 100. So at the true code phase position a correct detection can happen with probability P_D or no detection occurs with probability 1 - P_D. At any other code phase position a false alarm can happen with probability P_{FA}, causing a penalty of $K\tau_d$ sec, or no false alarm occurs with probability 1 - P_{FA}, resulting in a single dwell time of τ_d sec.

We assume that no code Doppler is present and that only one cell corresponds to a correct code phase alignment and that there are $q = 2L_c$ cells to be examined, where L_c is the code length in case of full period code correlation. The mean acquisition time is then given by [Simon, 1985]

$$\overline{T}_{ACQ} = \frac{2 + (2 - P_D)\cdot(q - 1)\cdot(1 + K\cdot P_{FA})}{2\cdot P_D}\cdot\tau_d \tag{5.19}$$

For the normal case of $q >> 1$ this results in

$$\overline{T}_{ACQ} = \frac{(2 - P_D)\cdot(1 + K\cdot P_{FA})}{2\cdot P_D}\cdot(q\cdot\tau_d) \tag{5.20}$$

In the presence of code Doppler the relative code phase between the received and the local PN codes will be varying during the dwell time resulting in a changing P_D. Also the search rate is sped up or slowed down depending on the sign of the code Doppler. This last effect results in a mean search update μ given by

$$\mu = \tfrac{1}{2} + \Delta f_c\cdot\tau_d + \Delta f_c\cdot K\cdot\tau_d\cdot P_{FA} \tag{5.21}$$

where $\frac{1}{2}$ is the step size of the search in absence of Doppler and Δf_c is the code Doppler in chips/sec. The mean acquisition time in the presence of Doppler is then given by

$$\overline{T}_{ACQ} = \frac{(2 - P_D)\cdot(1 + K\cdot P_{FA})\cdot L_c\cdot\tau_d}{2\cdot P_D\cdot[\frac{1}{2} + \Delta f_c\cdot\tau_d(1 + K\cdot P_{FA})]} = \frac{\overline{T}_{ACQ|\text{no code Doppler}}}{1 + \frac{1}{2}\cdot\Delta f_c\cdot\tau_d(1 + K\cdot P_{FA})} \tag{5.22}$$

In our system the effect of code Doppler generally can be neglected so equation 5.20 can be used.

For a given P_{FA} and pre-detection signal-to-noise ratio $SNR = C/BN_0$, P_D, P_{FA} and τ_d are related by [Simon, 1985]

$$P_D = Q\left[\frac{Q^{-1}(P_{FA}) - SNR\cdot\sqrt{B\cdot\tau_d}}{\sqrt{1 + 2\cdot SNR}}\right] \tag{5.23}$$

where no code Doppler is assumed to be present.

Since the PN code correlation curve is triangular over the interval $[-\tau_c, \tau_c]$ there are in reality several cells for which the signal could be considered present. For the worst case of two correlation points ¼ chip away from the correlation peak, SNR has to be reduced by 10 log $(0.75)^2$ = 2.5 dB. Also the effective probability of detection P_D' has to be used in computing the mean acquisition time where

$$P_D' = P_D + (1 - P_D)\cdot P_D = 2\cdot P_D - P_D^2 \tag{5.24}$$

Depending on the ratio of the pre-detection filter bandwidth B to the bit rate R_b there will be a power reduction when the data modulation passes through the filter. The influence of both chip misalignment and filtering loss can be accounted for by decreasing SNR with about 2 to 4 dB.

Mean acquisition times can be decreased by using more elaborate acquisition schemes. In a multiple dwell serial PN acquisition system the same phase cell is evaluated for 1 to N times with increasing dwell times for each evaluation. The first evaluation has a short integration time and leads to rejection of many incorrect cells. In case of a false alarm one or more evaluations with increasing integration times are used to reject these incorrect cells. The search is stopped and the correct cell is found after the thresholds have been exceeded during all N evaluations. As the average dwell time per cell will normally be shorter than in the single dwell system, mean acquisition time decreases. Other schemes which possibly lead to shorter acquisition times make use of matched filters or sequential detection. The use of a serial acquisition scheme in our system is proposed because of its simplicity.

5.7.4 Code tracking

As described in Section 4.5 a non-coherent delay-lock loop can be used for the code tracking process. The IF filters in the early, late and punctual channels have to be wide enough to pass the data modulation plus any Doppler frequency offset. The envelope detectors shown in Figure 4.4 are square-law detectors. The closed loop filter bandwidth has to be wide enough to track the dynamics of receiver motion. Normally B_n is chosen in the order of 1-10 Hz. Assuming that

1. The DS spreading modulation is BPSK or QPSK
2. Code self-noise and clock components can be ignored
3. The output noise at the discriminator output (= at the loop filter input) is Gaussian, which is allowed for $B_n << B_{IF}$
4. The early and late channels are precisely amplitude balanced

then the rms timing jitter in the delay measurement is given by [Spilker, 1977]

$$\sigma_\varepsilon = T_c \cdot \left[\frac{B_n}{2 \cdot C/N_0} \cdot \left(1 + \frac{2 \cdot B_{IF}}{C/N_0} \right) \right]^{\frac{1}{2}} \tag{5.25}$$

This will give a range error contribution of $\sigma_\varepsilon \cdot c$ meters.

One disadvantage of this loop is that improper balance of the early and late channels will offset the discriminator characteristic leading to non-zero voltages when the tracking error is zero. A tau-dither loop does not have this problem, but shows a loss in signal to noise ratio instead. As our system is already power limited a DLL will be used in the receiver design.

5.7.5 Receiver design

A block diagram of the main receiver elements is shown in Figure 5.5. After image reject filtering the received RF signal is down converted to a first IF frequency of f_{IF1} MHz. The output of the first mixer is passed through a BPF to reject the sum frequency output and out of band interference. Some sort of Gain Control is required in the IF chain to compensate for the variations in the incoming signal strength. These variations arise from the differences in satellites, antenna gain and path losses. The IF spread spectrum signal is then power divided for input to two acquisition loops, a Gold code tracking loop, a carrier tracking loop and a range channel despreader.

First the Gold code is acquired by means of a serial search method. The Gold code generator steps through the code phase cells in increments of half a chip until the correct phase is found. An early and late version of this code are the inputs to a non-coherent delay lock loop to align the Gold code more precisely. After code tracking has been established a punctual or "on time" version of the Gold code despreads the information channel IF signal. The output of IF bandpass filter 4 is a BPSK data-modulated carrier at f_{IF2} MHz. This signal is power divided and input to a Costas loop to generate a phase-locked version of the received carrier. The mixer output of the Costas loop I-channel is led to a BPSK demodulator to reproduce the transmitted general information. After carrier tracking has been established all carriers within the receiver are synchronized to the carrier VCO in the Costas loop.

Now synchronization of the range code can start. As the range code is epoch synchronous with the Gold code only 256 potential range code phase cells have to be evaluated, again using the serial search method. The range code generator is controlled by the code synchronization logic and code clock VCO which were employed in the Gold code acquisition and tracking. When the correct phase cell of the range code is found, the range code is already finely aligned so no second code tracking loop is needed. The output of IF bandpass filter 6 contains the data modulated range channel carrier. This signal is mixed with a phase shifted version of the synchronized carrier and the mixer output is led to a BPSK data modulator to reproduce the navigation message.

There is a wide range of usable IF frequencies in the receiver. The selection of IF frequencies should be based on the following criteria

1. The selected IF chain should be inexpensively implementable and reliable.
2. The IF's should avoid the frequency bands of known interference sources such as the TV, FM, CB and Amateur Radio bands.
3. To avoid the so called "self-jamming" phenomenon the IF after PN despreading (f_{IF2}) should not be an integer multiple of the clock frequency of the PN code.

As a starting point for f_{IF1} the common value of 70 MHz might be chosen and for f_{LO} 60 MHz, resulting in f_{IF2} of 10 MHz. The RF to IF conversion shown in Figure 5.5 is a single frequency conversion. It may be advisable to obtain the desired intermediate frequency f_{IF1} by dual frequency conversion.

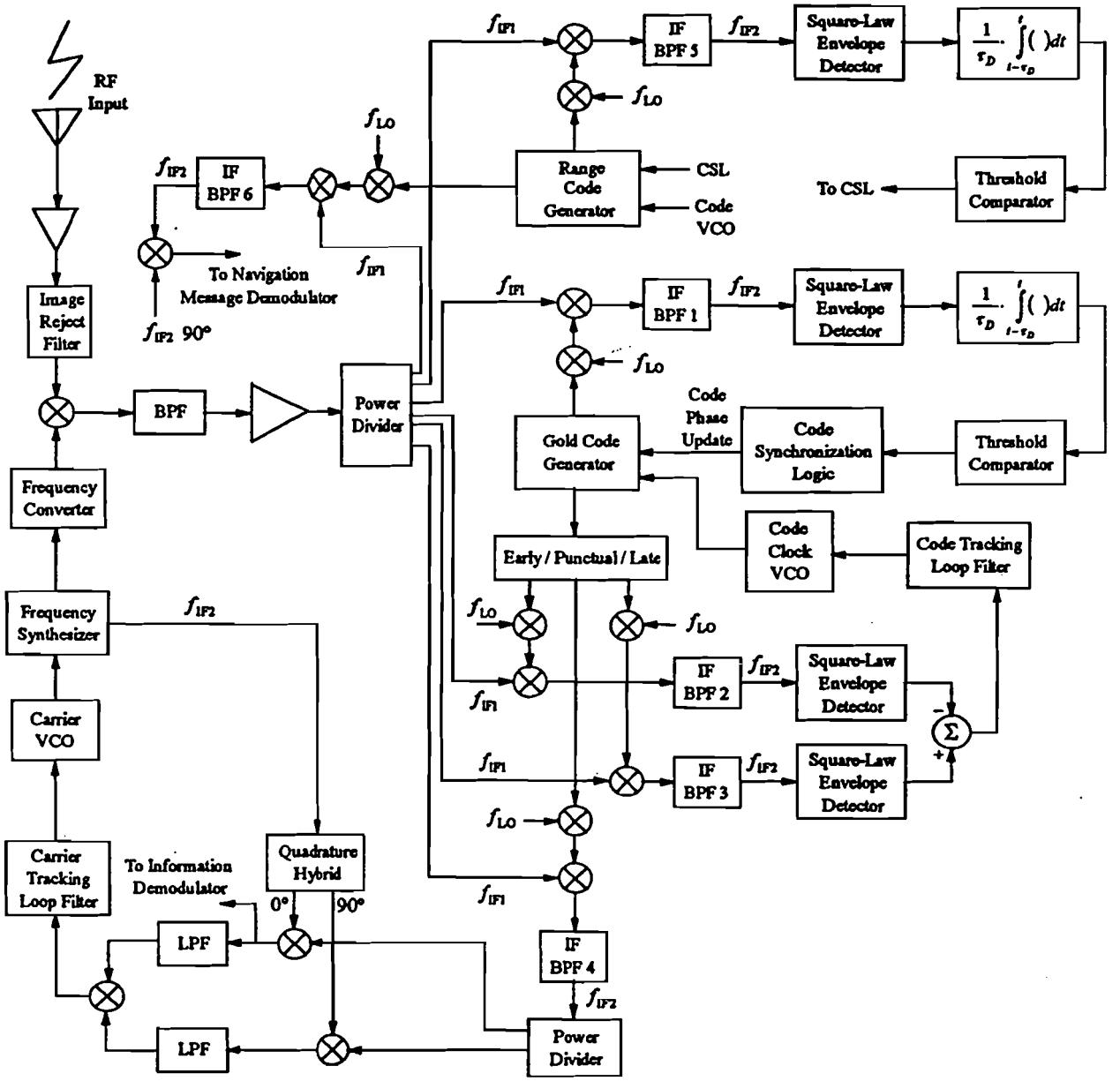

Figure 5.5 Dual-channel QPSK spread spectrum receiver

5.7.6 Functional antenna design

In this section it is assumed that the space segment of our system consists of four geostationary satellites. The task of the receiver antenna system is to receive signals from those four satellites simultaneously. The antenna system can either consist of one antenna with four independently steerable beams or four single-beam antennas. In order to achieve the datarates derived in Section 5.6 it is crucial that the underlying antenna gains of 8 dB for a C-band system and 12 dB for a Ku-band system are achieved. Another requirement is that the frequency response of the antenna has to support the required system bandwidth. In practice it is desirable that the antenna operate over the full 500 MHz frequency range used by C- or Ku-band satellites, so that a change in transponder channel is possible.

The antenna system has to be azimuth controlled such that it is always pointing to the south. Beam-steering is necessary as a user can be anywhere in or above the CONUS. As the orbital separation between two satellites can be as small as 22°, the antenna patterns have to show main lobes with narrow beamwidths. Beam-steering can either be done mechanically or electronically.

One option would be to use four mechanically steerable horn antennas. The beams have to be narrow in azimuth but are allowed to be quite broad in elevation. If the polarization of the incoming satellite signal is horizontal an *E*-plane sectoral horn can be used, for vertical polarization an *H*-plane sectoral horn is most appropriate. Pyramidal or conical horn antennas give narrow beamwidths in both planes but at the cost of larger aperture dimensions (also resulting in higher gain than required). As the antenna size has to be kept small, sectoral horns seem to be the best option. Assuming uniform phase across the horn aperture the gain of the horn can be approximated by [Pratt, 1986]

$$G = 0.81 \cdot \frac{4\pi \cdot a \cdot b}{\lambda^2} \tag{5.26}$$

where a is the width of the horn in the *H*- plane and b is the height of the horn in the *E*-plane respectively. *E*-plane horns give slightly narrower 3 dB beamwidths than *H*-plane horns. The beamwidths are given by [Stutzman, 1981]

$$\theta_{3dB} = 54 \cdot \frac{\lambda}{b} \quad \text{(degrees)} \tag{5.27}$$

and

$$\theta_{3dB} = 78 \cdot \frac{\lambda}{a} \quad \text{(degrees)} \tag{5.28}$$

respectively.

These equations only apply when both a and b have the size of at least one wavelength. Assuming a maximum beamwidth of 20° this leads to aperture dimensions ($a \times b$) of 7.5 cm by 20.2 cm at C-band and 2.5 by 6.8 cm at Ku-band, for an E-plane sectoral horn. In both cases the gain is 14.4 dB for an optimum horn. In reality gains will be lower, but they should be high enough to fulfill the gain requirements of 8 and 12 dB at C- and Ku-band respectively.

Disadvantages of the use of horn antennas include fairly high sidelobe levels (some improvement can be obtained by corrugating the inner walls), air-drag caused by their high profile and the need for sophisticated mechanics to steer them. Advantageous are their ruggedness and simplicity.

Another option is to use phased array antennas. In case of a uniformly excited equally spaced linear array the maximum broadside gain is approximated by [Stutzman, 1981]

$$G \approx \frac{2L}{\lambda} = \frac{2N \cdot d}{\lambda} \tag{5.29}$$

where $L = Nd$ is the array length, N and d are the number of and the distance between the array elements respectively. Equation 5.29 only applies to isotropic elements. Including the element pattern leads to a much more complicated formula but equation 5.29 will be used to get an indication of the necessary number of elements to achieve the desired gains. For $d = \frac{1}{2}\lambda$ this results in 8 (assuming the use of a corporate feed) and 16 elements at C- and Ku-band respectively. The 3-dB broadside beamwidth can be approximated by [Stutzman, 1981]

$$\theta_{3dB} = \frac{0.886 \cdot \lambda}{L} \quad \text{(radians)} \tag{5.30}$$

This results in 3-dB broadside beamwidths of 12.7° and 6.3° at C- and Ku-band respectively. The main beam pattern can be electronically scanned by applying a progressive phase difference between the elements given by [Stutzman, 1981]

$$\alpha = -\beta \cdot d \cdot \cos\theta_0 \tag{5.31}$$

where $\beta = 2\pi/\lambda$ and θ_0 is the direction of maximum gain (scan angle). As the beam is scanned from broadside ($\theta_0 = 90°$) the main beam broadens. The 3-dB beamwidth of a scanning array is given by [Balanis, 1982]

$$\theta_{3dB} = \cos^{-1}\left[\cos\theta_0 - 0.443\cdot\frac{\lambda}{L+d}\right] - \cos^{-1}\left[\cos\theta_0 + 0.443\cdot\frac{\lambda}{L+d}\right] \tag{5.32}$$

Short dipoles or microstrip patches may be used as array elements. The design of phased array antennas involves a great number of complexities. Mutual coupling between the elements has to be taken into account. Some degradation of the antenna pattern will always occur as a result of phase and amplitude errors and variations in element pattern [Rulf, 1987]. Major problem is to find low cost, low power, low loss, simple phase shifters which can be used in a PCB layout. For use on aircraft conformal arrays have to be considered. In this case the array element location must conform to the nonplanar surface of the airplane.

5.8 Control segment

The control segment of our system has to perform the following functions

- track the geostationary satellites
- provide timing and frequency control of the PN signals
- update the navigation message and general information

The control segment will consist of one Master Control Station (MCS) with uplink facilities and a number of monitor stations located throughout the continental US at precisely surveyed locations.

5.8.1 Satellite orbit determination

Positions of all satellites are calculated at the MCS. Each monitor station continuously makes pseudo-range measurements to all visible satellites and transmits these measurements to the MCS about twice per second via leased telephone lines. The positions of the satellites are determined by solving the following set of equations

$$\begin{aligned} PR_m^n - PR_r^n + CB_r = {} & [(X_m - X_n)^2 + (Y_m - Y_n)^2 + (Z_m - Z_n)^2]^{\frac{1}{2}} - \\ & [(X_r - X_n)^2 + (Y_r - Y_n)^2 + (Z_r - Z_n)^2]^{\frac{1}{2}} \end{aligned} \tag{5.33}$$

Known variables

PR_m^n = pseudo-range measurement from MCS to satellite n, n = 1,2,3,4(,5)

PR_r^n = pseudo-range measurement monitor station r to satellite n, n depends on location of monitor station and position of satellites

X_m, Y_m, Z_m = space coordinates of MCS

X_r, Y_r, Z_r = space coordinates of monitor station r

Unknown variables

CB_r = clock offset error between MCS and monitor station r

X_n, Y_n, Z_n = space coordinates of satellite n

Assuming the a space segment of four satellites the MCS has to solve for 12 satellite space coordinates plus clock offsets between each monitor station and the MCS. The minimum number of monitor stations is 5, assuming that every satellite is visible from each monitor station. This will probably not be the case, so a larger number is needed, also to have some redundancy to increase the confidence in the solution.

5.8.2 Timing and frequency control

Timing and frequency control of the transmitted PN signal is required to make the PN timing (epoch) and frequency of the signal resemble that of a signal whose clock and frequency references are located on the satellite rather than at the uplink ground station. The signal generation and timing equipment will consist of

- PN signal generator. The PN signal generator will use a clock signal at the chip rate frequency provided by the clock synthesizer to generate the PN code signal. This signal will be modulated with the general information.

- Clock synthesizer. A digital frequency synthesizer will be needed to provide the clock reference to the PN signal generator.

- IF signal generator. A frequency generator is required to generate a 70 MHz IF signal which is uplinked at C- or Ku-band to the satellite

- True time base. A true time generator (e.g. a high class GPS receiver) is required to measure the time delay between the received PN signal and UTC time (Δt_{RX}). This time difference will be used to

control clock and frequency offsets. The same generator will be used in the setup for every satellite to provide a common time frame.

- Time interval counter. A PC card can be used to measure the offset between the transmitted PN code and UTC time (Δt_{TX}).

The control software has to adjust the frequency of the clock synthesizer until the received time difference (Δt_{RX}) is equal to the transmitted time difference (Δt_{TX}). When this is established the transmitted signal has been advanced from UTC time by the same amount that the received signal is delayed from UTC time. As the uplink path from the ground station to the geostationary satellite is the same as the downlink path this will result in a signal that appears to be transmitted from the satellite synchronized with UTC.

The PN code generator will generate a signal, advanced from UTC time by an offset Δt_{TX} , which will be transmitted to a satellite. This time offset will be measured using the time interval counter so

$$\Delta t_{TX} = t_{TX} - t_{\mathrm{UTC}} \tag{5.34}$$

The signal will be received with a time offset Δt_{RX} determined by the range R between the satellite and the ground station. The time delay is measured relative to UTC time using the true time generator.

$$\Delta t_{RX} = t_{\mathrm{UTC}} - t_{RX} = t_{\mathrm{UTC}} - t_{TX} + 2 \cdot R/c \tag{5.35}$$

A control law will be needed to adjust the frequency F_c of the clock synthesizer to drive the difference between the received time offset and the transmitted time offset to zero. The transmission time t_{TX} is adjusted through the PN signal generator by the integral of the frequency offset from the nominal frequency.

$$\frac{dt_{TX}}{dt} = \frac{\delta F_c}{F_{c,0}} \tag{5.36}$$

In synchronization the transmission and receive times are offset by the same amount of time

$$\begin{aligned} t_{TX} &= t_{UTC} + R/c \\ t_{RX} &= t_{UTC} - R/c \end{aligned} \tag{5.37}$$

In the following analysis the signal is modeled without the data modulation, only the in-phase component of the carrier is considered and the signal amplitude is normalized to unity at each point. The signal transmitted from the ground station then has the form

$$s_{UT}(t) = C(t + \tau_c)\cdot\cos[\omega_u \cdot t + \delta f_c \cdot t + \theta_0] \tag{5.38}$$

where

$C(t)$ = the Gold code from the PN signal generator
τ_c = the time offset introduced by the clock synthesizer to synchronize the signal (sec)
ω_u = the uplink carrier frequency (rad/sec)
δf_c = the IF frequency offset introduced by the IF signal generator to control the signal frequency (Hz/sec)
θ_0 = an arbitrary phase (rad)

During the propagation from the uplink ground station to the receiver the signal is subject to group delay which affects both the code and carrier, and frequency translation, which only affects the carrier. The signal received by the satellite is given by

$$s_{UR}(t) = C(t + \tau_c - \tau_1)\cdot\cos[\omega_u \cdot (t - \tau_1) + \delta f_c \cdot (t - \tau_1) + \theta_1] \tag{5.39}$$

where

τ_1 = R_u/c
R_u = the range from the uplink ground station to the satellite (m)
c = the speed of light (m/s)
θ_1 = an arbitrary phase (rad)

The signal transmitted by the satellite is given by

$$s_{DT}(t) = C(t+\tau_c-\tau_1-\tau_2)\cdot\cos[\omega_u \cdot (t-\tau_1-\tau_2) + \delta f_c \cdot (t-\tau_1-\tau_2) + (\omega_d - \omega_u)\cdot t + \theta_2] \tag{5.40}$$

where

τ_2 = the group delay through the satellite (sec)
ω_d = the downlink carrier frequency (rad/sec)
θ_2 = an arbitrary phase (rad)

The signal received by the receiver is given by

$$s_{DR}(t) = C(t+\tau_c-\tau_1-\tau_2-\tau_3)\cdot\cos[\omega_u\cdot(t-\tau_1-\tau_2-\tau_3) + \delta f_c\cdot(t-\tau_1-\tau_2-\tau_3) + (\omega_d-\omega_u)\cdot(t-\tau_3) + \theta_3] \tag{5.41}$$

where

τ_3 = R_d/c

R_d = the range from the satellite to the receiver (m)

θ_3 = an arbitrary phase (rad)

The carrier frequency ω_r of the received signal is given by the time derivative of the argument of the cosine

$$\omega_r = \omega_u\cdot(1 - R_u'/c - R_d'/c) + \delta f_c\cdot(1 - R_u'/c - R_d'/c) + (\omega_d - \omega_u)\cdot(1 - R_d'/c) \tag{5.42}$$

where

τ_1' = R_u'/c is the uplink Doppler shift

τ_2' = 0 when the satellite group delay is assumed to be constant

τ_3' = R_d'/c is the downlink Doppler shift

The apparent carrier Doppler shift is

$$\omega_D = \omega_r - \omega_d = -R_d'/c\cdot(\delta f_c + \omega_d) + \delta f_c - R_u'/c\cdot(\delta f_c + \omega_u) \tag{5.43}$$

The first term is a function of the receiver position and dynamics. The other terms are the same for each receiver. The code rate τ' of the received signal is given by the time derivative of the argument of $C(t)$

$$\tau' = 1 - R_u'/c - R_d'/c + \tau_c' \tag{5.44}$$

where τ_c' is the relative frequency offset of the clock synthesizer. The apparent code Doppler rate is given by

$$\tau_D' = \tau' - 1 = - R_u'/c - R_d'/c + \tau_c' \tag{5.45}$$

In a receiver carrier tracking can be used to support the code tracking. Based on the frequency gradient of the carrier tracking loop (which is determined by the Doppler shift), the control signal of the VCO in

the code tracking loop can be computed. This allows for the use of a low-order delay lock loop with a narrow closed loop bandwidth. The code rate is obtained from the carrier Doppler shift by dividing by the carrier frequency. The "aided code loop rate" error is then given by

$$\tau'_{ERR} = \tau'_D - \omega_D/\omega_d = -\delta f_c/\omega_d + R'_u/c\cdot[(\omega_u+\delta f_c)/\omega_d - 1] + R'_d/c\cdot(\delta f_c/\omega_d) + \tau'_c \qquad (5.46)$$

The purpose of the timing and frequency control was to synchronize the signal relayed by a transponder of a geostationary communication satellite with UTC time so that it resembles a signal from a geostationary navigation satellite. To accomplish this the clock synthesizer is used to synchronize the code phase of the PN signal with UTC time and the IF frequency generator is used to synchronize the received frequency.

The frequency offset of the IF frequency generator is derived by setting equation 5.46 to zero. Ignoring errors to be corrected due to group delays in the satellite and the receiver, the required time offset τ_c is equal to R_u/c. Assuming $\tau'_c = R'_u/c$, equation 5.46 can be written as

$$\tau'_{ERR} = -\frac{\delta f_c}{\omega_d} + \frac{R'_d}{c\cdot\omega_d}\cdot\delta f_c + \frac{R'_u}{c\cdot\omega_d}\cdot(\omega_u + \delta f_c) \qquad (5.47)$$

Neglecting second order effects τ'_{ERR} equals zero when

$$\delta f_c = \omega_u \cdot R'_u/c \qquad (5.48)$$

Both the frequency of the PN code generator and the 70 MHz IF frequency can be adjusted by means of the closed loop control system shown in Figure 5.7. Two control loops are assumed here. The first control loop provides time synchronization control through adjusting the clock synthesizer's nominal frequency reference. The steps to be performed in computing the code phase adjustment are

1. Calculate $del = \Delta t_{TX} - \Delta t_{RX}$
2. Adjust F_c : $\delta F_c = K(\delta F_c , del)$

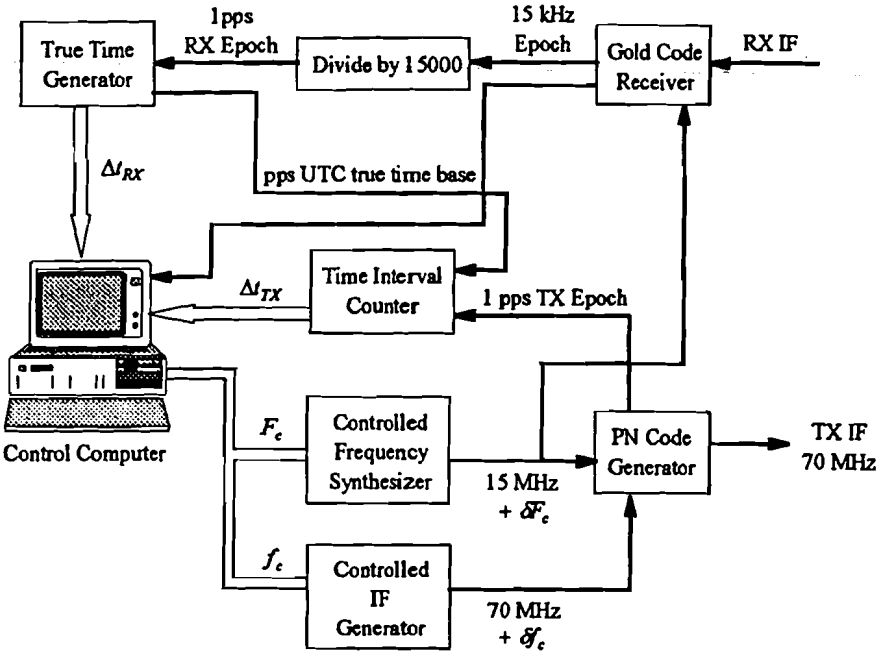

Figure 5.7 Closed loop control system

The second control loop provides carrier frequency control to maintain the carrier Doppler shift synchronized with the code Doppler shift by adjusting the IF signal generator 70 MHz frequency reference. The steps to be performed in the adjustment process are

1. Measure the delta-range dR
2. Adjust f_c : $\delta f_c = K(\delta f_c , dR , \delta F_c)$

The design of the control algorithms is outside the scope of this study. By careful design of the control loops it should be possible to maintain the satellite signal synchronous to UTC within 10 ns (1σ). The range equivalent of this time synchronization error is 3 m (1σ).

5.9 System performance analysis

5.9.1 Error budget

The error budget for both a C-band and Ku-band system is given in Table 5.13.

Table 5.13 Error budget

Error source	C-band	Ku-band
Time synchronization error	3.0	3.0
Ephemeris error	3.0	3.0
Tropospheric delay	2.0	2.0
Ionospheric delay	1.0	0.1
Multipath	1.0	1.0
Tracking error	0.5	0.6
Quantization error	0.2	0.2
URE (1σ)	4.9	4.8
Range of HDOP	5.3 - 13.4	7.3 - 16.0
Horizontal accuracy (2drms)	51.9 - 131.3	70.1 - 153.6

URE = User Range Error HDOP = Horizontal Dilution of Precision

drms = distance root mean square

All entities in meters, except HDOP (dimensionless)

Time synchronization - Closed loop timing control is assumed. As indicated in Section 5.8.2 the remaining range error is about 3 m, comparable to the satellite clock error in GPS

Ephemeris error - Satellites have to be tracked continuously by a network of monitor stations on well-defined locations in the US. Remaining ephemeris errors should be less than 3 m.

Multipath - Because of the cross-correlation properties of Gold codes, multipath can only lead to range errors in case of a difference in path length of less than 1.5 chip, which is equivalent to 30 m for a code rate of about 15 Mcps. Careful antenna design should be sufficient to avoid multipath errors. Even if some vehicle surface reflections still alter the code delay measurements, resulting range errors should be less than 1 m.

Tropospheric delay - Using similar models as in GPS, the residual range error caused by the tropospheric delay should be less than 2.0 m

Ionospheric delay - Both for C-band and Ku-band carrier frequencies the influence of the ionospheric delay is much smaller than in the GPS case, because the resulting range error is inversely proportional to the square of the frequency. Uncorrected zenith values for the ionospheric range error are 1.26 and 0.14 m for C-band and Ku-band frequencies respectively. Residual range errors over the entire range of elevations after modeling will be less than 1.0 and 0.1 m respectively.

Quantization error - In a digital implementation, pseudo-range measurements of a PN code can easily be quantized to 0.01 of a PN code chip. Based on a 15.3 Mcps code rate this gives a quantization size of 0.2 m, an upper limit for the quantization error.

Tracking error - Using equation 5.25 the range error caused by the timing jitter in the delay measurement can be calculated using the following parameters

T_c = $6.52*10^{-8}$ s
B_n = 1 - 10 Hz
C/N_0 = 44.5 - 47.5 dB-Hz , C-band
44.5 - 52.5 dB-Hz , Ku-band
B_{IF} = 5 - 36 kHz , C-band
7 - 68 kHz , Ku-band

The tracking error of the C-band system will be in the range of 0.06 to 0.49 m. For a Ku-band system this range will be 0.04 to 0.63 m. In Table 5.13 worst case tracking errors have been taken.

HDOP - For a range error of 5 m the altimeter error to range error ratio will be about 4. The range of HDOP values for both the C-band and Ku-band system is obtained from Table 5.8.

5.8.2 Acquisition time

As described in Section 5.7.3, the mean acquisition time depends on the carrier to noise ratio of the incoming signal, the symbol rate of the data modulation, the code length of the spreading code, the expected carrier Doppler shift, the pre-detection losses in the receiver and the probabilities of detection and false alarm. Using equations 5.20, 5.23 and 5.24, the mean acquisition time for the communication part of the system can be calculated using the following parameters

C/N_0 = 44.5 - 47.5 dB-Hz , C-band

		44.5 - 52.5 dB-Hz , Ku-band
R_b	=	2 - 14 kbps, C-band
		2 - 40 kbps, Ku-band
code length	=	1023 chips
B	=	5 - 36 kHz , C-band
		7 - 104 kHz , Ku-band
P_{fa}	=	10^{-3} - 10^{-6}
P_D'	=	0.9
pre-detection loss	=	2 - 4 dB

Acquisition times have been calculated for a large number of combinations of these parameters. A summary is given in the Tables 5.14 and 5.15.

Table 5.14 Mean acquisition time for information channel in C-band system

C/N_0 (dB-Hz)	R_b (kbps)	Doppler (kHz)	Loss (dB)	P_{fa}	$\overline{T}_{ACQ}$ (s)
47.5	2	0.5	2	10^{-3}	0.14
47.5	2	0.5	2	10^{-6}	0.23
47.5	2	0.5	4	10^{-3}	0.30
47.5	2	0.5	4	10^{-6}	0.51
47.5	2	4	2	10^{-3}	0.26
47.5	2	4	2	10^{-6}	0.45
47.5	2	4	4	10^{-3}	0.58
47.5	2	4	4	10^{-6}	1.04
47.5	14	0.5	2	10^{-3}	0.51
47.5	14	0.5	2	10^{-6}	0.95
47.5	14	0.5	4	10^{-3}	1.21
47.5	14	0.5	4	10^{-6}	2.27
47.5	14	4	2	10^{-3}	0.62
47.5	14	4	2	10^{-6}	1.15
47.5	14	4	4	10^{-3}	1.46
47.5	14	4	4	10^{-6}	2.77
44.5	2	0.5	2	10^{-3}	0.45
44.5	2	0.5	2	10^{-6}	0.77
44.5	2	0.5	4	10^{-3}	1.00
44.5	2	0.5	4	10^{-6}	1.77
44.5	2	4	2	10^{-3}	0.88
44.5	2	4	2	10^{-6}	1.59
44.5	2	4	4	10^{-3}	2.04
44.5	2	4	4	10^{-6}	3.80
44.5	7	0.5	2	10^{-3}	1.05
44.5	7	0.5	2	10^{-6}	1.94
44.5	7	0.5	4	10^{-3}	2.48
44.5	7	0.5	4	10^{-6}	4.66
44.5	7	4	2	10^{-3}	1.46
44.5	7	4	2	10^{-6}	2.74
44.5	7	4	4	10^{-3}	3.49
44.5	7	4	4	10^{-6}	6.64

Table 5.15 Mean acquisition time for information channel in Ku-band system

C/N_0 (dB-Hz)	R_b (kbps)	Doppler (kHz)	Loss (dB)	P_{fa}	$\overline{T}_{ACQ}$ (s)
52.5	2	1.5	2	10^{-3}	*0.07*
52.5	2	1.5	2	10^{-6}	*0.07*
52.5	2	1.5	4	10^{-3}	*0.08*
52.5	2	1.5	4	10^{-6}	0.09
52.5	2	12	2	10^{-3}	*0.09*
52.5	2	12	2	10^{-6}	0.11
52.5	2	12	4	10^{-3}	0.14
52.5	2	12	4	10^{-6}	0.25
52.5	40	1.5	2	10^{-3}	0.15
52.5	40	1.5	2	10^{-6}	0.27
52.5	40	1.5	4	10^{-3}	0.35
52.5	40	1.5	4	10^{-6}	0.65
52.5	40	12	2	10^{-3}	0.18
52.5	40	12	2	10^{-6}	0.33
52.5	40	12	4	10^{-3}	0.43
52.5	40	12	4	10^{-6}	0.80
44.5	2	1.5	2	10^{-3}	0.57
44.5	2	1.5	2	10^{-6}	1.01
44.5	2	1.5	4	10^{-3}	1.30
44.5	2	1.5	4	10^{-6}	2.36
44.5	2	12	2	10^{-3}	1.81
44.5	2	12	2	10^{-6}	3.41
44.5	2	12	4	10^{-3}	4.35
44.5	2	12	4	10^{-6}	8.32
44.5	7	1.5	2	10^{-3}	1.17
44.5	7	1.5	2	10^{-6}	2.17
44.5	7	1.5	4	10^{-3}	2.77
44.5	7	1.5	4	10^{-6}	5.22
44.5	7	12	2	10^{-3}	2.38
44.5	7	12	2	10^{-6}	4.54
44.5	7	12	4	10^{-3}	5.78
44.5	7	12	4	10^{-6}	11.13

The acquisition times in italics are the result of a dwell time of exactly one code period and an effective probability of detection larger than 0.9

The mean acquisition time of the positioning part of the system is the sum of the mean time to acquire the Gold code and the mean time to acquire the range code. As the data modulation rate on the range channel is much lower than on the information channel and only 256 instead of 2046 phase cells need to be examined, the time to acquire the range code could be much lower than the time to acquire the Gold code. For the C-band system mean acquisition times would be in the range of 0.02 - 0.72 s and for the Ku-band system this range would be 0.01 - 1.47 s. For both ranges however dwell times would be (much) less than one code period, so partial correlation in the detection scheme would be necessary. As this can more easily lead to a false code lock on, which would result in incorrect range measurements, full code period correlation is chosen instead.

In this case the dwell time τ_d is equal to 256*1023/15,345,000 = 0.01707 s. For any combination of carrier to noise ratio, Doppler shift and probability of false alarm, the effective probability of detection will be 1. As a result the mean times to acquire the range code are the same for both the C-band and Ku-band system, 1.09 s and 1.20 s for probabilities of false alarm of 10^{-3} and 10^{-6} respectively. As in most cases the mean time to acquire the Gold code will be less than 2 s, the total acquisition time for the range channel will be less than 4 s.

Chapter 6 Conclusions and recommendations

The horizontal position accuracy of a satellite positioning system is determined by the combination of the user range error and the geometry of the satellites, reflected by the Horizontal Dilution Of Precision. Of the currently existing satellite positioning systems only GPS has a continuous world-wide availability. Operation of TRANSIT will stop in 1996 and the viability of GLONASS is highly questionable.

The civil GPS user community is already large and growing continuously. The horizontal position error of the Standard Positioning Service meant for civil (= non-authorized) users is artificially kept high at 100 m by employing Selective Availability. Accuracies between 10 and 20 m are already achievable using some form of differential GPS and will be feasible world-wide once the INMARSAT geostationary overlay will come in use.

The optimal number of satellites for an integrated communication and positioning system to cover the Continental US is four. The use of only three satellites would result in position errors about two times as high. Although using five satellites could possibly lead to an improvement of position accuracy of about 20%, this advantage does not outweigh the resulting increase in system cost and complexity. For an elevation mask of 10°, 90% HDOP ranges are 5.3 - 13.0 and 7.3 - 15.0 based on optimal C- and Ku-band satellite constellations respectively. The position error will mainly be in the N-S direction.

At C-band, received carrier to noise ratios are 44.5 and 47.5 dB-Hz for ITU Region 1 & 3 and ITU Region 2 satellites, allowing maximum data rates of 3.7 and 7.4 kbps respectively. At Ku-band, there is a much wider range of carrier to noise ratios of 44.5 to 52.5 dB-Hz, leading to maximum data rates of 3.7 to 23.4 kbps. System operation at Ku-band allows for the use of higher data rates at the expense of a decrease in position accuracy compared to C-band operation.

By using QPSK spread spectrum modulation the general information and the navigation message are received on two different channels and total acquisition time can be less than 4 s. A complete navigation message can be received in less than 30 s.

Key to system operation is the possibility to design and produce antenna systems with four independent beams that achieve the required gains of 8 or 12 dB at C- or Ku-band respectively. Intensive research is required in the antenna area, keeping in mind that the antenna system has to be both low-cost and low-profile.

Assuming the use of closed loop timing and frequency control of the satellite signals, user range errors as low as 5 m are achievable. This will lead to 90% ranges of horizontal accuracy (2 drms) of 51.9 - 131.3 m and 70.1 - 153.6 m for optimal C- and Ku-band satellite constellations respectively. Compared to the 100 m accuracy of GPS as specified in the 1992 Federal Radionavigation Plan, these accuracies are certainly acceptable for system use in cars and aircraft.

The availability and cost of transponder bandwidth on geostationary satellites (both C- and Ku-band) needs to be examined to determine whether it is possible to implement the most favorable satellite constellations from a positioning point of view.

A large part of the components that make up the receiver design will already be available in blocks, i.e. standard or application specific ICs that can perform the different tasks of the receiver. To keep the total cost and complexity of the receiver as low as possible, it is necessary to inventory which off-the-shelf components can be used, possibly considering slight deviations from the original design. When designing the transmitters and receivers and choosing the final signal parameters, careful attention should be paid to the CCIR rules on Radiodetermination Satellite Services and other CCIR restrictions on power levels etc.

The feasibility of using C-band transponders in our system is determined very much by the interference levels that can be expected throughout the Continental US from terrestrial microwave transmitters. Some sort of "interference map" that locates and quantifies these sources of interference is required to determine whether a C-band system is feasible or not.

Depending on the design of the Kalman filter in the navigation processor of the receiver, the use of delta-range measurements and/or an external user velocity input may be advantageous. The impact of including these extra inputs on the position accuracy needs to be determined.

System implementation requires the lease of transponder bandwidth. To justify such a multi-million dollar investment, system operation first has to be examined by means of computer simulations. Afterwards tests of the transmitting and receiving equipment should be carried out by using terrestrial transmitters and a receiver installed in an aeroplane.

As an altimeter is already installed in every aeroplane, this would be the most obvious altitude input source. For system operation in cars, the use of so called digital terrain maps needs to be considered. Research is required to compare the altitude accuracy and cost of such a map with that of an altimeter. Drawback of a digital terrain map is the huge memory requirement in the receiver, but installation of an altimeter in a car may lead to all sort of practical problems.

From the marketing point of view, one big advantage of our system is that simpler and therefore less expensive receivers can be build and sold to users who don't want to make use of the positioning capabilities offered by the system but are only interested in the other information provided by the system. Should system implementation take place in the US and become a success, then building a similar system in Europe based on four different satellites is a possible next step.

References

M. Ananda,
"The Global Positioning System (GPS) constellation and coverage",
The NAVSTAR GPS System, AGARD Lecture Series No. 161, September 1988

M. Ananda,
"The Global Positioning System (GPS) accuracy, system error budget, space and control system overview",
The NAVSTAR GPS System, AGARD Lecture Series No. 161, September 1988

C.A. Balanis,
Antenna theory,
New York: Wiley, 1982

J. Beser and A. Balendra,
"Integrated GPS/GLONASS navigation results",
Proceedings of ION GPS-93, Salt Lake City, UT, pp. 171-183, September 1993

H.D. Black,
"An easily implemented algorithm for the tropospheric range correction",
Journal of geophysical research, Vol. 83, No. B4, pp. 1825-1828, 1978

W.F. Blanchard,
"Civil satellite navigation and location systems",
Journal of Navigation, Vol. 42, No. 2, pp. 202-220, 1989

F.J.J. Brouwer et al.,
GPS - Navigatie en geodetische puntsbepaling met het Global Positioning System,
Delft: Delft University of Technology, Faculty of Geodetic Engineering, 1989

D.J. Curtin & S.B. Salamoff,
"The Orion satellite system",
13th AIAA International Communication Satellite Systems Conference, pp. 375-385, 1990

P. Daly
"Aspects of the Soviet Union's GLONASS satellite navigation system",
The Journal of Navigation, Vol. 41, No. 2, pp. 186-197, 1988

P. Daly et al.,
"Recent advances in the implementation of GNSS",
Proceedings of ION GPS-93, Salt Lake City, UT, pp. 433-440, September 1993

R.P. Denaro and R.M. Kalafus,
"Differential operation of NAVSTAR GPS for enhanced accuracy",
The NAVSTAR GPS System, AGARD Lecture Series No. 161, September 1988

P. Diederich,
"The development of civil satellite navigation in Europe",
NAVIGATION: Journal of The Institute of Navigation, Vol. 36, No. 1, pp. 127-136, Spring 1989

A.J. van Dierendonck et al.,
"The GPS navigation message",
NAVIGATION: Journal of The Institute of Navigation, Vol. 25, No. 1, pp. 55-73, Spring 1978

A.J. van Dierendonck et al.,
"Inmarsat-3 navigation signal C/A code selection and interference analysis",
NAVIGATION: Journal of The Institute of Navigation, Vol. 39, No. 4, pp. 445-461, Winter 1992-1993

A.J. van Dierendonck et al.,
"Evolution to civil GNSS taking advantage of geostationary satellites",
Institute of Navigation: Proceedings of the 49th Annual Meeting "Future global navigation and guidance", Cambridge, MA, pp. 231-239, June 1993

R.C. Dixon,
Spread spectrum systems, second edition
New York: Wiley, 1984

W.A. Fees and S.G. Stephens,
"Evaluation of GPS ionospheric time-delay model",
IEEE Transactions on aerospace and electronic systems, Vol. AES-23, No. 3, pp. 332-338, May 1987

B. Forssell
Radionavigation systems.
London: Prentice Hall, 1991

W. Gracey,
Measurement of aircraft speed and altitude,
NASA Reference publication 1046, 1980

T.T. Ha,
Digital satellite communications, second edition,
New York: McGraw-Hill, 1990

H.S. Hopfield,
"Tropospheric effect on electromagnetically measured range: Prediction from surface weather data",
Radio Science, Vol. 6, No. 3, pp. 357-367, 1971

N. Ivanov and V. Salischev,
"The GLONASS System - An overview",
The Journal of Navigation, Vol. 45, No. 2, pp. 175-182, 1992

C.D. de Jong,
GPS - Satellite orbits and atmospheric effects.
Delft: Delft University of Technology, Faculty of Geodetic Engineering, February 1991

William M. Kaula,
Theory of satellite geodesy,
Waltham: Blaisdell, 1966

V.N. Kazantsev, M.F. Reshetnev, A.G. Kozlov and V.F. Cheremisin,
"Current status, development program and performance of the GLONASS system",
Proceeding of ION GPS-92, Albuquerque, NM, pp. 139-144, September 1992

M. Kihara and T. Okada,
"A satellite selection method and accuracy for the global positioning system",
Navigation (USA), Vol. 31, No. 1, pp. 8-20, 1984

G.V. Kinal and J.P. Singh,
"An international geostationary overlay for GPS and GLONASS",
NAVIGATION: Journal of The Institute of Navigation, Vol. 37, No. 1, pp. 81-93, Spring 1990

G.V. Kinal and J. Nagle,
"Geostationary augmentation of global satellite navigation - 1991 update",
The Journal of Navigation, Vol. 45, No. 2, pp. 166-174, Summer 1992

G.V. Kinal and A.J. van Dierendonck,
"Susceptibility of Inmarsat navigation payloads to jamming and spoofing: Fact or (science) fiction?",
Institute of Navigation: Proceedings of National Technical Meeting "Evolution through integration of current and emerging systems", San Francisco, CA, pp. 459-467, January 1993

J.A. Klobuchar,
"Ionospheric time-delay algorithm for single-frequency GPS users",
IEEE Transactions on aerospace and electronic systems, Vol. AES-23, No. 3, pp. 325-331, May 1987

M. Long,
The 1992/1993 World satellite almanac,
Winter Beach: MLE Inc., 1992

G. Maral and M. Bousquet,
Satellite communications systems, second edition
Chichester: Wiley, 1993

K. McDonald and J. Nussbaum,
"The feasibility of using small, low-cost satellites (Econosats) as an augmentation to GNSS and as an eventually fully capable GNSS",
Institute of Navigation: Proceedings of National Technical Meeting "Evolution through integration of current and emerging systems", San Francisco, CA, pp. 605-612, January 1993

R.J. Milliken and C.J. Zoller,
"Principle of operation of NAVSTAR and system characteristics",
Navigation (USA), Vol. 25, No. 2, pp. 3-14, 1978

Navsys Corporation,
Geostationary satellite navigation R&D study final report,
INMARSAT contract study INM/90-521/PR, January 1991

P.W. Nieuwejaar,
"GPS signal structure",
The NAVSTAR GPS System, AGARD Lecture Series No. 161, September 1988

L. Ott and W. Blanchard,
"The Starfix satellite navigation system",
IEE Fourth International Conference on Satellite systems for mobile communications and navigation,
London, pp. 208-213, October 1988

T. Pratt & C.W. Bostian,
Satellite communications,
New York: Wiley, 1986

C. Rosetti and C. Carnebianca,
"NAVSAT: A global satellite based navigation system",
IEEE PLANS 1986, pp. 5-12

G.J.J. Ruijgrok,
Elements of airplane performance,
Delft: Delft University Press, 1990

B. Rulf and G.A. Robertshaw,
Understanding antennas for radar, communications and avionics,
New York: Van Nostrand Reinhold, 1987

G. Seeber,
Satellite Geodesy,
Berlin: Walter de Gruyter, 1993

M.K. Simon, J.K. Omura, R.A. Scholtz & B.K. Levitt,
Spread spectrum communications, Volume III,
Rockville: Computer Science Press, 1985

E.K. Smith and S. Weintraub,
"The constants in the equation for atmospheric refractive index at radio frequencies",
Proceedings of the IRE, pp. 1035-1037, 1953

J.J. Spilker,
Digital commununications by satellite,
Englewood Cliffs: Prentice-Hall, 1977

J.J. Spilker,
"GPS signal structure and performance characteristics",
NAVIGATION: Journal of The Institute of Navigation, Vol. 25, No. 1, pp. 29-54, Spring 1978

T.A. Stansell
The TRANSIT Navigation Satellite System
Magnavox, 1978

B.A. Stein,
"Satellite selection criteria during altimeter aiding of GPS",
GPS: Papers published in NAVIGATION, Vol. III, Washington, 1986

W.L. Stutzman and G.L. Thiele,
Antenna theory and design,
New York: Wiley, 1981

G.D. Thayer,
"An improved equation for the radio refractive index of air",
Radio Science, Vol. 9, No. 10, pp. 803-807, 1974

US Department of Defense
Federal Radionavigation Plan 1992
Washington DC.: January 1993

D. Wells et al.,
Guide to GPS positioning,
Fredericton: Canadian GPS Associates, 1986

M. Wiedemer,
"GPS Development Program Status",
Proceedings of ION GPS-93, Salt Lake City, UT, pp. 3-22, September 1993

D. van Willigen,
Radioplaatsbepaling.
Delft: Collegedictaat ET03-31 TU Delft, 1993

G.W. Zachmann,
"Status, plans and potential capabilities of geostationary GPS transponders",
Proceeding of ION GPS-92, Albuquerque, NM, pp. 159-165, September 1992

R.E. Ziemer & R.L. Peterson,
Digital communications and spread spectrum,
New York: Macmillan, 1985

Appendix 1 Details on GPS navigation message

Table A1.1 Subframe 1 parameters

Parameter	Information
Code on L_2	Indicates if P code or C/A code is transmitted on L_2
Week No.	Number of the week in GPS time
Data flag for L_2 P-code	Modulation of navigation message on the P-code on L_2 (y/n)
Satellite accuracy	Predicted user range accuracy after double frequency ionospheric correction
Satellite health	Health status of the transmitting satellite
T_{GD}	Estimated group delay differential
t_{oc}, a_{f2}, a_{f1} and a_{f0}	Satellite clock correction parameters
IODC	Issue of Data Clock

Table A1.2 Ephemeris parameters (subframes 2 and 3)

Parameter	Information
IODE	Issue of Data Ephemeris
C_{rs}	Amplitude of the sine harmonic correction term to the orbit radius
Δn	Mean motion difference from computed value
M_0	Mean anomaly at reference time
C_{uc}	Amplitude of the cosine harmonic correction term to the argument of latitude
e	Eccentricity
C_{us}	Amplitude of the sine harmonic correction term to the argument of latitude
$(A)^{1/2}$	Square root of the semi-major axis
t_{oe}	Reference time of ephemeris
C_{ic}	Amplitude of the cosine harmonic correction term to the angle of inclination
Ω_0	Right ascension at reference time
C_{is}	Amplitude of the sine harmonic correction term to the angle of inclination
i_0	Inclination angle at reference time
C_{rc}	Amplitude of the cosine harmonic correction term to the orbit radius
ω	Argument of perigee
$\dot{\Omega}$	Rate of right ascension
$\dot{i}$	Rate of inclination angle

Table A1.3 Subframe 4 parameters

Page	Information
1, 6, 11, 12, 16, 19, 20, 21, 22, 23 and 24	Reserved
2, 3, 4, 5, 7, 8, 9 and 10	Almanac data for satellites 25 through 33
13, 14 and 15	Spare
17	Special messages
18	Ionospheric model parameters and Universal Time Coordinated data
25	Anti-Spoofing flags (A-S on or off) and SV configuration code (Block I or II) for 32 satellites plus SV health status for satellites 25 through 32

Table A1.4 Subframe 5 parameters (Almanac Data)

Pages 1 through 24	
Parameter	**Information**
e	Eccentricity
t_{oa}	Reference time of almanac
δi	Correction to inclination
$\dot{\Omega}$	Rate of right ascension
$(A)^{1/2}$	Square root of the semi-major axis
Ω_0	Right ascension at reference time
ω	Argument of perigee
M_0	Mean anomaly at reference time
a_{f1} and a_{f0}	Satellite clock correction parameters
Page 25	SV health status for satellites 1 through 24

Appendix 2A Matlab source code to calculate DOP values in case of four non-geostationary satellites

```
% receiver position
long=-80.44/180*pi;
lat=37.23/180*pi;
h=0.646;

% calculation of sidereal time
GMST=219.6778;
UTC=0;
t=(GMST+UTC*0.25068447)*pi/180;

% calculation of CTS user coordinates
N=40680632/sqrt(40680632*(cos(lat))^2+40408296*(sin(lat))^2);
x0=(N+h)*cos(lat)*cos(long);
y0=(N+h)*cos(lat)*sin(long);
z0=(N+h)*sin(lat);
orig=[x0 y0 z0];

% satellite positions at given time in CIS coordinates
c1=[-21810.471 7749.521 -12338.383];
c2=[-12680.386 11089.597 20621.213];
c3=[4327.213 26253.668 -401.210];
c4=[-15141.137 -16117.047 14907.644];

% transformation of satellite positions to CTS coordinates
co=[c1;c2;c3;c4]';
cn=[cos(t) sin(t) 0;-sin(t) cos(t) 0;0 0 1]*co;

% calculation of user to satellite vectors with origin at user
position
A=[-sin(long) cos(long) 0;-sin(lat)*cos(long) -sin(lat)*sin(long)
cos(lat);cos(lat)*cos(long) cos(lat)*sin(long) sin(lat)];
or=[orig;orig;orig;orig]';
coords=cn-or;
nc=A*coords;

% calculation of dilution of precision values
r1=sqrt((nc(1,1))^2+(nc(2,1))^2+(nc(3,1))^2);
r2=sqrt((nc(1,2))^2+(nc(2,2))^2+(nc(3,2))^2);
r3=sqrt((nc(1,3))^2+(nc(2,3))^2+(nc(3,3))^2);
r4=sqrt((nc(1,4))^2+(nc(2,4))^2+(nc(3,4))^2);
G=[nc(1,1)/r1 nc(2,1)/r1 nc(3,1)/r1 -1;nc(1,2)/r2 nc(2,2)/r2
nc(3,2)/r2 -1;nc(1,3)/r3 nc(2,3)/r3 nc(3,3)/r3 -1;nc(1,4)/r4
nc(2,4)/r4 nc(3,4)/r4 -1];
DOP=inv(G'*G);
GDOP=sqrt(trace(DOP));
PDOP=sqrt(DOP(1,1)+DOP(2,2)+DOP(3,3));
HDOP=sqrt(DOP(1,1)+DOP(2,2));
VDOP=sqrt(DOP(3,3));

dil=[GDOP PDOP HDOP VDOP]
```

Table A2.1 Comparison of calculated DOP values (left) and values from GSS (right)

Time (UTC)	GDOP		PDOP		HDOP		VDOP	
00.00 h	2.354	2.4	2.1903	2.2	1.3945	1.4	1.6890	1.7
06.00 h	2.2671	2.3	2.0850	2.1	1.4208	1.4	1.5260	1.5
12.00 h	2.6345	2.7	2.4131	2.4	1.3619	1.4	1.9921	2.0
18.00 h	2.5745	2.6	2.3051	2.3	1.3023	1.3	1.9020	1.9

Appendix 2B Matlab source code for calculation of DOP when using 3 GEO satellites and an altimeter

```
% El=15 and 5 GEO satellites at 158W, 128W, 98W, 67W and 37W
% r is the ratio of altimeter to pseudo-range error
% f and l are the latitudes and longitudes of the 72 grid points
% re and rs are the earth radius and satellite orbit radius
% dl is the maximal longitudinal separation for different user
latitudes
% ls represents the longitudes of the GEO satellites
r=1;
f=[50 45 40 35 30 25];
l=[125 120 115 110 105 100 95 90 85 80 75 70];
dl=[52 56 59 61 63 64];
ls=[158 128 98 67 37];
re=6370;
rs=42164.2;
th=0;

% calculation of DOP values for all grid points
for i=1:6
  for j=1:12

    % user position
    lat=f(i)/180*pi;
    long=-l(j)/180*pi;
    x0=re*cos(lat)*cos(long);
    y0=re*cos(lat)*sin(long);
    z0=re*sin(lat);
    orig=[x0 y0 z0];

    % satellite selection
    l1=ls(1);
    if l1-l(j)>dl(i)
       l1=ls(2);
       if l1-l(j)>dl(i)
          l1=ls(3);
       end
    end

    l2=ls(5);
    if l(j)-l2>dl(i)
       l2=ls(4);
       if l(j)-l2>dl(i)
          l2=ls(3);
       end
    end
```

```
    l3=ls(2);
    d=abs(l3-l(j));
    if (abs(ls(3)-l(j))<=d)|(l1==ls(2))&(l2~=ls(3))
       l3=ls(3);
       d=abs(l3-l(j));
       if (abs(ls(4)-l(j))<=d)&(l2~=ls(4))
          l3=ls(4);
          d=abs(l3-l(j));
       end
    end
    L3(i,j)=l3;

    % determination and transformation of satellite coordinates
    lo1=-l1/180*pi;
    lo2=-l2/180*pi;
    lo3=-l3/180*pi;
    x1=rs*cos(lo1);
    y1=rs*sin(lo1);
    x2=rs*cos(lo2);
    y2=rs*sin(lo2);
    x3=rs*cos(lo3);
    y3=rs*sin(lo3);
    coord1=[x1 y1 0];
    coord2=[x2 y2 0];
    coord3=[x3 y3 0];
    A=[-sin(long) cos(long) 0;-sin(lat)*cos(long) -sin(lat)*sin(long)
         cos(lat);cos(lat)*cos(long) cos(lat)*sin(long) sin(lat)];
    coords=[coord1-orig;coord2-orig;coord3-orig]';
    nc=A*coords;

    % calculation of DOP elements
    r1=sqrt((nc(1,1))^2+(nc(2,1))^2+(nc(3,1))^2);
    r2=sqrt((nc(1,2))^2+(nc(2,2))^2+(nc(3,2))^2);
    r3=sqrt((nc(1,3))^2+(nc(2,3))^2+(nc(3,3))^2);
    G=[0 0 -1 0;nc(1,1)/r1 nc(2,1)/r1 nc(3,1)/r1 -1;nc(1,2)/r2
     nc(2,2)/r2 nc(3,2)/r2 -1;nc(1,3)/r3 nc(2,3)/r3 nc(3,3)/r3 -1];
    R=[1/r^2 0 0 0;0 1 0 0;0 0 1 0;0 0 0 1];
    DOP=inv(G'*R*G);
    PD=sqrt(DOP(1,1)+DOP(2,2)+DOP(3,3));
    PDOP(i,j)=PD;
    HD=sqrt(DOP(1,1)+DOP(2,2));
    HDOP(i,j)=HD;
    th=th+HD;
  end
end

% display average HDOP for CONUS
th/72
```

Appendix 2C Final Matlab source code for horizontal accuracy evaluation

```
% El=15
% 5 available GEO satellites at positions indicated in ls1 to ls5
% r is the ratio of altimeter to pseudo-range error
% total of 1456 grid points
% re and rs are the earth radius and satellite orbit radius
% dl is the maximal longitudinal separation for different user
latitudes
r=1;
ls5=[34.5 34.5 41 41 53 53 34.5 34.5 34.5 34.5 34.5 34.5 41 41 41 41
41 41 53 53 53 53 53 53];
ls4=[74 74 74 74 74 74 53 53 53 69 69 69 69 69 69 74 74 74 69 69 69 74
74 74];
ls3=[99 99 99 99 99 99 89 89 99 89 89 99 89 89 99 89 89 99 89 89 99 89
89 99];
ls2=[133 137 133 137 133 137 103 103 125 103 103 125 103 103 125 103
103 125 103 103 125 103 103 125];
ls1=[174 174 174 174 174 174 133 137 137 133 137 137 133 137 137 133
137 137 133 137 137 133 137 137];
re=6370;
rs=42164.2;

% do calculations for all satellite combinations
for p=1:24
  th=0;
  tew=0;
  tns=0;

  % calculation of DOP values for all grid points
  for i=0:25
    for j=0:55

      % user position
      l=125-j;
      lat=(50-i)/180*pi;
      long=-l/180*pi;
      dl=abs(acos(cos(pi*66.6/180)/cos(lat)))*180/pi;
      x0=re*cos(lat)*cos(long);
      y0=re*cos(lat)*sin(long);
      z0=re*sin(lat);
      orig=[x0 y0 z0];

      % satellite selection
      l1=ls1(p);
      if l1-l>dl
         l1=ls2(p);
         if l1-l>dl
            l1=ls3(p);
         end
      end

      l2=ls5(p);
      if l-l2>dl
         l2=ls4(p);
         if l-l2>dl
            l2=ls3(p);
         end
      end
```

```
      l3=ls2(p);
      d=abs(l3-l);
      if (abs(ls3(p)-l)<=d)|(l1==ls2(p))&(l2~=ls3(p))
         l3=ls3(p);
         d=abs(l3-l);
         if (abs(ls4(p)-l)<=d)&(l2~=ls4(p))
            l3=ls4(p);
            d=abs(l3-l);
         end
      end

      % determination and transformation of satellite coordinates
      lo1=-l1/180*pi;
      lo2=-l2/180*pi;
      lo3=-l3/180*pi;
      x1=rs*cos(lo1);
      y1=rs*sin(lo1);
      x2=rs*cos(lo2);
      y2=rs*sin(lo2);
      x3=rs*cos(lo3);
      y3=rs*sin(lo3);
      coord1=[x1 y1 0];
      coord2=[x2 y2 0];
      coord3=[x3 y3 0];
      A=[-sin(long) cos(long) 0;-sin(lat)*cos(long)
         -sin(lat)*sin(long) cos(lat);cos(lat)*cos(long)
         cos(lat)*sin(long) sin(lat)];
      coords=[coord1-orig;coord2-orig;coord3-orig]';
      nc=A*coords;

      % calculation of HDOP, E-W and N-S error factor
      r1=sqrt((nc(1,1))^2+(nc(2,1))^2+(nc(3,1))^2);
      r2=sqrt((nc(1,2))^2+(nc(2,2))^2+(nc(3,2))^2);
      r3=sqrt((nc(1,3))^2+(nc(2,3))^2+(nc(3,3))^2);
      G=[0 0 -1 0;nc(1,1)/r1 nc(2,1)/r1 nc(3,1)/r1 -1;nc(1,2)/r2
       nc(2,2)/r2 nc(3,2)/r2 -1;nc(1,3)/r3 nc(2,3)/r3 nc(3,3)/r3 -1];
      R=[1/r^2 0 0 0;0 1 0 0;0 0 1 0;0 0 0 1];
      DOP=inv(G'*R*G);
      HD=sqrt(DOP(1,1)+DOP(2,2));
      HDOP(i+1,j+1)=HD;
      EWD=sqrt(DOP(1,1));
      EWDOP(i+1,j+1)=EWD;
      NSD=sqrt(DOP(2,2));
      NSDOP(i+1,j+1)=NSD;
      th=th+HD;
      tew=tew+EWD;
      tns=tns+NSD;
    end
  end

  HP(p)=th/1456;
  EWP(p)=tew/1456;
  NSP(p)=tns/1456;
end

% display results
HP
EWP
NSP
```

Appendix 3A Available satellites at C-band

Satellite	Orbit	Operator	Launch	Uplink (MHz)	Downlink (MHz)	Transponders	Polarization	Beam	EIRP (dBW)	G/T (db/K)	Remarks
Intelsat VI F1	27.5 W	Intelsat	1991	5.854-6.423	3.629-4.198	26 of 72 MHz 12 of 36 MHz 2 of 41 MHz	RH RH & LH	Hemi Global	> 31 26.5-27.5		What is nominal east-US EIRP ?
Intelsat VI F3	34.5 W	Intelsat	1990	5.854-6.423	3.629-4.198	26 of 72 MHz 12 of 36 MHz 2 of 41 MHz	RH RH & LH	Hemi Global	> 31 26.5-27.5		What is nominal east-US EIRP ?
TDRSS-41	41 W	NASA	1991	5.945-6.385	3.720-4.160	12 of 36 MHz			31.9 - 33.4 nom: 32	-6.5	Lease of bandwidth through Columbia at US $ 1,350,000 per year ?
Intelsat VII F3	53 W	Intelsat	1994	5.929-6.423	3.704-4.198	2 of 36 MHz 16 of 72 MHz	RH & LH RH & LH	Hemi & Zone	> 33		
Spacenet II	69 W	GTE Spacenet	1984	5.925-6.405	3.7-4.2	6 of 72 MHz 12 of 36 MHz	12 Vertical 12 Horizontal	CONUS	36.1-38.1 35-37 nom : 35	> -4.6	To be replaced with Spacenet IIR in 1997
Spacenet IIR	69 W	GTE Spacenet	1997	5.925-6.405	3.7-4.2	24 of 36 MHz	12 Horizontal 12 Vertical	CONUS	36.8 - 38.8 nom : 37	> -2	
Galaxy VI	74 W	Hughes	1990	5.925-6.425	3.7-4.2	24 of 36 MHz	12 Horizontal 12 Vertical	CONUS	35 - 39 nom : 35	> -5	Final orbit in 1994
Satcom Hybrid-1	79 W	GE Americom	1994	5.925-6.425	3.7-4.2	24 of 36 MHz	12 Horizontal 12 Vertical	CONUS	nom : 38		Launch in 1994
Spacenet III-R	87 W	GTE Corp.	1988	5.925-6.405	3.7-4.2	6 of 72 MHz 12 of 36 MHz	Vertical Horizontal	CONUS	36 - 38.4 34 - 37 nom : 35	> -5	Carries L-band Geostar payload
Telstar 402	89 W	AT&T	1994	5.925-6.425	3.7-4.2	24 of 36 MHz	12 Horizontal 12 Vertical	CONUS	35 - 39 nom : 37	> -1	
Galaxy VII-H	91 W	Hughes	1993	5.925-6.425	3.7-4.2	24 of 36 MHz	12 Horizontal 12 Vertical	CONUS	36 - 39 nom : 38	nom : -1	
Galaxy III-H	95 W	Hughes	1994	5.925-6.425	3.7-4.2	24 of 36 MHz	12 Horizontal 12 Vertical	CONUS	36 - 39 nom : 38	nom : -1	
Telstar 401	97 W	AT&T	1993	5.925-6.425	3.7-4.2	24 of 36 MHz	12 Horizontal 12 Vertical	CONUS	35 -39 nom : 37	> -1	

Appendix 3A Available satellites at C-band

Satellite	Orbit	Operator	Launch	Uplink (MHz)	Downlink (MHz)	Transponders	Polarization	Beam	EIRP (dBW)	G/T (db/K)	Remarks
Galaxy IV-H	99 W	Hughes	1993	5.925-6.425	3.7-4.2	24 of 36 MHz	12 Horizontal 12 Vertical	CONUS	nom : 38	nom : 1	
Spacenet IV	101 W	GTE Spacenet	1991	5.925-6.405	3.7-4.2	6 of 72 MHz 12 of 36 MHz	Vertical Horizontal	CONUS	35 - 37 nom : 35		
Spacenet IR	103 W	GTE Spacenet	1994	5.925-6.425	3.7-4.2	24 of 36 MHz	12 Horizontal 12 Vertical	CONUS	> 35 nom : 36	> -2	
Galaxy V	125 W	Hughes	1992	5.925-6.425	3.7-4.2	24 of 36 MHz	12 Horizontal 12 Vertical	CONUS	37.5 - 40.3 nom : 38	> -0.5	
Satcom C4	131 W	GE Americom	1992	5.925-6.425	3.7-4.2	24 of 36 MHz	12 Horizontal 12 Vertical	CONUS	38-40 nom : 38	> -2	
Galaxy I-R	133 W	Hughes	1992	5.925-6.425	3.7-4.2	24 of 36 MHz	12 Horizontal 12 Vertical	CONUS	36 - 40 (37) 35 - 39 (36)	> -1.5	
Satcom C3	135 W	GE Americom	1992	5.925-6.425	3.7-4.2	24 of 36 MHz	12 Horizontal 12 Vertical	CONUS	38-40 nom : 38	> -2	
Aurora II (Satcom C5)	137 W	Alascom	1991	5.925-6.425	3.7-4.2	24 of 36 MHz	12 Horizontal 12 Vertical	CONUS	36 -38 nom : 37	> -3	
TDRSS-174	174.3 W	NASA	1988	5.925-6.425	3.7-4.2	12 of 36 MHz	Horizontal	CONUS	32 (nom)	> -6	

Appendix 3B Available satellites at Ku-band

Satellite	Orbit	Operator	Launch	Uplink (MHz)	Downlink (MHz)	Transponders	Polarization	Beam	EIRP (dBW)	G/T (dB/K)	Remarks
Intelsat VI F1	27.5 W	Intelsat	1991	14.004-14.498	10.954-11.698	6 of 72 MHz 2 of 77 MHz 2 of 150 MHz		West Spot	44.7 - 51.7 nom : 48		
Intelsat VI F3	34.5 W	Intelsat	1990	14.004-14.498	10.954-11.698	6 of 72 MHz 2 of 77 MHz 2 of 150 MHz		West Spot	44.7 - 51.7 nom : 48		
Orion 1	37.5 W	Orion	1993	14.0-14.5	11.7-12.2	3 of 36 MHz 14 of 54 MHz	Vertical Vertical & Horizontal	West spot	48 - 52.4 nom : 50	5.6 --10	[Cartin, 1990]
PAS-3	39.5 W	Alpha Lyracom	1994	14.0-14.5	11.7-12.2	6 of 72 MHz	Vertical & Horizontal	Conus	nom : 50.1	nom : 6.4	
Orion 2	47 W	Orion	1994	14.0-14.5	11.7-12.2	3 of 36 MHz 14 of 54 MHz	Vertical Vertical & Horizontal	West spot	48 - 52.4 nom : 50	5.6 - 10	[Cartin, 1990]
Intelsat VII F3	53 W	Intelsat	1994	14.004-14.498	10.954-11.698	72 or 112 MHz	Linear	Spot	nom : 47		What coverage ?
Spacenet II	69 W	GTE Spacenet	1984	14.0-14.5	11.7-12.2	6 of 72 MHz	Horizontal	CONUS	38.6-44.6 nom : 43		To be replaced with IIR in 1997
Spacenet IIR	69 W	GTE Spacenet	1997	14.0-14.5	11.7-12.2	8 of 54 MHz 4 of 36 MHz 10 of 27 MHz	Horizontal & Vertical	CONUS	43.8 - 47.8 nom : 46	> -1	
Satcom Hybrid-1	79 W	GE Americom	1994	14.0-14.5	11.7-12.2	16, 27 and 54 MHz	Linear	CONUS	nom : 45	nom : 0	
Spacenet III-R	87 W	GTE Corp.	1988	14.0-14.5	11.7-12.2	6 of 72 MHz	Horizontal	East & West Regional	35 - 47 36 - 48 nom : 40	> -4	Low EIRP (<40) in middle of US
Telstar 402	89 W	AT&T	1994	14.0-14.5	11.7-12.2	8 of 54 MHz 8 of 2*27 MHz	Vertical & Horizontal	CONUS	nom : 46	> 0	

Appendix 3B Available satellites at Ku-band

Satellite	Orbit	Operator	Launch	Uplink (MHz)	Downlink (MHz)	Transponders	Polarization	Beam	EIRP (dBW)	G/T (dB/K)	Remarks
Galaxy VII-H	91 W	Hughes	1992	14.0-14.5	11.7-12.2	8 of 54 MHz 16 of 27 MHz	Vertical Horizontal	CONUS	nom : 45	nom : 2.0	
Telstar 401	97 W	AT&T	1993	14.0-14.5	11.7-12.2	16 of 54 MHz	8 Horizontal 8 Vertical	CONUS	nom : 46	> 0	
Galaxy IV-H	99 W	Hughes	1993	14.0-14.5	11.7-12.2	8 of 54 MHz 16 of 27 MHz	Vertical Horizontal	CONUS	nom : 45	nom : -1	
Spacenet IV	101 W	GTE Spacenet	1991	14.0-14.5	11.7-12.2	3 of 72 MHz	Vertical	CONUS	42 and 44.7 ?		Footprint ?
Spacenet IR	103 W	GTE Spacenet	1995	14.0-14.5	11.7-12.2	8 of 54 MHz 4 of 36 MHz 10 of 27 MHz	Linear	CONUS	41.8 - 47.8 nom : 46		
GSTAR IIR	105 W	GTE Spacenet	1995	14.0-14.5	11.7-12.2	16 of 54 MHz or 32 of 27 MHz	Vertical & Horizontal	CONUS	43.1 - 49.1 nom : 47	> 1	
SBS 5	123 W	Hughes	1988	14.0-14.5	11.7-12.2	10 of 43 MHz 4 of 110 MHz	Horizontal Vertical	CONUS	39-46 nom : 42		
GSTAR IV	125 W	GTE Spacenet	1990	14.0-14.5	11.7-12.2	16 of 54 MHz	8 Horizontal 8 Vertical	CONUS	37-44.6 nom : 42	> -6	
Columbiasat 1	165 W	CCC		14.0-14.5	11.7-12.2	?	?	?	?		Need to know more about Columbia
TDRSS-174	174.3 W	NASA	1988	14.0-14.5	11.7-12.2	4 of 225 MHz	2 Horizontal 2 Vertical	?	45 ?		
Intelsat V-A F11	177 W	Intelsat	1993	14.004-14.498	10.954-11.698	4 of 72 MHz 2 of 241 MHz	Linear	West spot	> 44.4		

Appendix 4A Horizontal error factors for C-band system of 4 satellites

	Elevation mask = 15°			Elevation mask = 10°		
Satellite positions	<HDOP>	<EW>	<NS>	<HDOP>	<EW>	<NS>
34.5 69 97 137	8.84	1.45	8.71	7.60	1.32	7.47
34.5 69 97 135	8.93	1.48	8.80	7.79	1.39	7.66
34.5 69 97 133	9.08	1.53	8.93	8.06	1.47	7.91
34.5 69 99 137	8.64	1.42	8.51	7.51	1.32	7.39
34.5 69 99 135	8.77	1.46	8.64	7.73	1.39	7.59
34.5 69 99 133	8.96	1.52	8.82	8.03	1.48	7.88
34.5 69 101 137	8.50	1.40	8.38	7.47	1.33	7.34
34.5 69 101 135	8.68	1.45	8.54	7.72	1.40	7.58
34.5 69 101 133	8.91	1.52	8.77	8.04	1.50	7.89
34.5 69 103 137	8.42	1.39	8.30	7.47	1.34	7.34
34.5 69 103 135	8.64	1.45	8.51	7.75	1.42	7.61
34.5 69 103 133	8.92	1.53	8.77	8.11	1.52	7.95
34.5 74 97 137	10.13	1.54	10.00	8.53	1.35	8.41
34.5 74 97 135	10.24	1.56	10.10	8.74	1.41	8.62
34.5 74 97 133	10.40	1.61	10.26	9.05	1.49	8.91
34.5 74 99 137	9.75	1.50	9.62	8.31	1.34	8.20
34.5 74 99 135	9.90	1.53	9.77	8.56	1.41	8.43
34.5 74 99 133	10.11	1.58	9.98	8.89	1.49	8.75
34.5 74 101 137	9.47	1.47	9.35	8.17	1.34	8.05
34.5 74 101 135	9.67	1.51	9.54	8.44	1.41	8.31
34.5 74 101 133	9.93	1.57	9.79	8.80	1.50	8.66
34.5 74 103 137	9.27	1.45	9.15	8.08	1.34	7.96
34.5 74 103 135	9.52	1.50	9.39	8.39	1.42	8.26
34.5 74 103 133	9.83	1.57	9.69	8.78	1.51	8.63
41 69 97 137	8.86	1.41	8.74	7.50	1.39	7.36
41 69 97 135	8.89	1.46	8.75	7.66	1.46	7.51
41 69 97 133	8.96	1.54	8.82	7.90	1.55	7.74
41 69 99 137	8.69	1.40	8.56	7.45	1.39	7.31
41 69 99 135	8.76	1.46	8.63	7.64	1.47	7.49
41 69 99 133	8.88	1.54	8.74	7.91	1.56	7.74
41 69 101 137	8.57	1.39	8.45	7.45	1.40	7.31
41 69 101 135	8.69	1.46	8.55	7.67	1.49	7.51
41 69 101 133	8.86	1.54	8.72	7.97	1.58	7.79
41 69 103 137	8.51	1.39	8.39	7.48	1.42	7.34
41 69 103 135	8.67	1.47	8.54	7.73	1.51	7.57
41 69 103 133	8.90	1.56	8.75	8.06	1.61	7.89
41 74 97 137	9.85	1.46	9.74	8.12	1.38	8.00
41 74 97 135	9.88	1.50	9.76	8.29	1.46	8.15
41 74 97 133	9.96	1.56	9.83	8.56	1.55	8.40
41 74 99 137	9.52	1.43	9.40	7.97	1.38	7.84
41 74 99 135	9.60	1.48	9.48	8.17	1.46	8.03
41 74 99 133	9.74	1.55	9.60	8.46	1.55	8.31
41 74 101 137	9.28	1.41	9.16	7.88	1.38	7.75
41 74 101 135	9.41	1.47	9.28	8.11	1.47	7.97
41 74 101 133	9.60	1.55	9.46	8.43	1.56	8.27
41 74 103 137	9.11	1.40	8.99	7.84	1.39	7.71
41 74 103 135	9.29	1.47	9.16	8.11	1.48	7.96
41 74 103 133	9.53	1.56	9.39	8.46	1.58	8.30

41 79 97 137	11.61	1.55	11.49	9.25	1.40	9.13
41 79 97 135	11.62	1.58	11.50	9.43	1.47	9.30
41 79 97 133	11.70	1.64	11.58	9.72	1.57	9.58
41 79 99 137	10.97	1.49	10.85	8.90	1.38	8.78
41 79 99 135	11.05	1.54	10.93	9.12	1.46	8.98
41 79 99 133	11.19	1.60	11.06	9.43	1.56	9.29
41 79 101 137	10.49	1.46	10.37	8.66	1.38	8.54
41 79 101 135	10.62	1.51	10.50	8.91	1.46	8.77
41 79 101 133	10.83	1.58	10.70	9.25	1.56	9.11
41 79 103 137	10.13	1.44	10.02	8.50	1.38	8.37
41 79 103 135	10.32	1.49	10.20	8.78	1.47	8.64
41 79 103 133	10.59	1.58	10.46	9.16	1.57	9.01
53 69 97 137	10.44	1.62	10.30	8.58	1.73	8.38
53 69 97 135	10.25	1.71	10.09	8.67	1.81	8.46
53 69 97 133	10.14	1.81	9.96	8.88	1.89	8.65
53 69 99 137	10.28	1.63	10.14	8.62	1.75	8.42
53 69 99 135	10.17	1.72	10.01	8.74	1.83	8.53
53 69 99 133	10.13	1.84	9.94	8.99	1.92	8.77
53 69 101 137	10.19	1.65	10.04	8.69	1.78	8.49
53 69 101 135	10.15	1.75	9.98	8.86	1.86	8.64
53 69 101 133	10.18	1.87	9.98	9.15	1.95	8.91
53 69 103 137	10.16	1.68	10.00	8.80	1.81	8.60
53 69 103 135	10.18	1.78	10.00	9.01	1.89	8.79
53 69 103 133	10.28	1.90	10.08	9.34	1.98	9.10
53 74 97 137	10.50	1.59	10.36	8.38	1.65	8.20
53 74 97 135	10.33	1.67	10.18	8.46	1.73	8.27
53 74 97 133	10.23	1.77	10.06	8.67	1.81	8.47
53 74 99 137	10.22	1.59	10.08	8.34	1.66	8.16
53 74 99 135	10.13	1.68	9.97	8.47	1.74	8.27
53 74 99 133	10.10	1.78	9.93	8.71	1.83	8.50
53 74 101 137	10.02	1.60	9.88	8.34	1.68	8.16
53 74 101 135	10.00	1.69	9.84	8.51	1.76	8.31
53 74 101 133	10.04	1.79	9.87	8.80	1.85	8.58
53 74 103 137	9.89	1.61	9.75	8.39	1.70	8.20
53 74 103 135	9.94	1.71	9.78	8.60	1.78	8.40
53 74 103 133	10.05	1.82	9.87	8.92	1.88	8.70
53 79 97 137	11.31	1.59	11.18	8.56	1.61	8.39
53 79 97 135	11.10	1.67	10.96	8.62	1.69	8.44
53 79 97 133	10.95	1.76	10.80	8.82	1.78	8.63
53 79 99 137	10.80	1.57	10.67	8.42	1.62	8.25
53 79 99 135	10.68	1.65	10.54	8.53	1.70	8.35
53 79 99 133	10.63	1.75	10.47	8.77	1.78	8.57
53 79 101 137	10.43	1.57	10.30	8.34	1.62	8.17
53 79 101 135	10.39	1.65	10.25	8.50	1.70	8.31
53 79 101 133	10.42	1.76	10.26	8.77	1.80	8.57
53 79 103 137	10.16	1.57	10.03	8.31	1.64	8.14
53 79 103 135	10.20	1.66	10.05	8.51	1.72	8.32
53 79 103 133	10.30	1.77	10.14	8.83	1.82	8.62

Appendix 4B Horizontal error factors for C-band system of 5 satellites

	Elevation mask = 15°			Elevation mask = 10°		
Satellite positions	<HDOP>	<EW>	<NS>	<HDOP>	<EW>	<NS>
27.5 69 99 133 174	-	-	-	6.66	1.08	6.56
27.5 69 99 137 174	-	-	-	6.44	1.07	6.35
27.5 74 99 133 174	-	-	-	7.33	1.17	7.23
27.5 74 99 137 174	-	-	-	7.12	1.18	7.01
34.5 69 99 133 174	-	-	-	6.28	1.09	6.18
34.5 69 99 137 174	-	-	-	6.14	1.06	6.05
34.5 74 99 133 174	8.65	1.27	8.55	6.67	1.13	6.56
34.5 74 99 137 174	8.59	1.28	8.49	6.56	1.12	6.45
41 69 99 133 174	-	-	-	6.26	1.15	6.15
41 69 99 137 174	-	-	-	6.16	1.10	6.06
41 74 99 133 174	8.27	1.24	8.17	6.38	1.16	6.27
41 74 99 137 174	8.36	1.21	8.27	6.33	1.12	6.22
53 69 99 133 174	-	-	-	7.70	1.47	7.55
53 69 99 137 174	-	-	-	7.60	1.42	7.45
53 74 99 133 174	8.75	1.44	8.62	7.22	1.37	7.08
53 74 99 137 174	9.15	1.35	9.04	7.14	1.33	7.01
34.5 53 89 103 133	11.54	1.60	11.41	8.60	1.60	8.43
34.5 53 89 103 137	11.22	1.45	11.12	8.03	1.38	7.89
34.5 69 89 103 133	8.97	1.54	8.82	7.87	1.49	7.71
34.5 69 89 103 137	8.57	1.42	8.44	7.27	1.32	7.14
41 69 89 103 133	8.76	1.55	8.61	7.75	1.58	7.57
41 69 89 103 137	8.48	1.39	8.35	7.21	1.39	7.07
41 74 89 103 133	9.36	1.54	9.22	8.26	1.57	8.10
41 74 89 103 137	9.01	1.40	8.89	7.68	1.38	7.54
53 69 89 103 133	9.75	1.84	9.56	8.66	1.91	8.43
53 69 89 103 137	9.76	1.62	9.61	8.19	1.73	7.99
53 74 89 103 133	9.68	1.78	9.50	8.55	1.84	8.33
53 74 89 103 137	9.61	1.58	9.46	8.06	1.66	7.88

Longitudes 95 or 97 can be used instead of 99 with difference less than 0.2

Longitude 135 can be used for the fourth satellite instead of 137 with difference less than 0.1

Longitude 91 can be used instead of 89 with difference less than 0.1

Longitude 101 can be used instead of 103 with difference less than 0.2

Appendix 4C Horizontal error factors for Ku-band system of 4 satellites

	Elevation mask = 15°			Elevation mask = 10°		
Satellite positions	<HDOP>	<EW>	<NS>	<HDOP>	<EW>	<NS>
37.5 69 97 123	11.13	2.18	10.88	10.26	2.23	9.99
37.5 69 97 125	10.49	1.99	10.27	9.66	2.03	9.42
37.5 69 99 123	11.29	2.23	11.03	10.45	2.29	10.16
37.5 69 99 125	10.58	2.02	10.36	9.78	2.07	9.54
37.5 69 101 123	11.56	2.29	11.29	10.73	2.36	10.44
37.5 69 101 125	10.77	2.07	10.53	9.99	2.13	9.73
37.5 69 103 123	11.96	2.38	11.68	11.13	2.46	10.82
37.5 69 103 125	11.05	2.13	10.81	10.28	2.20	10.01
37.5 79 97 123	15.07	2.37	14.84	13.26	2.38	13.02
37.5 79 97 125	14.19	2.16	14.00	12.47	2.14	12.26
37.5 79 99 123	14.73	2.36	14.51	13.05	2.38	12.80
37.5 79 99 125	13.80	2.14	13.60	12.21	2.14	12.00
37.5 79 101 123	14.63	2.38	14.40	13.03	2.42	12.78
37.5 79 101 125	13.61	2.15	13.41	12.12	2.16	11.90
37.5 79 103 123	14.74	2.42	14.51	13.19	2.48	12.93
37.5 79 103 125	13.61	2.17	13.41	12.18	2.20	11.95
47 69 97 123	11.09	2.32	10.81	10.94	2.33	10.04
47 69 97 125	10.49	2.14	10.24	9.75	2.15	9.48
47 69 99 123	11.32	2.38	11.03	10.60	2.39	10.28
47 69 99 125	10.65	2.18	10.40	9.95	2.20	9.67
47 69 101 123	11.65	2.45	11.35	10.34	2.47	10.61
47 69 101 125	10.89	2.23	10.63	10.22	2.26	9.93
47 69 103 123	12.09	2.55	11.77	11.38	2.58	11.04
47 69 103 125	11.22	2.30	10.95	10.56	2.34	10.26
47 79 97 123	13.38	2.44	13.13	11.67	2.45	11.38
47 79 97 125	12.64	2.22	12.42	10.99	2.23	10.74
47 79 99 123	13.24	2.45	12.99	11.66	2.47	11.37
47 79 99 125	12.44	2.22	12.22	10.93	2.24	10.68
47 79 101 123	13.28	2.49	13.02	11.78	2.52	11.48
47 79 101 125	12.40	2.24	12.17	10.99	2.28	10.73
47 79 103 123	13.48	2.55	13.21	12.04	2.59	11.72
47 79 103 125	12.49	2.28	12.26	11.15	2.33	10.88
53 69 97 123	11.89	2.50	11.59	11.26	2.47	10.94
53 69 97 125	11.27	2.33	11.00	10.64	2.31	10.34
53 69 99 123	12.19	2.56	11.88	11.59	2.53	11.25
53 69 99 125	11.50	2.37	11.22	10.90	2.36	10.60
53 69 101 123	12.58	2.64	12.26	12.00	2.62	11.65
53 69 101 125	11.81	2.43	11.52	11.23	2.43	10.92
53 69 103 123	13.08	2.74	12.74	12.51	2.72	12.14
53 69 103 125	12.20	2.51	11.90	11.64	2.51	11.32
53 79 97 123	12.87	2.54	12.59	11.27	2.46	10.96
53 79 97 125	12.18	2.33	11.93	10.63	2.27	10.35
53 79 99 123	12.86	2.56	12.58	11.39	2.50	11.08
53 79 99 125	12.11	2.34	11.86	10.70	2.30	10.42
53 79 101 123	12.99	2.60	12.70	11.61	2.56	11.29
53 79 101 125	12.16	2.37	11.91	10.85	2.34	10.56
53 79 103 123	13.26	2.67	12.96	11.94	2.64	11.60
53 79 103 125	12.33	2.42	12.07	11.09	2.41	10.79

47 69 105 165	-	-	-	9.66	1.52	9.52
47 69 123 165	-	-	-	7.57	1.15	7.47
47 69 125 165	-	-	-	7.48	1.15	7.38
47 79 105 165	-	-	-	9.64	1.58	9.48
47 79 123 165	-	-	-	6.86	1.12	6.76
47 79 125 165	-	-	-	6.74	1.11	6.64
47 87 105 165	-	-	-	11.63	1.87	11.45
47 87 123 165	-	-	-	6.98	1.17	6.88
47 87 125 165	-	-	-	6.79	1.15	6.69
53 69 105 165	-	-	-	12.42	1.69	12.28
53 69 123 165	-	-	-	9.51	1.38	9.39
53 69 125 165	-	-	-	9.37	1.39	9.25
53 79 105 165	-	-	-	10.86	1.61	10.72
53 79 123 165	-	-	-	7.69	1.24	7.58
53 79 125 165	-	-	-	7.55	1.24	7.44
53 87 105 165	-	-	-	12.27	1.78	12.11
53 87 123 165	-	-	-	7.41	1.22	7.30
53 87 125 165	-	-	-	7.21	1.21	7.10

Appendix 4D Horizontal error factors for Ku-band system of 5 satellites

	Elevation mask = 15°			Elevation mask = 10°		
Satellite positions	<HDOP>	<EW>	<NS>	<HDOP>	<EW>	<NS>
27.5 53 89 123 165	-	-	-	6.05	1.08	5.95
27.5 53 89 125 165	-	-	-	5.91	1.05	5.81
27.5 53 89 123 165	-	-	-	6.19	1.10	6.08
27.5 53 91 125 165	-	-	-	6.03	1.07	5.93
27.5 53 91 123 165	-	-	-	6.74	1.20	6.62
27.5 53 97 125 165	-	-	-	6.49	1.15	6.38
27.5 53 99 123 165	-	-	-	6.98	1.24	6.87
27.5 53 99 125 165	-	-	-	6.70	1.18	6.58
27.5 53 103 123 165	-	-	-	7.61	1.35	7.48
27.5 53 103 125 165	-	-	-	7.22	1.28	7.10
27.5 69 97 123 165	8.83	1.28	8.73	6.85	1.18	6.74
27.5 69 97 123 177	-	-	-	8.42	1.35	8.30
27.5 69 97 125 165	8.48	1.24	8.38	6.67	1.15	6.56
27.5 69 97 125 177	-	-	-	8.01	1.27	7.90
27.5 69 99 123 165	8.89	1.28	8.79	6.86	1.18	6.75
27.5 69 99 123 177	-	-	-	8.52	1.37	8.40
27.5 69 99 125 165	8.50	1.24	8.40	6.66	1.15	6.56
27.5 69 99 125 177	-	-	-	8.07	1.28	7.96
27.5 69 103 123 165	9.22	1.29	9.12	6.96	1.18	6.85
27.5 69 103 123 177	-	-	-	8.92	1.42	8.80
27.5 69 103 125 165	8.70	1.25	8.60	6.71	1.14	6.60
27.5 69 103 125 177	-	-	-	8.35	1.32	8.24
34.5 53 89 123 165	-	-	-	6.11	1.09	6.01
34.5 53 89 125 165	-	-	-	5.96	1.06	5.86
34.5 53 91 123 165	-	-	-	6.30	1.12	6.19
34.5 53 91 125 165	-	-	-	6.13	1.08	6.02
34.5 53 97 123 165	-	-	-	6.98	1.22	6.87
34.5 53 97 125 165	-	-	-	6.73	1.18	6.62
34.5 53 99 123 165	-	-	-	7.27	1.27	7.15
34.5 53 99 125 165	-	-	-	6.98	1.22	6.86
34.5 53 103 123 165	-	-	-	7.99	1.38	7.86
34.5 53 103 125 165	-	-	-	7.58	1.32	7.46
34.5 69 97 123 165	8.15	1.25	8.05	6.51	1.16	6.40
34.5 69 97 123 177	-	-	-	7.80	1.40	7.66
34.5 69 97 125 165	7.87	1.21	7.77	6.36	1.13	6.25
34.5 69 97 125 177	-	-	-	7.44	1.31	7.32
34.5 69 99 123 165	8.24	1.26	8.13	6.57	1.17	6.46
34.5 69 99 123 177	-	-	-	7.94	1.43	7.80
34.5 69 99 125 165	7.91	1.21	7.81	6.39	1.13	6.28
34.5 69 99 125 177	-	-	-	7.54	1.34	7.42
34.5 69 103 123 165	8.54	1.30	8.43	6.71	1.19	6.60
34.5 69 103 123 177	-	-	-	8.37	1.51	8.22
34.5 69 103 125 165	8.11	1.23	8.01	6.49	1.15	6.38
34.5 69 103 125 177	-	-	-	7.87	1.40	7.73
37.5 53 89 123 165	-	-	-	6.25	1.10	6.14
37.5 53 89 125 165	-	-	-	6.09	1.07	5.99
37.5 53 91 123 165	-	-	-	6.46	1.13	6.35
37.5 53 91 125 165	-	-	-	6.28	1.10	6.18

37.5 53 97 123 165	-	-	-	7.24	1.24	7.13
37.5 53 97 125 165	-	-	-	6.97	1.20	6.86
37.5 53 99 123 165	-	-	-	7.57	1.29	7.45
37.5 53 99 125 165	-	-	-	7.26	1.24	7.14
37.5 53 103 123 165	-	-	-	8.35	1.41	8.22
37.5 53 103 125 165	-	-	-	7.93	1.34	7.80
37.5 69 97 123 165	7.96	1.27	7.85	6.51	1.15	6.40
37.5 69 97 123 177	-	-	-	7.63	1.43	7.48
37.5 69 97 125 165	7.69	1.22	7.59	6.35	1.12	6.25
37.5 69 97 125 177	-	-	-	7.29	1.34	7.15
37.5 69 99 123 165	8.06	1.29	7.95	6.59	1.16	6.48
37.5 69 99 123 177	-	-	-	7.79	1.46	7.64
37.5 69 99 125 165	7.76	1.23	7.65	6.41	1.13	6.30
37.5 69 99 125 177	-	-	-	7.41	1.37	7.27
37.5 69 103 123 165	8.38	1.33	8.27	6.76	1.19	6.65
37.5 69 103 123 177	-	-	-	8.24	1.55	8.08
37.5 69 103 125 165	7.98	1.26	7.87	6.53	1.15	6.43
37.5 69 103 125 177	-	-	-	7.76	1.44	7.61
24.5 47 79 103 123	12.69	2.44	12.43	10.90	2.49	10.59
24.5 47 79 103 125	11.73	2.17	11.51	10.06	2.21	9.80
24.5 47 79 105 123	13.06	2.53	12.79	11.29	2.60	10.96
24.5 47 79 105 125	11.97	2.23	11.74	10.33	2.29	10.06
24.5 47 89 103 123	17.97	2.65	17.74	14.40	2.71	14.11
24.5 47 89 103 125	16.60	2.34	16.41	13.29	2.38	13.05
24.5 47 89 105 123	17.62	2.66	17.39	14.30	2.75	14.00
24.5 47 89 105 125	16.13	2.33	15.94	13.08	2.39	12.84
24.5 53 79 103 123	12.01	2.45	11.73	10.15	2.42	9.82
24.5 53 79 103 125	11.12	2.19	10.88	9.38	2.16	9.10
24.5 53 79 105 123	12.43	2.55	12.14	10.58	2.53	10.24
24.5 53 79 105 125	11.41	2.26	11.17	9.70	2.24	9.41
24.5 53 89 103 123	15.53	2.66	15.27	11.95	2.59	11.63
24.5 53 89 103 125	14.36	2.35	14.15	11.05	2.30	10.78
24.5 53 89 105 123	15.42	2.69	15.16	12.08	2.66	11.75
24.5 53 89 105 125	14.14	2.36	13.92	11.09	2.34	10.81
24.5 69 89 103 123	13.42	2.48	13.14	12.00	2.31	11.73
24.5 69 89 103 125	12.46	2.26	12.21	11.11	2.09	10.88
24.5 69 89 105 123	13.84	2.57	13.54	12.44	2.41	12.16
24.5 69 89 105 125	12.76	2.33	12.51	11.44	2.15	11.19
27.5 47 79 103 123	12.60	2.44	12.33	10.85	2.51	10.54
27.5 47 79 103 125	11.64	2.17	11.42	10.02	2.26	9.76
27.5 47 79 105 123	12.97	2.53	12.70	11.24	2.61	10.91
27.5 47 79 105 125	11.88	2.23	11.65	10.29	2.30	10.01
27.5 47 89 103 123	17.91	2.65	17.68	14.39	2.71	14.07
27.5 47 89 103 125	16.54	2.34	16.35	13.25	2.38	13.01
27.5 47 89 105 123	17.56	2.66	17.32	14.25	2.75	13.96
27.5 47 89 105 125	16.07	2.33	15.88	13.04	2.40	12.79
27.5 53 79 103 123	11.82	2.44	11.55	10.03	2.44	9.70
27.5 53 79 103 125	10.94	2.18	10.70	9.27	2.17	8.99
27.5 53 79 105 123	12.25	2.55	11.96	10.45	2.55	10.11
27.5 53 79 105 125	11.24	2.25	10.99	9.58	2.25	9.29
27.5 53 89 103 123	15.42	2.66	15.16	11.86	2.60	11.54
27.5 53 89 103 125	14.26	2.34	14.05	10.97	2.31	10.70
27.5 53 89 105 123	15.31	2.69	15.05	11.99	2.67	11.66
27.5 53 89 105 125	14.04	2.35	13.82	11.01	2.35	10.73
27.5 69 89 103 123	12.94	2.40	12.67	11.54	2.30	11.26

27.5	69	89	103	125	12.01	2.18	11.77	10.67	2.06	10.43
27.5	69	89	105	123	13.36	2.50	13.07	11.98	2.39	11.69
27.5	69	89	105	125	12.31	2.25	12.06	11.00	2.13	10.75
34.5	53	79	103	123	11.62	2.48	11.34	9.98	2.49	9.63
34.5	53	79	103	125	10.76	2.20	10.52	9.24	2.23	8.94
34.5	53	79	105	123	12.02	2.58	11.72	10.38	2.61	10.02
34.5	53	79	105	125	11.03	2.27	10.78	9.53	2.31	9.22
34.5	53	89	103	123	15.32	2.69	15.06	11.83	2.64	11.50
34.5	53	89	103	125	14.18	2.37	13.96	10.95	2.35	10.67
34.5	53	89	105	123	15.21	2.72	14.94	11.96	2.71	11.62
34.5	53	89	105	125	13.96	2.38	13.73	10.98	2.40	10.69
34.5	69	89	103	123	11.98	2.34	11.71	10.79	2.35	10.50
34.5	69	89	103	125	11.11	2.10	10.87	10.00	2.11	9.74
34.5	69	89	105	123	12.39	2.43	12.10	11.19	2.45	10.88
34.5	69	89	105	125	11.40	2.17	11.15	10.28	2.18	10.01
37.5	53	79	103	123	11.65	2.50	11.36	10.05	2.51	9.70
37.5	53	79	103	125	10.79	2.23	10.54	9.31	2.25	9.01
37.5	53	79	105	123	12.04	2.60	11.74	10.45	2.63	10.09
37.5	53	79	105	125	11.05	2.30	10.80	9.61	2.33	9.29
37.5	53	89	103	123	15.38	2.71	15.12	11.93	2.67	11.60
37.5	53	89	103	125	14.24	2.39	14.02	11.05	2.38	10.77
37.5	53	89	105	123	15.27	2.74	15.00	12.05	2.74	11.71
37.5	53	89	105	125	14.01	2.40	13.79	11.08	2.42	10.79
37.5	69	89	103	123	11.71	2.36	11.43	10.62	2.40	10.31
37.5	69	89	103	125	10.86	2.12	10.62	9.85	2.15	9.58
37.5	69	89	105	123	12.10	2.45	11.81	11.00	2.50	10.68
37.5	69	89	105	125	11.14	2.18	10.89	10.12	2.22	9.84

Appendix 5 Computation of satellite coordinates from Kepler elements

Based on the data in the navigation message, shown in Table A5.1 satellite coordinates can be calculated using the following steps

1. Compute the elapsed time since the ephemeris reference epoch

$$t_k = t - t_{oe}$$

where t is the system time at time of (virtual) transmission.

2. Compute the corrected mean motion

$$n = n_0 + \Delta n = \sqrt{\mu / A^3} + \Delta n$$

where $\mu = 3.986005 \cdot 10^{14}\ \mathrm{m^3/s^2}$, the WGS 84 value of the geocentric gravitational constant.

3. Compute the mean anomaly at t_k

$$M_k = M_0 + n \cdot t_k$$

4. Solve Kepler's equation of the eccentric anomaly by iteration

$$E_k = M_k + e \cdot \sin(E_k)$$

$$E_0 = M$$

$$E_i = M + e \cdot \sin(E_i)\ ,\ i = 1,2,3\cdots$$

5. Compute the true anomaly

$$v_k = \tan^{-1}\left(\frac{\sin(v_k)}{\cos(v_k)}\right) = \tan^{-1}\left(\frac{\sin(E_k)\cdot\sqrt{1-e^2}}{\cos(E_k - e)}\right)$$

6. Compute the argument of latitude

$$\varphi_k = v_k + \omega$$

7. Compute corrections of the argument of latitude, radius and inclination

$$\delta u_k = C_{uc} \cdot \cos(2\varphi_k) + C_{us} \cdot \sin(2\varphi_k)$$

$$\delta r_k = C_{rc} \cdot \cos(2\varphi_k) + C_{rs} \cdot \sin(2\varphi_k)$$

$$\delta i_k = C_{ic} \cdot \cos(2\varphi_k) + C_{is} \cdot \sin(2\varphi_k)$$

8. Compute the corrected argument of latitude, radius and inclination

$$u_k = \varphi_k + \delta u_k$$

$$r_k = A \cdot [1 - e \cdot \cos(E_k)] + \delta r_k$$

$$i_k = i_0 + \dot{i} \cdot t_k + \delta i_k$$

9. Compute positions in the orbital plane

$$x'_k = r_k \cdot \cos(u_k)$$

$$y'_k = r_k \cdot \sin(u_k)$$

10. Compute corrected longitude of ascending node

$$\Omega_k = \Omega_0 + (\dot{\Omega} - \omega_e) \cdot t_k - \omega_e \cdot t_{oe}$$

where $\omega_e = 7.2921151467 \cdot 10^5$ rad/s , the WGS 84 value of the earth rotation rate

11. Compute ECEF satellite coordinates

$$x_k = x'_k \cdot \cos(\Omega_k) - y'_k \cdot \cos(i_k) \cdot \sin(\Omega_k)$$

$$y_k = x'_k \cdot \sin(\Omega_k) - y'_k \cdot \cos(i_k) \cdot \cos(\Omega_k)$$

$$z_k = y'_k \cdot \sin(i_k)$$

Table A5.1 Navigation message parameters based on use of Kepler orbital elements

Group	Parameter	No. of bits	Scale factor	Information
Ephemeris	IODE	8		Issue of Data Ephemeris
	t_{oe} (s)	16	2^{4}	Reference time of ephemeris
	$(A)^{½}$ ($m^{½}$)	32	2^{-19}	Square root of the semi-major axis
	e	32	2^{-37}	Eccentricity
	i_0 (semicircles)	32*	2^{-31}	Inclination angle at reference time
	Ω_0 (semicircles)	32*	2^{-31}	Right ascension at reference time
	ω (semicircles)	32*	2^{-31}	Argument of perigee
	M_0 (semicircles)	32*	2^{-31}	Mean anomaly at reference time
	Δn (semicircles/s)	16*	2^{-43}	Mean motion difference from computed value
	$\dot{\Omega}$ (semicircles/s)	24*	2^{-43}	Rate of right ascension
	$\dot{i}$ (semicircles/s)	14*	2^{-43}	Rate of change of inclination
	C_{us} (rad)	16*	2^{-29}	Amplitude of the sine harmonic correction term to the argument of latitude
	C_{uc} (rad)	16*	2^{-29}	Amplitude of the cosine harmonic correction term to the argument of latitude
	C_{is} (rad)	16*	2^{-29}	Amplitude of the sine harmonic correction term to the angle of inclination
	C_{ic} (rad)	16*	2^{-29}	Amplitude of the cosine harmonic correction term to the angle of inclination
	C_{rs} (m)	16*	2^{-5}	Amplitude of the sine harmonic correction term to the orbit radius
	C_{rc} (m)	16*	2^{-5}	Amplitude of the cosine harmonic correction term to the orbit radius
Almanacs of	t_{oa} (s)	8	2^{12}	Reference time of almanac
other system	$(A)^{½}$ ($m^{½}$)	24	2^{-19}	
satellites	e	24	2^{-21}	
	i_0 (semicircles)	24*	2^{-23}	
	Ω_0 (semicircles)	24*	2^{-23}	
	ω (semicircles)	24*	2^{-23}	
	M_0 (semicircles)	24*	2^{-23}	
	$\dot{\Omega}$ (semicircles/s)	16*	2^{-35}	
	$\dot{i}$ (semicircles/s)	8*	2^{-37}	

Appendix 6 Correction model for ionospheric delays

The ionospheric model developed for one-frequency users of GPS [Klobuchar, 1987] consists of a cosine representation of the daily fluctuation in TEC. By including a frequency scaling term this model can be used for any single frequency positioning system.

The model assumes a diurnal maximum of TEC at 14.00 hr local time. The positive portion of a cosine wave is used to model the ionospheric delay during the day and a constant nighttime offset is used to model the diurnal behavior. Third order polynomials are used to depict cosine amplitude and period as functions of user geomagnetic latitude. The polynomial coefficients are chosen daily from a set of constants that reflect the sensitivity to solar-flux and seasonal variation. The coefficients are transmitted as part of the navigation message. The ionospheric delay is then given by

$$T_g = DC + A \cdot \cos\left(\frac{2\pi \cdot (t - T_p)}{P}\right)$$

where DC, A, T_p and P (constant offset, amplitude, phase and period) are the four parameters required to obtain a complete diurnal representation of T_g at any location. To limit the required computational power in the receiver, a truncated cosine expansion is used

$$T_g = DC + A \cdot \left[1 - x^2/4 + x^4/24\right] \quad , \quad |x| \leq \pi/2 \qquad \text{(seconds)}$$

with

$$x = \frac{2\pi \cdot (t - T_p)}{P} \qquad \text{(rad)}$$

where t is the local time of the Earth subpoint of the signal intersection with the mean atmospheric height, assumed to be 350 km. DC and T_p are held constant at 5 ns and 14 h (50400 s) respectively. A and P are modeled as third order polynomials

$$A = \sum_{n=0}^{3} \alpha_n \cdot \varphi_m^n \qquad \text{(seconds)}$$

$$P = \sum_{n=0}^{3} \beta_n \cdot \varphi_m^n \qquad \text{(seconds)}$$

where φ_m is the geomagnetic latitude of the subpoint and α_n and β_n are part of the navigation message. Based on an estimate of the user position, the ionospheric delay can be calculated through the following steps

1. Calculate the subtended Earth angle (EA) between user and satellite using the approximations

$$EA = \frac{445}{El+20} - 4 \quad \text{(degrees)}$$

where El is the (estimated) elevation angle of the satellite with respect to the user.

2. Compute the geodetic latitude and longitude of the ionospheric subpoint using the approximations

$$\varphi_I = \varphi_u + EA \cdot \cos(Az) \quad \text{(degrees)}$$

$$\lambda_I = \lambda_u + EA \cdot \frac{\sin(Az)}{\cos(\varphi_I)} \quad \text{(degrees)}$$

where φ_u and λ_u are the (estimated) geodetic latitude and longitude of the user and Az is the (estimated) azimuth of the satellite with respect to the user.

3. Convert the geodetic to a geomagnetic latitude using the approximation

$$\varphi_m = \varphi_I + 11.6 \cdot \cos(\lambda_I - 291) \quad \text{(degrees)}$$

4. Find the local time

$$t = 240 \cdot \lambda_I + \text{UTC time} \quad \text{(seconds)}$$

if $t > 86400$ use $t = t - 86400$. If $t < 0$, add 86400.

5. Account for elevation angle by scaling with an obliquity or slant factor F

$$F = 1.0 + 2.0 \cdot \left(\frac{96 - El}{90}\right)^3$$

6. Compute the ionospheric time delay

$$T_{IONO} = q \cdot F \cdot [5 \cdot 10^{-9} + (1 - x^2/2 + x^4/24) \cdot \sum_{n=0}^{3} \alpha_n \cdot \varphi_m^n]$$

where

$$x = \frac{2\pi \cdot (t - 50{,}400)}{\sum_{n=0}^{3} \beta_n \cdot \varphi_m^n}$$

and q is the frequency scaling term to allow for the use of the algorithm at a carrier frequency different than L_1

$$q = (1.57542/f)^2$$

where f is the carrier frequency of our system in GHz.

This model leads to an overall reduction in rms ionospheric range error of about 60% [Fees, 1987].

Appendix 7 Receiver noise model

The noise model of a receiving system is shown in Figure A7.1

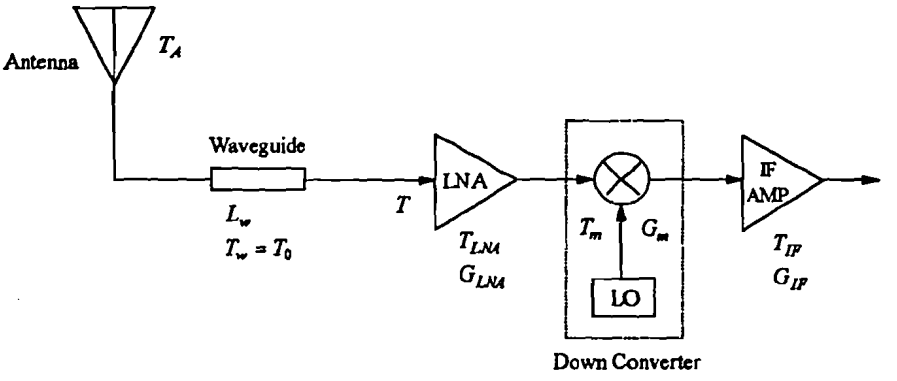

Figure A7.1 Receiver system noise model

The system noise temperature at the input of the low-noise amplifier is given by

$$T = \frac{T_A}{L_W} + \left(\frac{L_W - 1}{L_W}\right)\cdot T_0 + T_{LNA} + \frac{T_m}{G_{LNA}} + \frac{T_{IF}}{G_{LNA}\cdot G_m}$$

where L_w is a ratio >1, not in dB.

Typical values are: L_W = 0.5 dB, T_{LNA} = 150 K, G_{LNA} = 50 dB, T_m = 850 K, G_m = -10 dB, T_{IF} = 400 K and G_{IF} = 30 dB. If G_{LNA} = 50 dB, the last two terms of the equation are negligible.

In clear-sky conditions the antenna noise temperature is given by

$$T_A = T_{sky} + T_{ground}$$

The sky noise contribution is a function of the downlink frequency and the elevation angle. At 4 GHz T_{sky} is about 2.2 K and 12 K for elevation angles of 90° and 10° respectively. The respective values at 12 GHz are 4 K and 20 K. T_{ground} is determined by the radiation from the earth in the vicinity of the antenna captured by the sidelobes and partly by the main lobe of the antenna radiation pattern. Typical clear-sky antenna temperatures at 4 GHz and 12 GHz are 50 K and 65 K respectively. Combined with

the mentioned typical receiver parameters this gives system noise temperatures of 227 K and 240 K at 4 GHz and 12 GHz respectively.

During rain the antenna temperature increases and is given by

$$T_A = T_{sky} / A_{rain} + T_m \cdot (1 - 1/A_{rain}) + T_{ground}$$

where A_{rain} is the rain attenuation and T_m is the mean rain temperature (270 - 290 K).